

UC Irvine

UC Irvine Previously Published Works

Title

Recent Advances in Photo-Initiated Electron Transfer at the Interface of Anatase TiO₂ Nanocrystallites and Transition-Metal Polypyridyl Compounds

Permalink

<https://escholarship.org/uc/item/1kf8h276>

ISBN

9781119951438

Authors

Ardo, S

Meyer, GJ

Publication Date

2010-11-01

DOI

10.1002/9781119951438.eibc0468

Copyright Information

This work is made available under the terms of a Creative Commons Attribution License, available at

<https://creativecommons.org/licenses/by/4.0/>

Peer reviewed

Recent Advances in Photo-Initiated Electron-Transfer at the Interface between Anatase TiO₂ Nanocrystallites and Transition-Metal Polypyridyl Compounds

Shane Ardo and Gerald J. Meyer

Johns Hopkins University, Baltimore, MD, USA

1	Introduction	1
2	Solar Light Harvesting	3
3	Photoinduced Electron Injection	11
4	Sensitizer Regeneration	16
5	Sensitization at the Power Point	23
6	Conclusions	25
7	Acknowledgments	26
8	End Notes	26
9	Related Articles	26
10	Abbreviations and Acronyms	26
11	Further Reading	26
12	References	26

1 INTRODUCTION

Hoffert and colleagues documented recent energy needs on the terawatt (TW = 10¹² W) scale.^{1,2} They described the pitfalls of a “wait-and-see” approach and recommended immediate action that has now been dubbed the Terawatt Challenge.³ As the worldwide rate of energy expenditure is related to the number of people on Earth, the population growth experienced over the last quarter-century is staggering: a 45% increase which equates to roughly two billion people and 6 TW of energy (~63% increase).⁴ This coupled with the urbanism of third-world and nonindustrialized nations and cities has led to an increase in the demand for fossil fuel.⁴ However, as mentioned by Hoffert, the continued use of fossil fuels is not a long-term solution, and the deleterious environmental consequences of their combustion have become evident. Ice-core data over the past three-quarters-of-a-million years that correlate temperature with greenhouse gas concentration are sobering.^{5,6} The current atmospheric CO₂ levels of >380 ppm⁷ exceed any values attained over this same time period.^{5,8,9} The increased average global temperature and rates of glacial melting measured over the last few decades are telling signs.¹⁰ Regardless, if one thinks that these “signs” are the results

of global climate change, it is very difficult to argue with two key points: our civilization needs to better appreciate the “cost” of energy and begin to implement sustainable renewable power-conversion technologies.

The sun is the one source that *on its own* could supply the world’s projected energy demand in a sustainable fashion.⁷ To put it in perspective, the amount of solar energy reaching the earth *in one day* could power the planet for *an entire year*.^{3,11} More realistically, covering roughly 1/800th of the land on Earth with 10% efficient solar cells would generate enough power to compensate the world’s average power usage,^{3,4} while the land area occupied by the nation’s federally numbered highways would approximately power the United States.³ Remaining is the challenge of harvesting and storing this energy in a cost-effective way.

It has been 19 years since Grätzel, O’Regan, and Anderson first introduced thin films comprised of ~20-nm anatase TiO₂ particles interconnected in a mesoporous 10-micron thick film for applications in regenerative, dye-sensitized solar cells (DSSCs).^{12,13} Global conversion efficiencies greater than 11% have now been confirmed by several certified national laboratories.^{14–19} This efficiency is encouraging as future advancements could assist in solving

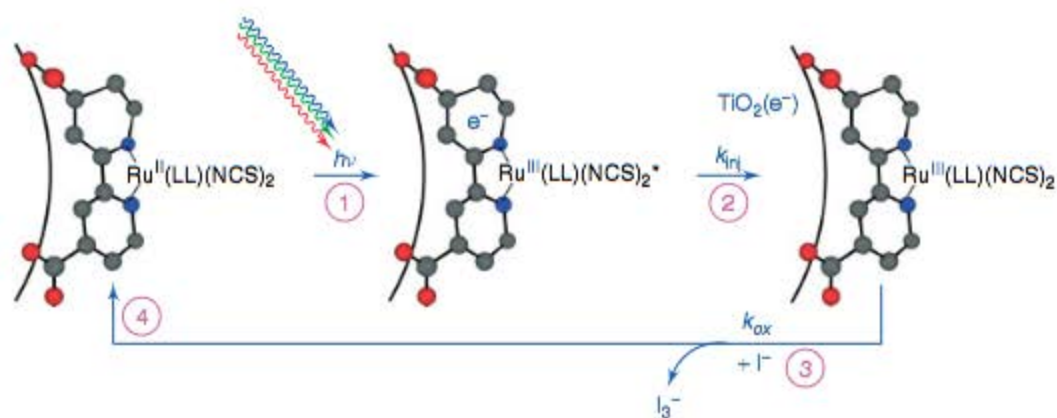
the Terawatt Challenge and allow for the replacement of traditional silicon solar cells, whose purification procedure is highly energy intensive and expensive.³ A solar cell that can be manufactured inexpensively with the use of nontoxic and abundant precursors would undoubtedly enhance the sustainability of our civilization.²⁰

Inorganic chemistry has and will continue to be important for the optimization of DSSCs and for advancement of our fundamental knowledge of photoinduced electron transfer at molecular–semiconductor interfaces. The light-harvesting and redox properties of transition-metal coordination compounds are well understood and continue to be optimized for applications in DSSCs. This is particularly true for $d\pi^6$ transition-metal polypyridyl compounds, such as Ru(II) tris-bipyridine, Ru(bpy)₃²⁺.^{21–23} Coordination compounds based on Cu, Ir, and Pt have recently received renewed attention as sensitizers. Transition-metal compounds and halide chemistry is also highly relevant to redox mediation in DSSCs. Alkali and alkaline earth cations are known to have large impacts on the solar conversion efficiencies, yet our understanding of this behavior is currently lacking. Also important is the synthesis of new inorganic materials with tailored architectures on the nano- and micrometer length scales. DSSCs, therefore, provide many exciting opportunities for chemists interested in these diverse areas of inorganic chemistry.

In this article, we highlight some of the recent (roughly, publication year from 2004 to present) inorganic advances, techniques, and avenues for further exploration that involve photoinduced electron transfer at anatase TiO₂ nanocrystallites which are often at the heart of current DSSC-related research. The focus is predominantly on those related to the steps comprising the metal-to-ligand charge-transfer (MLCT) “sensitization cycle” Scheme 1, for TiO₂-based DSSCs, which is described further below. As such, this article

is not exhaustive. A comprehensive review, including historical background, can be found elsewhere;²¹ however as this article expands on certain areas highlighted in the comprehensive review, descriptions of some of the historical studies may be similar. First, a brief overview of the mechanism of DSSC operation and the current–voltage (i – V) curves that characterize the power-conversion efficiencies of solar cells has been presented.

The most practically useful “sensitizers” in DSSCs are polypyridyl compounds of Ru^{II} and, to a lesser extent, Os^{II}.^{21–23} The photophysical properties of MLCT excited states are well characterized in fluid solution,^{24–32} yet identifying their behavior at sensitized TiO₂ interfaces remains an unresolved issue. Ruthenium polypyridyl compounds, such as N3, [*cis*-Ru(dcb)₂(NCS)₂], where dcb is 4,4′-(COOH)₂-2,2′-bipyridine, are generally the optimum sensitizers for this application due to their photochemical and thermal stability and broad spectral light harvesting.^{33,34} In sunlight, such sensitizers bind to TiO₂ rapidly and quantitatively undergo three consecutive charge-transfer reactions^{20,21,35}: (i) MLCT excitation; (ii) excited-state electron injection into TiO₂; and (iii) reduction *via* iodide oxidation, at which time the sensitizer is “regenerated” and can repeat the “sensitization cycle” of light absorption, excited-state injection, and iodide oxidation as shown in Scheme 1. Not shown, but necessary to the function of the DSSC, is the transport of the injected electron through the mesoporous thin film to the external circuit with eventual arrival at the counter electrode, where it uses its remaining free energy to reduce tri-iodide. Hence, the solar cell is termed “regenerative” as all oxidation chemistry at the dye-sensitized photoanode is reversed at a dark counter electrode such that no net chemistry occurs. Building on the success of the DSSC and developing low-cost architectures for solar energy conversion and storage is just one of many motivations for understanding the interfacial sensitization cycle in precise molecular detail.



Scheme 1 Light absorption, excited-state injection, and iodide oxidation termed the “sensitization cycle.” In the operational DSSC, under 1 sun, AM1.5 spectral irradiance each sensitizer repeats this sensitization cycle roughly twice per second. (Reproduced from Ref. 36. © American Chemical Society, 2010.)

2 SOLAR LIGHT HARVESTING

2.1 Determination of the Light-Harvesting Efficiency

The fraction of light that is absorbed by a DSSC is wavelength dependent and is often called the *light-harvesting efficiency (LHE)* or *absorptance* (α).³⁸ When light scattering is absent, the absorptance is simply one minus the transmittance.³⁸ The absorptance of a monolayer of sensitizers anchored to a surface is related to the molar extinction coefficient of the sensitizer ($M^{-1} \text{ cm}^{-1}$), ϵ , and the surface area occupied by the sensitizer on a planar surface in \AA^2 , $A_{\text{sensitizer}}$, i.e., the footprint:

$$\alpha(\lambda) = 1 - \frac{I(\lambda)}{I_0(\lambda)} = 1 - 10^{-\text{Absorbance}(\lambda)}, \quad \text{where} \quad (1)$$

$$\text{Absorbance}(\lambda) = 1000 \cdot \epsilon(\lambda) \cdot \Gamma = \frac{10^{19} \cdot \epsilon(\lambda)}{N_A \cdot A_{\text{sensitizer}}} \quad (2)$$

where I_0 is the intensity of the incoming incident light, I is the intensity of the light transmitted through the sample, Γ is the macroscopic surface coverage in moles per square centimeter, and N_A is Avogadro's number. Calculations show that even a monolayer of phthalocyanines or porphyrins, which have among the highest extinction coefficients known, packed within van der Waals distance of one another on planar surfaces, absorbs <10% of light at their maximum absorbance and far less than 1% of the 1 sun, AM1.5 spectrum.³⁹ This underscores the need for high surface-area materials to increase the LHE of a molecular monolayer of sensitizers. It is for this reason that DSSCs typically consist of anatase TiO_2 nanocrystallites ($\sim 20 \text{ nm}$ in diameter) sintered into a transparent, sponge-like network on transparent fluorine- or indium-doped SnO_2 -conductive substrates.²¹

2.2 Evaluation of Solar Cell Performance

The success of a solar cell is quantified by its light-to-electrical power-conversion efficiency, η :

$$\eta = \frac{V_{\text{oc}} \cdot i_{\text{sc}} \cdot \text{FF}}{A_{\text{cell}} \cdot P_0} \quad (3)$$

where V_{oc} is the open-circuit photovoltage, i_{sc} is the short-circuit photocurrent, FF is the fill factor, A_{cell} is the cell's projected area, and P_0 is the incident irradiance.⁴⁰ P_0 is usually fixed to 1 sun (100 mW cm^{-2}) of solar irradiance and an air mass 1.5 (AM1.5) spectral distribution, which is often taken as an average irradiance and spectral distribution of sunlight in the United States. The AM1.5 spectrum can be downloaded from the National Renewable Energy Laboratory (NREL) website.⁴¹ V_{oc} is the maximum Gibbs free energy that one can abstract from a regenerative solar cell while i_{sc} is the maximum rate at which the charge can flow through the external circuit and is ultimately limited by the photon flux.

The theoretical, detailed-balance limit for the light-to-electrical power-conversion efficiency of a solar cell with a single light absorber was elegantly derived by Shockley and Quissar in 1961.⁴² Under 1 sun of AM1.5 irradiance, this efficiency has been deemed to be $\eta = 29\text{--}33\%$.^{42–47} Similar values have been obtained *via* derivations based on molecular light absorbers and first-principles thermodynamics,^{46,47} indicating that DSSCs would possess a similar upper limit.

What cannot be stressed enough is that the i_{sc} of a solar cell is directly related to its *absorptance*, (α), not its *absorbance*.²¹ In the absence of nonlinear effects, the measured absorptance spectrum can be used to calculate the fraction of AM1.5 solar photons absorbed, which provides an upper limit to the i_{sc} of a DSSC. Likewise, the optimal incident photon-to-current efficiency (IPCE) can be calculated from the absorptance spectrum of the solar cell. When the IPCE is measured as a function of the wavelength of light, the so-called photocurrent action spectrum is obtained. The IPCE is the product of three terms: the absorptance (α), the injection quantum yield (φ_{inj}), and the quantum yield for electron collection (φ_{coll}). In fact, the integral of the IPCE (λ)-weighted solar flux is mathematically *identical* to the i_{sc} . This equality can actually be used to test the validity of the 1-sun, AM1.5-simulated light source used for the power-conversion-efficiency measurements.⁴⁸ Thus, ultimately, the i_{sc} is solely based on the sensitizer's (i) extinction coefficient, (ii) molecular footprint and surface roughness as they relate to the surface coverage, (iii) quantum yield for injection, and (iv) collection efficiency. Recent advances in each are discussed in detail in the sections that follow, as they relate to the aforementioned sensitization cycle.

The FF can be related to i_{sc} and V_{oc} through the corresponding current and voltage at the power point (PP):

$$\text{FF} = \frac{i_{\text{PP}} \cdot V_{\text{PP}}}{i_{\text{sc}} \cdot V_{\text{oc}}} \quad (4)$$

where the PP occurs at the maximum product of the cell output photovoltage and photocurrent obtained along the current–voltage curve, Figure 1(a). While an FF of unity is ideal, such a value cannot be achieved because of various loss mechanisms such as charge recombination. Under short-circuit conditions, the injected electrons in DSSCs are rapidly and quantitatively collected in the external circuit. At open circuit, current does not flow and the concentration of electrons injected into the TiO_2 nanoparticles, $\text{TiO}_2(e^-)$ s, increases to a steady-state value. At the PP, roughly 10 electrons have been estimated to reside in each TiO_2 nanocrystallite.⁴⁹

Rough estimates of the theoretical ultimate (ideal) values for V_{oc} , i_{sc} , and power-conversion efficiency can be obtained by straightforward analysis of the AM1.5 solar irradiance spectrum (Figure 1b) and the absorptance spectrum of the surface-anchored sensitizers. As described previously,²¹ the long-wavelength absorption edge (the ‘‘effective bandgap’’) sets a (thermodynamic) limit to the V_{oc} while integration of the 1-sun solar photon flux to this

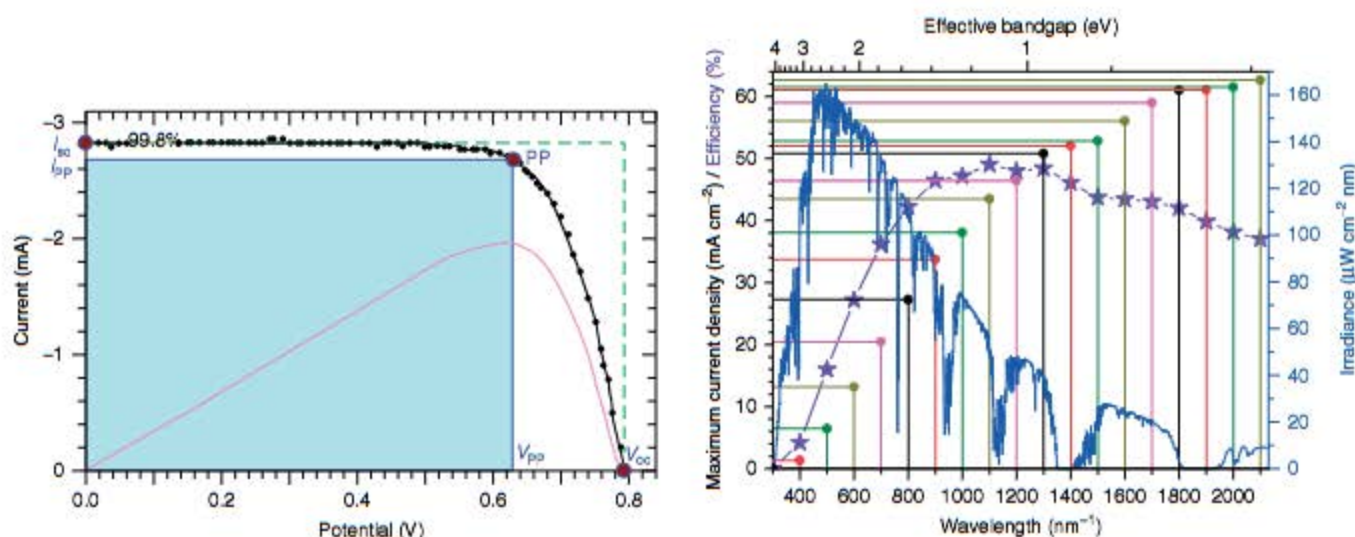


Figure 1 (a) Typical current–voltage curve for a champion DSSC under approximately 1 sun, AM1.5 illumination. Labeled are the short-circuit photocurrent (i_{sc}), open-circuit photovoltage (V_{oc}), and power point (PP) along with its corresponding photovoltage (V_{pp}) and photocurrent (i_{pp}). The fill factor (FF) is the area of the shaded region, which is bounded by the V_{pp} and i_{pp} , divided by the area of the region outlined by the dashed line, which is bounded by the V_{oc} and i_{sc} . The curve in magenta represents the power as a function of voltage in arbitrary units further illustrating that the PP coincides with the condition of maximum power output. (Reproduced from Ref. 52. © Elsevier, 2003.) (b) Circular figures represent the maximum current density that can be obtained from a complete light absorber whose “effective bandgap” corresponds to the wavelength or energy indicated on the abscissa axes. Also shown, as stars, are the maximum possible efficiencies obtainable from the said light absorber assuming the unrealistic case where there are neither current nor voltage losses. The spectral irradiance for 1 sun of AM1.5 sunlight is shown in blue and corresponds to the right axis

“effective bandgap,” and conversion to current density, sets a limit to the i_{sc} . Thus, assuming a fill factor of unity, the largest possible efficiency (Figure 1b, purple stars) can be estimated from the absorbance spectrum. For champion DSSCs based on the so-called “black dye” (N749) sensitizer, maximum V_{oc} and i_{sc} values of 0.74 V and 21 mA cm^{-2} have been achieved.^{17,50,51} Based on these assumptions, with an absorption edge of 900 nm, this yields theoretical maximum values for V_{oc} and i_{sc} of 1.38 V and 33.7 mA cm^{-2} (red), and $\eta = 46.5\%$. This approximate value not only greatly exceeds the actual value obtained, $\eta \approx 11\%$,^{17,51} but is also clearly impossible as it exceeds the Shockley–Quissar limit described above. The crude analysis fails to account for entropic and resistive voltage and recombination losses at the PP of operational DSSCs, which have thus far proven impossible to prevent.

Theoretical efficiencies estimated in this manner far exceed those obtained in practice. The optimal i_{sc} is within experimental error practically realized in champion DSSCs.³³ However, for V_{oc} , this is not the case and the spectroscopically estimated maximum V_{oc} values are at least a full volt larger than those that have been observed experimentally.²¹ Also, while a fill factor of unity is ideal, in reality such a value cannot be achieved because of various loss mechanisms and overpotential requirements.⁴⁸ Notwithstanding, most of the recent advances in DSSCs are from increases in i_{sc} because of enhancements in extinction coefficient, spectral bandwidth, and charge-separated lifetime; optimizing V_{oc} and FF values

has proven to be a much more difficult undertaking. For these reasons, inorganic advances related to the ultimate enhancement of i_{sc} are predominantly covered throughout this article.

2.3 Tuning Orbitals for Increased Light Harvesting

The MLCT excited states of $d\pi^6$ coordination compounds have emerged as the most efficient states for solar harvesting and sensitization of wide-bandgap semiconductor materials. As the name implies, light absorption promotes an electron from the metal d orbitals to the ligand π^* orbitals, $d(\pi) \rightarrow \pi^*$; where the $d(\pi)$ nature of the highest occupied molecular orbital (HOMO) is due to mixing of the t_{2g} states of the metal with the π orbitals of the ligands.^{53–55} A number of electric-dipole-allowed charge-transfer transitions are observed, which give rise to intense absorption bands in the visible region with moderate extinction coefficients. There is no formal spin for each excited state due to heavy-atom spin–orbit coupling from the transition-metal center (especially for 4d and 5d metals).^{24,28,56,57} Crosby *et al.* have proposed that the excited state is accurately described solely by the symmetry label of the molecular point group to which it belongs and not the spin and an orbital individually.⁵⁶ Furthermore, the effects of spin–orbit coupling must be introduced in order to rationalize the relative oscillator strengths and absorption spectra of $M(\text{bpy})_3^{2+}$ ($M = \text{Fe}^{\text{II}}$, Ru^{II} , and Os^{II}) compounds, where bpy is 2,2'-bipyridine.

The classical example of a compound with such transitions is $\text{Ru}(\text{bpy})_3^{2+}$, which is arguably the most well-studied coordination compound. The ground state is threefold symmetric and is best described by the symmetry label D_3 . Demas and colleagues have shown that intersystem crossing from the charge-localized, C_2 -symmetrical, $^1\text{MLCT}$ excited state to a manifold of relaxed states occurs with a quantum yield near unity in fluid solution.^{58–60} Although not formally triplet or singlet in nature, the predominantly triplet character of the lowest energy excited state, $^1E'$,^{61,62} and singlet character of the initial, Franck–Condon state allow the transition between them to be labeled as intersystem crossing. It is for this reason that these states will be labeled as $^3\text{MLCT}$ and $^1\text{MLCT}$, respectively, throughout this article. Crosby, Hager, and colleagues have shown that photoluminescence arises from three closely spaced electronic states.^{63–67} Rapid thermal equilibrium between this manifold of states, $<kT$ in energy apart, happens such that photoluminescence occurs from what appears to be a single thermally equilibrated, or thexi,^{68,69} state. Yersin, *et al.* discovered evidence for two more highest energy states by temperature-dependent emission polarization experiments and labeled them per the D_3' double symmetry group, which takes into account the spin–orbit coupling.^{61,62} Recently, these transitions have generally been supported by those obtained from computational density functional theory (DFT) calculations.⁷⁰ These calculations also revealed that there was a D_3 and C_2 excited state within a few wavenumbers of one another, thus rationalizing the discrepancies found in the literature for the identity of the symmetry of the initial, Franck–Condon excited state.^{71–76} A dissociative, metal-centered state from a ligand-field (LF) transition ($d \rightarrow d$) was also identified, at roughly the same energy, where it was proposed that a four-coordinate species may result.

Recently, Chergui and coworkers have shown by polychromatic femtosecond fluorescence upconversion that intersystem crossing to the $^3\text{MLCT}$ excited state of $\text{Ru}(\text{bpy})_3^{2+}$ occurs within 15 ± 10 fs; as this corresponds to the vibrational period of a high-frequency mode, this points to a strongly nonadiabatic process.⁷⁷ Subsequent dissipation of the excess thermal energy within the thexi state manifold in <300 fs is also rather rapid and was suggested to be because of intramolecular vibrational-energy redistribution, where the excess thermal energy in the predominant 1607 cm^{-1} higher frequency mode was transferred to low-energy metal–ligand modes.⁷⁸

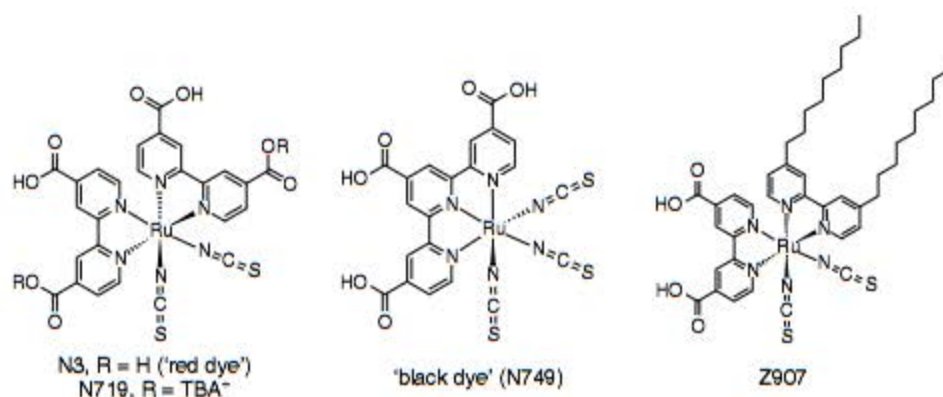
Hammarström and colleagues have shown by transient-absorption anisotropy measurements in acetonitrile that 1 ps following photoexcitation, the electron has no memory of which bipyridine was initially photoselected.^{71,79} This was also found to be true in ethanol solution and with $\text{Ru}(\text{bpy})_2(\text{mcb})/\text{TiO}_2$ thin films, where mcb is 4-COOH-4'-CH₃-bpy.⁸⁰ These findings are in contrast to older models where electron hopping randomization among ligands was

proposed to explain the time evolution of the spectroscopically isotropic signal.^{81,82}

The excited-state lifetime of $[\text{Ru}^{\text{II}}(\text{bpy})_2(\text{bpy}^-)]^{2+*}$ is $\sim 1\ \mu\text{s}$ in water.⁸³ The radiative rate constant, k_r , is typically about two orders-of-magnitude smaller than the nonradiative rate constant, k_{nr} , and hence the excited-state lifetime is generally controlled by the latter.⁸³ Often Ru^{II} - and Os^{II} -polypyridyl excited states have been shown to follow Jortner's energy gap law, where k_{nr} increases exponentially with decreasing energy gap.^{84–88} For this reason, preparation of compounds that emit in the infrared region and have long-lived excited states has proven difficult. However, small k_{nr} values are not sufficient to realize long-lived excited states. A large ligand-field splitting parameter is also required in this class of excited states as the presence of low-lying, LF states can rapidly deactivate the thexi states. A classical example of this is $\text{Fe}(\text{bpy})_3^{2+}$ that until recently was thought to be completely nonemissive due to rapid and quantitative internal conversion/intersystem crossing through ligand-field states. Notwithstanding, realization of efficient sensitization by Fe^{II} polypyridyl compounds would decrease the cost of DSSCs. However, efficient power-conversion with Fe^{II} sensitizers has not been realized.

Chergui and coworkers provided clear transient femtosecond structural and absorption evidence that the mechanism of relaxation in $\text{Fe}(\text{bpy})_3^{2+}$ is intersystem crossing from the $^1\text{MLCT}$ to $^3\text{MLCT}$ state followed by direct relaxation to the high-spin 5T_2 state in ~ 150 fs,^{89–94} termed spin crossover or light-induced excited spin-state trapping (LIESST) when the state is long-lived. The MLCT intersystem crossing was in a strongly non-Born Oppenheimer regime mediated by high-frequency modes of the molecule. Ultimately, thermally activated relaxation to the energy-minimum initial low-spin 1A_1 state completed the cycle. These data were obtained by time-resolved optical-pump experiments, where the probe technique was based on extended X-ray absorption fine spectroscopy (EXAFS), X-ray absorption near-edge structure (XANES), or visible transient-absorption spectroscopy. McCusker and colleagues observed similar behavior with a hexadentate Fe^{II} coordination compound.^{95–97} Evidence for light-induced spin trapping on TiO_2 was obtained in our laboratories with surface-anchored $\text{Fe}(\text{pymbA})_3^{2+}$, where pymbA is 4-(2-pyridin-2-yl-benzimidazol-1-ylmethyl)-benzoic acid.⁹⁸ Although not proven, the rapid spin trapping observed probably accounts for the inefficient excited-state electron injection into TiO_2 . An Arrhenius analysis of the high-spin to low-spin re-equilibration revealed a Gaussian distribution of activation energies.⁹⁹

An important aspect of $d\pi^6$ coordination compounds is that their colors can be controlled with synthetic chemistry. The MLCT absorption bands can be tuned in energy by altering the substituents on the bpy ligands or, simplistically, by controlling the extent of σ -donation from the nonchromophoric ligands or $d(\pi) \rightarrow \pi^*$ back-bonding donation to ligands.²⁸ How these changes affect the photophysical



Scheme 2 The chemical structures of historically the most successful Ru^{II}-polypyridyl sensitizers employed in champion DSSCs

properties of the compounds has been the subject of many investigations affording further insights into the factors that govern radiative and nonradiative excited-state decay.^{24–32,100}

As many of the sensitizers employed in champion DSSCs are of the form *cis*-Ru(LL)₂X₂, where LL is a bpy-like ligand and X is an anionic nonchromophoric ligand, their spectral differences and similarities to Ru(bpy)₃²⁺ are discussed. In terms of DSSC light-to-electrical power-conversion efficiency, N3/N719, where LL = dcb^{0/-} and X = SCN⁻,^{33,34} and closely related analogs, until recently, remained unsurpassed, Scheme 2.³ Although slightly solvatochromic, the visible absorption spectrum of N3, and that of its ‘‘LL = bpy’’ derivative, exhibit two well-resolved bands because of its symmetry. The symmetry of the ground state is C₂ whereas that for Ru(bpy)₃²⁺ is D₃. It has been postulated that the spectroscopic signatures are due in part to a shift in the electron density of the HOMO from the Ru^{II} metal center to the isothiocyanate ligands.^{101–103} Roughly, 75% of the HOMO density was calculated to reside on the isothiocyanate ligands, mainly on the sulfur atom. The gain in red absorption over Ru(dcb)₃²⁺ and subsequent increase in LHE occurs at the expense of the driving force for iodide oxidation and the excited-state lifetime, by the energy gap law. However, the performance of the DSSC is generally not affected by either of these undesirable traits because of the many orders-of-magnitude faster rates of the competing processes (i.e., interfacial charge recombination and excited-state injection, respectively).^{104,105} Also, a recent Raman study has shown that when anchored to TiO₂, the solvent reorganization energy of N3 decreased by a factor of 6.¹⁰⁶

In champion DSSCs, the presence of Li⁺ in the electrolyte is a requirement.²¹ This hard Lewis acidic cation affects all of the steps related to the sensitization cycle.^{21,107,108} In a step toward controlling this chemistry, Grätzel and coworkers recently synthesized a novel N3 analog where one dcb ligand was replaced with 4,4'-(triethylene oxide methyl ether)-bpy.^{109,110} The 12-crown-4 ether groups on the bipyridine ligand provide a coordination environment for Li⁺. Interestingly, in comparative photoelectrochemical studies,

N3-like sensitizers with these crown ether ligands displayed a significant increase in *i*_{sc} with little-to-no variation in V_{oc}. This was unusual as the loss of Li⁺ from the TiO₂ surface was expected to destabilize the TiO₂ acceptor states, presumably resulting in less efficient excited-state injection and hence a lower photocurrent.^{21,107} Similar results have since been observed with a more hydrophobic version of the sensitizer.¹¹¹ Such amphiphilic sensitizers have also recently gained interest as possible sensitizers that are more forgiving toward trace amounts of water and are also often found to be more stable toward temperature stress and light soaking.^{112–121}

Recently, a new motif for Ru^{II} sensitizer chelation was employed using an N3-like compound, where one dcb was replaced with two pyridines linked in their 2 positions by the nitrogen atom of an aniline.¹²² The photoelectrochemical properties were all found to be very similar to those of N719.^{122,123} Another novel motif involved replacement of the two isothiocyanate ligands with a single sulfur-donor bidentate ligand.¹²⁴ Although these first-generation sensitizers had lower efficiencies than N719, it was interesting that of these sensitizers, the ones with the most favorable photophysical characteristics did not perform as well. This was proposed to be due to the terminal cyano groups of the sulfur-donor ligands, which may have directly bound to the TiO₂ surface, thus speeding interfacial charge recombination.

2.3.1 Increasing the Extinction Coefficient

Although the excited-state lifetime of Ru^{II}-polypyridyl compounds is sufficiently long-lived for realization of near-quantitative excited-state injection and sensitization, a shortcoming of sensitization by these visible-light MLCT transitions is their relatively low extinction coefficients as compared to intraligand (IL) π → π* transitions. Ru(bpy)₃²⁺ has a molar extinction coefficient of roughly 15 000 M⁻¹ cm⁻¹ for its MLCT electronic transitions.¹²⁵ In contrast, natural and synthetic organic and porphyrin/phthalocyanine pigments also absorb solar photons,

but with extinction coefficients that are often in excess of $200\,000\text{ M}^{-1}\text{ cm}^{-1}$ for their IL transitions.³⁹ Thus 5–10 μm thick films of nanocrystallite TiO_2 , with internal surface areas up to 1000 times larger,^{126–128} are required for efficient solar harvesting with Ru^{II} -polypyridyl coordination compounds.

Fermi's so-called "Second Golden Rule" states that $k_{\text{ET}} = \frac{2\pi}{\hbar} \cdot |\langle \hat{H}_{\text{ab}} \rangle|^2 \cdot \rho_{\text{FCW}}$, where k_{ET} is the rate constant for electron transfer, H_{ab} is the electronic-coupling matrix element between the initial and final states, and ρ_{FCW} is the Franck–Condon weighted density of vibronic states.^{129–132} As electronic transitions follow this rule, both Einstein's *A* and *B* transition probability coefficients relate to the square of the transition dipole moment, under electric dipole-induced conditions. Under the approximation of a two-level system, Einstein's *A* coefficient, which is equal to k_{r} , is also related to the cube of the average energy gap¹³⁰; as the oscillator strength, absorption cross section, and extinction coefficient all relate to Einstein's *B* coefficient, they too are directly related to the square of the transition dipole moment and to the average energy gap.^{130,133} Taken together, increases in extinction coefficient should most often be accompanied by similar enhancements in k_{r} . It has long been known that addition of substituents with low-lying π orbitals (such as aromatics, esters, carboxylic acids, or unsaturated organics) to polypyridines can enhance MLCT extinction coefficients relative to unsubstituted polypyridines.^{134–147} However, as described above, it is often k_{nr} , and not k_{r} , that determines the excited-state lifetime of Ru^{II} polypyridyl compounds. Thus, the question begs, could enhancements in extinction coefficient be coupled to *increases* in the lifetime of the excited state if k_{nr} simultaneously decreased?

Indeed, this has been observed in MLCT compounds employing 4,4'-aryl- or 4,4'-vinyl-disubstituted bpy, 2,2':6',2''-terpyridine (tpy), and 1,10-phenanthroline (phen) ligands.^{134–136,138,139,143–151} As expected, when the transition dipole moment was extended by LUMO π^* delocalization, both the extinction coefficient, or oscillator strength if the band's width was altered, and k_{r} increased.^{134,139,150} When compared to sensitizers lacking this extended conjugation, k_{nr} decreased because of less electron–vibrational coupling, i.e., smaller Huang–Rhys factors, from the further delocalization of the π^* electron over the entire ligand.¹³⁴ Thus the excited-state lifetimes increased as well!

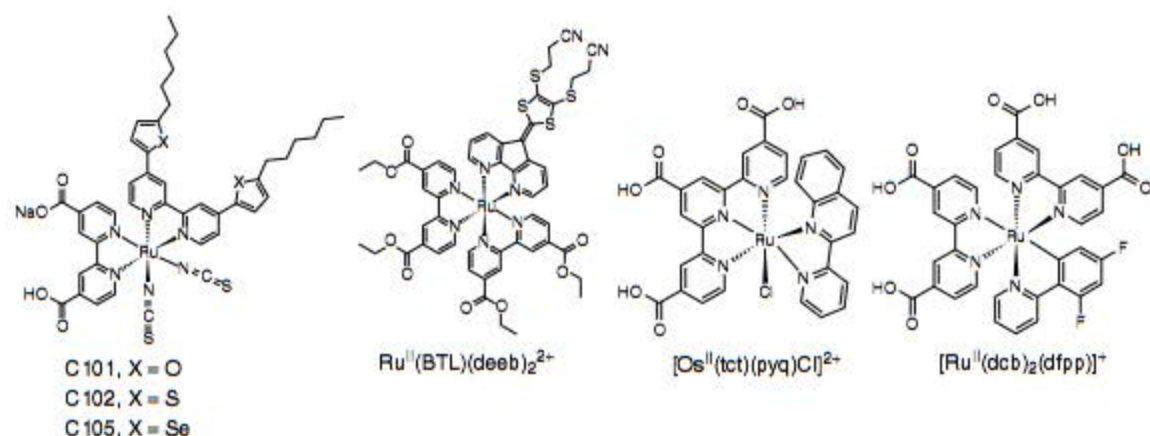
Smaller extinction-coefficient enhancements were observed with 5,5'-aryl-disubstitution,¹³⁹ even though 5,5'-disubstitution increased the conjugation relative to 4,4'-disubstitution. Albeit, 5,5'-aryl-disubstituted ligands did lead to the expected decrease in energy gap and red-shifted MLCT transition because of enhanced conjugation and a lowering of the LUMO energy.¹³⁹ These conflicting findings were rationalized using Mulliken charge-transfer theory,¹³⁹ where the degree of charge transfer is directly proportional to the overlap between the HOMO and LUMO.^{136,152–154} It was determined that the extended intraligand delocalization afforded by the increased conjugation in the 5,5'-disubstituted

ligand actually resulted in *less* electron density on the nitrogen p_z orbital chelated to Ru^{II} as compared to the less-conjugated 4,4'-disubstituted ligand.¹³⁹ Conversely, when delocalization of the ligand π^* orbital was extended in the opposite direction of the MLCT band, e.g., with 6,6'-disubstitution, the magnitude of the transition dipole moment and the extinction coefficient actually decreased.¹³⁶

For these reasons, the preparation of high extinction coefficient, and still rather long-lived, heteroleptic N3 derivatives, where one of the dcbl ligands is replaced by a 4,4'-disubstituted bpy, is an extremely active area of research.^{16,115,116,140–142,155–169} This synthetic enhancement, coupled with covalent attachment of thiophene^{16,19,160–163,170–175} or tri-alkyl-/aryl-amine^{156,162,164,167} donor functional groups, has led to great enhancements in extinction coefficient and charge-separated lifetime. The lifetime of the $\text{TiO}_2(\text{e}^-)$ and oxidized sensitizer charge-separated state is known to increase when the hole is transferred away from the interface.^{21,176,177} This is not surprising as polythiophenes are often employed as efficient hole conductors in organic and solid-state solar cells.

In a comparative study of N3 analogs containing one chalcogen-substituted, 5-coordinate heteroarene, i.e., selenophene, thiophene, or furan (Scheme 3), it was shown that the extinction coefficient increased with the electropositivity and size of the heteroatom.¹⁷⁸ Calculations revealed that the extent of hole localization on the isothiocyanate ligands decreased as the extinction coefficient increased. The selenophene sensitizer showed great promise in DSSCs as the power-conversion efficiency was superior to that of Z907.

We recently found that employing bpy ligands bridged in the 3,3' positions by dithioline is a viable alternative to the more traditional and widely pursued approach of introducing conjugated groups in the 4 and 4' positions.¹⁶⁵ Substituent effects in this position are not as well documented as they sterically force the two pyridyl rings out of planarity, behavior that can decrease the stability of the compound. This issue is circumvented with bridging ligands but at the expense of opening up the N–Ru–N bite angle, thereby stabilizing LF states and increasing k_{nr} . Nevertheless, it was notable that this first-derivative, MLCT-dithioline compound, $[\text{Ru}(\text{BTL})(\text{deeb})_2]^{2+}$, where BTL is 9'-[4,5-bis-(cyanoethylthio)]-1,3-dithiol-2-ylidene]-4',5'-diazfluorene and deeb is 4,4'-(CO_2Et)₂-bpy (Scheme 3), had extinction coefficients for their lowest energy transitions that were comparable to the highest ever reported based on Ru^{II} (4,4'-disubstituted-bpy) compounds, $4.4 \times 10^4\text{ M}^{-1}\text{ cm}^{-1}$ at $\lambda_{\text{max}} = 470\text{ nm}$. In a similar absorption region, to the best of our knowledge, only four other efficient sensitizers exceed this value: $4.54 \times 10^4\text{ M}^{-1}\text{ cm}^{-1}$ at $\lambda_{\text{max}} = 471\text{ nm}$ (D16),¹⁵⁶ $7.85 \times 10^4\text{ M}^{-1}\text{ cm}^{-1}$ at $\lambda_{\text{max}} = 449\text{ nm}$ (D6),¹⁵⁶ $7.21 \times 10^4\text{ M}^{-1}\text{ cm}^{-1}$ at $\lambda_{\text{max}} = 442\text{ nm}$ (DCSC13),¹⁷⁹ and $5.43 \times 10^4\text{ M}^{-1}\text{ cm}^{-1}$ at $\lambda_{\text{max}} = 453\text{ nm}$ (C107).¹⁷¹ It should be noted that each of the former three sensitizers contained four phenylene and four vinylene groups on one bpy, while the latter



Scheme 3 The chemical structures of recently developed promising sensitizers with increased extinction coefficients, C101/C102/C105 and $\text{Ru}^{\text{II}}(\text{BTL})(\text{deeb})_2^{2+}$, or enhanced light-harvesting to the red without isothiocyanate ligands, $[\text{Os}^{\text{II}}(\text{tct})(\text{pyq})\text{Cl}]^{2+}$ and $[\text{Ru}^{\text{II}}(\text{dcb})_2(\text{dfpp})]^+$

contained four thiophene groups on one bpy. Part of the success with the dithioline-bpy ligands is that they themselves have IL absorption bands, in addition to the MLCT absorption bands, in the visible region. Regardless, their similar absorption, but with decreased conjugation, relative to the other four highly absorbing sensitizers was quite unexpected and intriguing.

An alternative strategy for increasing the LHE is to use nature's antenna effect, Figure 2.^{180–186} Multiple pigments that are suitably arranged can absorb light and vectorally transfer their energy to a central pigment that can then inject an electron into the semiconductor. If the additional pigments do not increase the footprint of the sensitizer on the semiconductor surface, the LHE could be enhanced. Indeed, the trinuclear Ru^{II} sensitizer utilized in the celebrated 1991 Nature paper¹³ had been previously designed in Italy to function as an antenna.¹⁸³

An issue with the *cis*- $\text{Ru}(\text{dcb})_2(\text{CN})_2$ group used as the energy-transfer acceptor and surface anchor is the *cis* geometry of the ambidentate cyano ligands. This resulted in a larger footprint as the number of Ru^{II} pigments was increased. In this regard, a *trans* geometry is more preferred, Figure 2.¹⁸⁷ The synthesis of molecules that function as antennae and their use in DSSCs continues to be an active area of research that may one day enable the efficient sensitization of planar semiconductor materials.¹⁸⁵

2.3.2 Broad Spectral Light-Harvesting

Given the usual values for the properties that determine the overall light absorbance of the TiO_2 -based DSSCs—i.e., the film thickness = 5–10 μm , roughness = 300–1000, porosity \approx 50%, and MLCT extinction coefficient \approx 15 000 $\text{M}^{-1} \text{cm}^{-1}$ —already \sim 90% of the incident light is absorbed at the absorption maximum. Larger extinction coefficients would allow for a more planar film to be employed, i.e., thinner or less roughened, that would most likely manifest itself as an enhancement of V_{oc} . However, the spectral sensitivity of the DSSC would hardly increase. Instead, advancements in LHE can be attained via increasing the region over which the sensitizer absorbs.

$\text{Ru}(\text{bpy})_3^{2+}$ and most other tris-heteroleptic d^6 polypyridyl compounds have redox and optical properties that are fairly insensitive to their environments.^{25,73} This is not the case when ammine or cyano ligands are present in compounds of the type $[\text{M}(\text{bpy}')(\text{X})_4]^{2-/2+}$ or $[\text{cis-}\text{M}(\text{bpy}')_2(\text{X})_2]^{0/2+}$, X = NC^- or NH_3 .²⁵ Outer-sphere interactions with the cyano ligands have a profound influence on $E^\circ(\text{Ru}^{\text{III/II}})$ and hence the color of the compound. For $[\text{Fe}(\text{bpy})(\text{CN})_4]^{2-}$ compounds, the excited-state reorganization energy in acetonitrile was found to be significantly larger on TiO_2 than in fluid solution ($\lambda = 0.32$ eV versus 0.10 eV, respectively).¹⁹⁰ This increased reorganization energy may be due to the restricted translational mobility of the semiconductor-bound iron compounds and

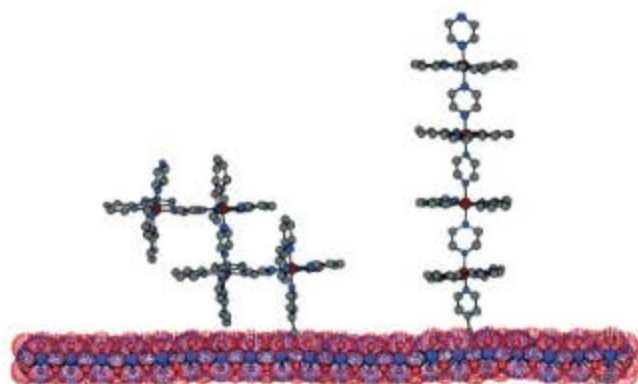


Figure 2 A scheme depicting an array of sensitizers bound to a planar TiO_2 surface consisting of *cis*- and *trans*- $[(\text{Ru}(\text{LL})_2(\text{pz}))_4(\text{ina})]^{8+}$ on the left and right, respectively, where pz is an ambidentate pyrazine ligand and ina is isonicotinic acid. The *trans* orientation enables increased absorbance, α , without changes in the projected footprint of the sensitizer. (Reproduced from Ref. 187. © Elsevier, 2008.)

the ambidentate $\text{Fe}^{\text{II}}\text{-CN-Ti}^{\text{IV}}$ linkages. $[\text{Ru}(\text{dcb})(\text{CN})_4]^{2-}$ is also highly solvatochromic¹⁹¹; the maximum of the lower energy MLCT band of $\text{Ru}(\text{dcb})(\text{CN})_4/\text{TiO}_2$ was observed at $450 \pm 10 \text{ nm}$ in tetrahydrofuran and at $500 \pm 20 \text{ nm}$ in dimethylformamide.¹⁹¹ The color change was due to a shift of $E^\circ(\text{Ru}^{\text{III/II}})$ with solvent. The compound maintained this solvatochromism upon attachment to mesoporous, nanocrystalline anatase (TiO_2) thin films although the magnitude of the effect decreased. Solvent tuning altered the spectral responses of DSSCs based on these materials in a predictable way and could in theory be used to enhance the LHE of solvatochromic sensitizers.

The position of attachment of the surface-anchoring carboxylic acid groups to bpy has also been examined for N3-like sensitizers of the type $\text{cis-Ru}(X,X'-(\text{COOH})_2\text{-bpy})_2(\text{NCS})_2$, where $X = 3, 4$, or 5 . When compared to the 4,4'-disubstituted bpy, 5,5' disubstitution resulted in a gain in red absorbance, because of a more favorable ligand reduction, but also decreased excited-state lifetime; taken together, this resulted in a smaller photocurrent but a similar V_{oc} .¹⁹² The decreased lifetime was rationalized based on the energy gap law,¹⁹² whereas the red enhancement was most likely due to increased conjugation from 5,5' disubstitution.¹³⁹ The lower photocurrent was also later found to be due to inefficient injection from the lower energy thexi state, as photocurrents on lower conduction-band edge SnO_2 were comparable regardless of the substitution position.¹⁹³ Similar decreases in photocurrent were seen for 5,5'-disubstituted N3-like compounds, vs their 4,4'-disubstituted version, containing the related NC^- and Cl^- nonchromophoric ligands.¹⁹² The same 5,5'- vs 4,4'-disubstitution trends in absorbance, ligand reduction, lifetime, and photocurrent were observed with N3-like sensitizers where the carboxylic acid functional groups were replaced with phosphonic acid groups, as well as those containing NC^- and Cl^- nonchromophoric ligands.¹⁹⁴

For 3,3'-disubstituted bpy, the photocurrent and V_{oc} were even worse, behavior attributed in part to lower maximum surface coverages.^{195,196} In addition, the steric hindrance induced by 3,3'-disubstitution led to a less-than-ideal bite angle for Ru^{II} chelation and thus a stabilization of the antibonding ligand-field states.^{28,83,197} This increased the k_{nr} values and results in a faster deactivation of the thexi state back to the ground state. Although difficult to quantify in such short-lived isothiocyanato-based compounds, similar photophysical studies with $\text{Ru}(\text{bpy})_2(\text{dcb})^{2+}$ with 3,3'- vs 4,4'-COOH-disubstitution have shown that the excited-state lifetime and quantum yield for emission decreased for compounds substituted in the 3,3' position,¹⁹⁸ implying that the nonradiative rate constant increased substantially.

A "black dye" that was discovered in the late 1990s is $[\text{Ru}(\text{tct})(\text{NCS})_3]^-$, where tct is 4,4', 4''-tricarboxylic acid-tpy, Scheme 2.⁵⁰ This compound extends the spectral sensitivity of DSSCs significantly toward the red relative to N3. However, the restricted tridentate nature of the terpyridyl ligand results in a far less than octahedral chelation range

that lowers the extinction coefficient throughout the visible region. Quantitative light harvesting at wavelengths near the absorption maximum of the black dye therefore requires thicker TiO_2 films than the $10\text{-}\mu\text{m}$ films typically used. The tradeoff in the effective bandgap and strength of light absorption over the absorbing regions for "black dye" vs N3 results in very similar power-conversion efficiencies in DSSCs.^{17,33,50,51}

Thummel and colleagues recently synthesized a series of N3 derivatives where the dcb ligands were replaced by 1,8-naphthyrid-2-yl ligands functionalized with binding groups.¹⁹⁹ These compounds extended the red-edge absorption beyond 800 nm , which is roughly 100 nm beyond that of N3. Also, Grätzel and colleagues, recently reported the synthesis and characterization of a *trans*- $\text{Ru}^{\text{II}}(\text{NCS})_2$ tetrapyrrolyl ligand.²⁰⁰ Interestingly, its absorption spectrum extended beyond 800 nm with an MLCT transition maximum near 637 nm . This first-generation sensitizer showed great promise with the proposed feasibility of introducing 4,4', 4'', 4'''-conjugated donor and acceptor groups in order to increase the extinction coefficient and charge-separated state lifetime.

Replacement of Ru^{II} with Os^{II} enhances the electric-dipole allowance of the ground state to ³MLCT absorbance in the near-infrared thereby providing better spectral overlap with the 1 sun, AM1.5 solar irradiance spectrum. Introduction of Os^{II} was calculated to result in up to three times more singlet character in the lower lying excited states,⁵⁷ which would thus make radiative recombination more spin allowed and thus faster.²⁰¹⁻²⁰⁴ Recently, Bignozzi and coworkers synthesized and investigated Os^{II} -based "black dye" analogs, i.e., each contained a tct ligand, in DSSCs (Scheme 3), where the absorbance was extended out to 1100 nm .¹⁸⁸ Although the photocurrent was $\sim 20\%$ inferior to that measured in champion DSSCs in the mid-visible region, the increased light absorbance in a rather intense region of the AM1.5 solar spectrum highlights promise for future sensitizers. This same group also synthesized $\text{Ru}(\text{dcb})_2\text{LL}$ compounds, where LL is a dioxolene, that can be oxidized to a semiquinone and then a quinone.²⁰⁵ Although reported for use in electrochromic devices, the absorption spectra of the semiquinone forms also extended to 1100 nm because of charge transfer to the semiquinone moiety.

Of note is that none of the sensitizers synthesized by Bignozzi and colleagues contained isothiocyanate ligands. This is desirable as the isothiocyanate ligands are thought to influence the stability of the sensitizer to the greatest extent.⁴⁸ It is for this reason that the newly synthesized and characterized cyclometallated $[\text{Ru}^{\text{II}}(\text{dcb})_2(\text{dfpp})]^+$ sensitizer, where dfpp^- is 2-(2,4-difluorophenyl)pyridine (Scheme 3), with a reported 10.1% light-to-electrical conversion efficiency under simulated 1 sun, AM1.5 conditions, is a significant advancement.¹⁸⁹ Interestingly, the calculated HOMO was almost entirely t_{2g} metal-centered, with a minor contribution from the dfpp^- ligand. Nevertheless, it was proposed that

the anionic nature of the carbon atom bound to the Ru helped to further stabilize the oxidized sensitizer such that the diffuse hole could be transferred away from the Ru toward the solution-based redox mediator. This is in line with the paradigm illustrated above where generally the most efficient sensitizers exhibit partial to entire hole transfer from Ru^{III} to a ligand: isothiocyanate, amine, thiophene, and now difluorophenyl groups.

Lastly, what if instead of tuning the optical properties of the surface-anchored sensitizer for broad solar harvesting, higher energy photons were absorbed by sensitizers in solution followed by efficient energy transfer to the surface-anchored sensitizers? This idea was recently realized by Grätzel and colleagues who dissolved an efficient organic energy relay dye in the solution electrolyte of a DSSC.²⁰⁶ The efficient light harvesting of the organic dye at shorter wavelengths, where surface-anchored Zn-phthalocyanines had a low absorptance, and overlap of its emission spectrum with the Zn-phthalocyanine's absorption spectrum resulted in efficient Förster energy transfer to the surface. This resulted in a 28% increase in i_{sc} and a 26% increase in η . It is interesting to note that energy transfer occurred even in the presence of a redox-active, red-colored electrolyte.

2.4 Sensitization by Pt, Cu, and Ir Polypyridyl Compounds

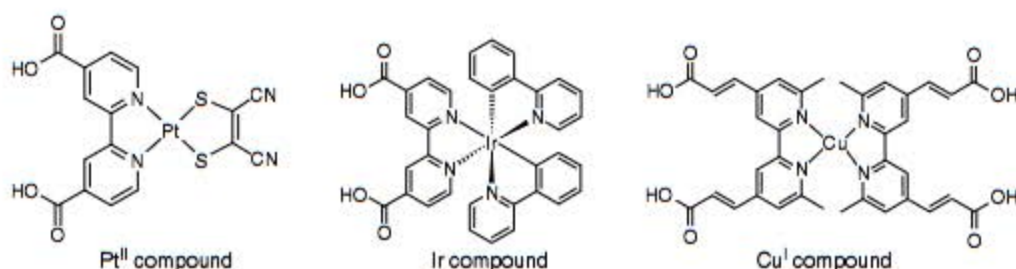
There now exists a large body of literature on the sensitization of TiO₂ by MLCT excited-states of octahedral, $d\pi^6$ low-spin Fe^{II}-, Ru^{II}-, Os^{II}-,²² and Re^I(CO)₃-polypyridyl compounds.^{138,207–214} There have also been some reports of MLCT sensitization by d^{10} Cu^I-polypyridyl compounds^{215–217} and square-planar d^8 compounds based on Pt^{II}^{218–224} that possesses MLCT-like excited states. A single report on d^5 Mn^{II}-tpy sensitizers has also appeared.^{225–227}

Durrant, Robertson, and colleagues investigated the effects of 3,3'- and 5,5'- vs 4,4'-(COOR)₂-bipyridine ligands (R = H is dcb and R = CH₂CH₃ is deeb) on square-planar [Pt^{II}(X,X'-(COOR)₂ bpy)(maleonitriledithiolate)]²⁺ sensitizers. The ground-state possesses partial localization of the highest molecular orbitals on the dithiolate ligand

(Scheme 4).²²³ It was found that disubstitution in the 5,5' or 3,3' position of deeb resulted in a 10–20-nm red-shifted absorption band, respectively, with first ligand reduction potentials being lowered by up to 130 mV. However, contrary to Ru^{II} 4,4'-disubstituted sensitizers, the extinction coefficients were approximately the same (to within 4%) regardless of the disubstitution position. Also of note was that 3,3'-disubstituted sensitized TiO₂ films had a longer lived charge-separated state, i.e., Pt^{III}/TiO₂(e⁻), and larger V_{oc} as compared to the 4,4'-disubstituted sensitized thin films. This was rationalized by EPR results. The 3,3'-disubstituted compound was far from planar²²⁸ and the HOMO was calculated to have much more dithiolate, and less Pt^{II} character. With 5,5'-disubstitution the location of orbital density was reversed.²²⁹

Although fundamentally important, current Ir^{III} sensitizers absorb far less visible light than those based on Ru^{II}, etc. Regardless, it has been shown that TiO₂ can be sensitized to ligand-to-ligand charge-transfer (LLCT) bands using cyclometallated, dcbq- or dcb-containing, octahedral Ir^{III} sensitizers, where dcbq is 4,4'-(COOH)₂-2,2'-biquinoline.²³¹ The novelty in these is that upon light excitation, a larger charge-separated-state distance is generated whereby the hole immediately resides on a ligand not bound to TiO₂. These first-generation sensitizers resulted in values for V_{oc} and FF that were similar to those for Ru(bpy)₂(dcb)²⁺. Grätzel and colleagues have since synthesized a cyclometallated Ir^{III} sensitizer with a chelating acac ligand whose i_{sc} is practically twofold larger, V_{oc} is over 150 mV larger, and η of 1.87% is almost three times higher.²³² In addition, Tian and coworkers reported a novel Ir^{III} sensitizer (Scheme 4) with a 2.86% light-to-electrical power-conversion efficiency.²³⁰

Cu^I-polypyridyl sensitizers represent an interesting alternative to the other sensitizers outlined in this article. They differ from other first-row transition-metal analogs, i.e., Fe^{II} and Mn^{II}, in that they possess long-lived MLCT excited states that can be explained by their filled d^{10} subshell.²³³ In addition, the rather low cost and high abundance of Cu relative to Re, Ru, Os, Ir, and Pt makes them commercially viable alternatives. Recently a 2.3% efficient DSSC was constructed with a Cu^I sensitizer containing two 4,4'-disubstituted conjugated bpy ligands (Scheme 4) for increased LHE.²¹⁵ The ligands also contained two methyl groups in the 6 and 6' positions to



Scheme 4 The chemical structures of recently developed non-Ru^{II}, Os^{II}, Fe^{II}, or Re^I sensitizers that exhibit significant photovoltaic performance when incorporated into a DSSC, based on Pt^{II}, Ir^{III}, and Cu^I

destabilize the Cu^{I} state via a Jahn–Teller distortion toward the expected more planar orientation in the excited state. Although η was four times lower than that for N719, the cost to manufacture such a DSSC was determined to be an order-of-magnitude lower. Chen and colleagues have shown by XANES and EXAFS that sterically similar $[\text{Cu}^{\text{I}}(2,9\text{-}(\text{CH}_3)_2\text{-phen})_2]^+$ adopts a four-coordinate, tetrahedral ground-state geometry but that the equilibrated excited state is five-coordinate, likely a distorted trigonal bipyramidal geometry.²³⁴

3 PHOTOINDUCED ELECTRON INJECTION

There are three means by which surface-anchored transition-metal sensitizers can achieve interfacial charge separation at anatase TiO_2 nanocrystalline interfaces (Figure 3): (a) metal-to-particle charge transfer (MPCT) sensitization where light absorption promotes an electron from the metal d orbitals directly to TiO_2 ; (b) excited-state sensitization, where an electronically excited compound transfers an electron to TiO_2 ; (c) reduced sensitizer injection that results from reductive quenching of the excited state by a donor, followed by electron transfer from the reduced sensitizer to TiO_2 . What follows is a discussion of each from a brief historical perspective accompanied by recent advances and techniques to monitor/verify such mechanisms of sensitization.

3.1 Direct Metal-to-Particle Charge Transfer

There is a less well-studied mechanism of photoinduced electron injection that has been observed for metal-cyano compounds anchored to TiO_2 and is termed MPCT.²³⁷ This mechanism is apparent based on the observations that (i) sensitizer– TiO_2 reactions yield a new absorption band that is not a result of Bronsted acid–base chemistry;

and (ii) light excitation into said absorption band results in immediate formation of $\text{S}^+/\text{TiO}_2(\text{e}^-)$. A useful feature of this sensitization mechanism is that the injection yield is by definition unity on an absorbed photon basis as electron transfer to TiO_2 is one in the same process. This is in contrast to excited-state injection, whose injection efficiency has been shown to be a function of the pH, ionic strength, excitation wavelength, and temperature.²³⁸ MPCT absorption bands were observed for the first time upon binding $\text{M}(\text{CN})_x^{4-}$ compounds to TiO_2 nanocrystallites ($\text{M} = \text{Fe}^{\text{II}}$, Ru^{II} , Os^{II} , Re^{III} , Mo^{IV} , W^{IV}).^{239,240} Some of these adducts extended the visible light photoresponse of TiO_2 beyond 700 nm. Hupp *et al.* discovered that the resonance Raman spectrum of $[\text{Fe}(\text{CN})_6]^{4-}/\text{TiO}_2$ colloids exhibited the coupling of ten vibrational modes to MPCT, three of which were surface modes.^{241,242} Jortner and colleagues have previously described an applicable theoretical model for describing such multimode electron transfer^{129,243–247}; however, the coupling of multiple surface modes to interfacial electron transfer was unprecedented experimentally.

Intervalence charge-transfer (IVCT) absorption bands are known for mixed-valence $\text{Fe}^{\text{II}}\text{-CN-Ti}^{\text{IV}}$ cyano compounds and are speculated to be related to MPCT bands in $[\text{Fe}(\text{CN})_6]^{4-}/\text{TiO}_2$.²⁴⁸ From this, an interesting question arises: does light absorption promote an electron from Fe^{II} to an adjacent Ti^{IV} site or to a Ti^{IV} site within the interior of a TiO_2 nanocrystallite? This question was addressed by electroabsorption (Stark) spectroscopy. Previously, Boxer and Oh reported Stark spectra of $\text{Ru}(\text{diimine})_3^{2+}$ compounds⁷⁵ and others have since studied related Ru^{II} compounds.^{249–251} Stark spectra are generally obtained in amorphous solid-state media with the application of a unidirectional, oscillating electric field relative to the laboratory frame-of-reference. The electric field induces changes in the extinction coefficient and energetic shifts in absorption and/or photoluminescence maxima.^{252,253} Spectral modeling allows for the assignment

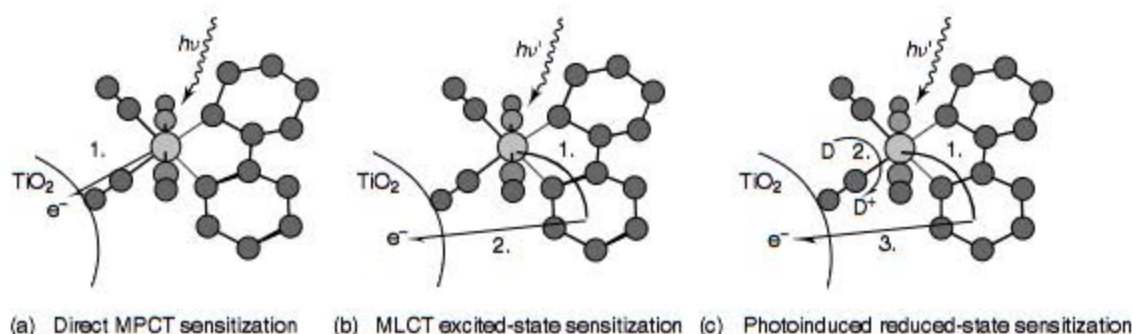


Figure 3 Ball-and-stick models for $[\text{Fe}(\text{bpy})(\text{CN})_4]^{2-}/\text{TiO}_2$ depicting the three possible mechanisms for photoinduced electron injection into TiO_2 : (a) direct, metal-to-particle charge-transfer (MPCT) sensitization; (b) excited-state injection, sensitization by means of a metal-to-ligand charge-transfer (MLCT) excitation followed by excited-state electron injection; (c) reduced-state sensitization, sensitizer injection that results from reductive quenching of the excited state with a donor, D, and then dark electron injection from the reduced sensitizer. To the best of our knowledge, only the former two have been reported in the literature for iron polypyridyl sensitizers. (Reproduced from Ref. 235. and Ref. 236. © American Chemical Society, 2000 and 2003.)

of these shifts as alterations in the transition moment (via the transition polarizability and hyperpolarizability) or peak position (via the difference dipole moment and polarizability), and from these data the charge-transfer dipole moment and distance can be determined via the Liptay treatment.²⁴⁸

For $[\text{Fe}(\text{CN})_6]^{4-}/\text{TiO}_2$, the charge-transfer distance was determined to be 5.3 Å based on the dipole moment change.²⁴⁸ This was within error of the distance from Fe^{II} to Ti^{IV} using molecular modeling on $[(\text{CN})_5\text{Fe}^{\text{II}}-\text{CN}-\text{Ti}^{\text{IV}}(\text{H}_2\text{O})_4\text{O}]^{2-}$, although the distance was slightly larger than empirical values measured for related $\text{Fe}^{\text{II}}-\text{CN}-\text{M}$ compounds. Similar values were found for Ru^{II} -, Mo^{IV} -, and W^{IV} -cyano compounds on TiO_2 and support the hypothesis that MPCT bands represent electronic transitions to an orbital on a Ti^{IV} atom that is in close proximity to the bound cyano nitrogen atom.²⁵⁴ In addition, on the basis of the above calculated distance and the fact that the unbound cyano ligands were even further from the surface than the metal center, identification of the process as MPCT and not ligand-to-metal charge transfer (LMCT), i.e. from a free NC^- to Ti^{IV} , was substantiated.

Some organic molecules are also known to display direct, ligand-to-particle charge-transfer (LPCT) absorption bands when anchored to TiO_2 , the most well known being catechol.^{238,255} Electroabsorption techniques are also useful in these cases; although most studies concluded that the excitation bands are LPCT in nature,^{256,257} excited-state injection was deduced for a select few sensitizers, i.e. eosin Y and alizarin.^{256,258} For this reason, a catechol group was covalently incorporated into tpy-^{226,259} and bpy-based^{260–262} ligands as a strong anchoring group for transition-metal, coordination-compound sensitizers. Two Os^{II} ²⁶⁰ and a *cis*- $\text{Ru}^{\text{II}}(\text{NCS})_2$ -polypyridyl²⁶² compounds with bpy-catechol derivatives for surface attachment were recently reported that extended the visible light absorption to beyond 750 nm. Absorption features assigned as direct catechol \rightarrow particle LPCT on TiO_2 , ZrO_2 and MLCT were observed. The observation of a direct charge-transfer band in the visible region was unexpected for ZrO_2 due to its large bandgap and the unfavorable reduction of $\text{Zr}(\text{IV})$.

3.2 Excited-State Injection

After light absorption, the MLCT excited state of the sensitizer may inject an electron into the anatase nanocrystallite, a process also referred to as interfacial charge separation. For sensitizers like N3, light absorption formally promotes an electron from the Ru^{II} metal center to a dcB ligand that is directly bound to the semiconductor surface. Therefore, excited-state charge separation occurs from the π^* orbitals of the organic ligand to the acceptor states in TiO_2 . There is now an overwhelming body of data that indicates that such charge separation occurs on a femto- to picosecond timescale. Experimentally, ultrafast

spectroscopists have all found that excited-state electron injection into TiO_2 is nonexponential, behavior attributed to the surface heterogeneity of TiO_2 and its density of acceptor states (DOS), distributions of sensitizer binding modes, strengths, and interactions, and multiple ultrafast injection processes occurring from various states in the thermal relaxation pathway, i.e., Franck–Condon singlet injection, internally converted singlet injection, intersystem crossing to the ³MLCT thexi state(s) followed by injection. This has been thoroughly reviewed for both organic and transition-metal coordination compounds bound to semiconductor metal oxides.^{212,263,264} While the explanations given to rationalize the complex kinetics observed for excited-state injection for Ru^{II} sensitizers are often reasonable, satisfactory mechanistic models are still lacking.

It has been suggested that ultrafast, interfacial charge separation, following light absorption, occurs from the Franck–Condon excited state. Evidence for room-temperature injection occurring with a lifetime faster than a molecular vibration, i.e., $k_{\text{B}}T/h = 1.6 \times 10^{-13} \text{ s} = 160 \text{ fs}$,^{265,266} eludes this phenomenon.^{207,208,212,213,263,264,267–278} This would imply that injection occurs before thermal relaxation of the molecular excited state. Willig and coworkers found that excited-state electron injection from N3^* into TiO_2 occurred in $<25 \text{ fs}$ under ultrahigh vacuum conditions.²⁷¹ The process therefore did not involve redistribution of vibrational excitation energy by exchange with phonons in the solid, and thus was entirely different from the weak-electronic-coupling case of Marcus–Levich–Jortner–Gerischer-type electron transfer.^{279–284} The finite reaction time for injection ruled out direct excitation of an electron from the Ru^{II} metal center to the semiconductor, yet the sub-100 fs rise-time implied vibrational wave packet motion-induced electron transfer. A detailed analysis of theoretical and empirical results supporting these conclusions using a perylene sensitizer can be found elsewhere.^{270,285–289} The quantitative, ultrafast excited-state electron injection reported for $\text{N3}/\text{TiO}_2$ under ultrahigh vacuum conditions was not always observed when the sensitized thin films were placed in organic solvents or electrolytes. Under such conditions, injection was nonexponential and occurred on the femtosecond to hundreds-of-picoseconds timescale.

Sundström and colleagues have recently further investigated the ultrafast injection of N3 into TiO_2 by femtosecond transient-absorption anisotropy techniques.²⁹⁰ They reported that for N3, the fast, $<100 \text{ fs}$, injection component occurred from the ¹MLCT excited state whereas the slower, picosecond injection process proceeded from the ³MLCT excited state. Anisotropy measurements indicated that the slower injection was due to interligand electron transfer from a free nonsurface-anchored dcB ligand to one that was in intimate contact with TiO_2 . This interligand hopping could be altered by chemical modification of the ligands and by solvent environment and was the rate-limiting step for injection from the ³MLCT thexi state. They also

showed that excited-state electron injection is slowed and gradually becomes less efficient as the excitation wavelength moves to the red of the absorption maximum.²⁷⁶ This was proposed to be due to direct ³MLCT population and thermal electron-transfer injection from the differences in population of the thexi states. These same authors also determined that by varying the method of TiO₂ film preparation, both rate constants for the biphasic injection kinetics for N3* into TiO₂ were directly related to the degree of TiO₂ crystallinity.²⁷²

Lian and coworkers found by femtosecond time-resolved infrared (TRIR) spectroscopy that excited-state electron injection into TiO₂ was biphasic for three [*cis*-Ru(dcb)₂(X)₂]^{0,0.2+} compounds (X = NCS, X = CN, or (X)₂ = dcb).²⁶⁷ The rate of the slower component was directly related to the sensitizer excited-state reduction potential. No noticeable changes were apparent for the fast component within the time resolution of the measurement, i.e., ~200 fs. Later, the same group compared the injection dependence for N3 sensitizers containing carboxylic acid or phosphonic acid linkers.²¹³ The amplitude of the fast component was larger for N3, which suggested stronger electronic coupling between the carboxylate and the TiO₂. However, the slow component for the phosphonated version of N3 was faster, which was assigned to injection from the relaxed ³MLCT thexi state and attributed to the slightly more favorable energetics for injection from the bpy-PO₃H₂ group orbitals. This led to more efficient excited-state injection from the ³MLCT of the phosphonated version of N3.

Durrant and coworkers found that an N3 sensitizer in which two of the carboxylic acid groups were deprotonated, N719, prior to sensitizer surface binding had a 30-fold slower rate of injection than N3*.²⁹¹ In a followup paper, it was determined that the concentration of potential-determining ions, e.g., H⁺ and Li⁺,^{21,107} and factors that influence the TiO₂ DOS resulted in N719's less-efficient excited-state injection.²⁹² After performing multiple washings of the N3/TiO₂ films in neat ethanol, the injection rates were found to be very similar to those of N719/TiO₂ thin films.²⁹¹ It was suggested that the labile protons from the carboxylic-acid binding groups of N3 had lowered the DOS in TiO₂ and promoted more favorable energetics for injection. To control this variable, Lian and coworkers pretreated N3/TiO₂ thin films for one day in aqueous buffer solutions at pH 2, 4, 6, or 8.²⁶⁷ After removing weakly bound and desorbed sensitizers, the biphasic kinetics and injection yields were found to be pH dependent. As the pH was raised from 2 to 8, there was a decrease in the rate of the slower component to injection, the ratio of the slower-to-faster components to injection, and the injection yield. Such behavior is consistent with the expected Nernstian shift of the TiO₂ conduction-band edge toward the vacuum level as the pH is raised.

Grätzel and coworkers reported that the slower picosecond components for excited-state electron injection could be removed with low concentration or sonicated dyeing solution, or by employing a lower surface-coverage thin

film.^{293,294} Under such conditions, only an ultrafast component (<20 fs) for injection remained. In support of this, Piotrowiak and coworkers found that dialysis of sensitized TiO₂ colloids resulted in much shorter excited-state lifetimes as measured by time-correlated single photon counting.²⁹⁵ However, in this case multiexponential kinetics were required to adequately fit the observed data.

The multiphasic character of the picosecond dynamics of excited-state electron injection into TiO₂ alludes to the consideration that at least some injection is occurring from a thexi state. This state, which can be described by a Boltzmann population, may exhibit behavior typical of nonadiabatic thermal electron transfer and/or electron tunneling. (The latter is clearly evident by temperature- and distance-dependent studies.) At low temperatures, a constant, nonzero rate for injection may persist while the room-temperature injection rate ought to exhibit an exponential dependence on distance, given that the inaccessible LUMOs are of similar energy:

$$A = A_0 \exp[-\beta \cdot x] \quad (5)$$

where β is the dampening factor. A dampening factor, $\beta = 1.0 \text{ \AA}^{-1}$, is often indicative of saturated hydrocarbon, through-bond superexchange tunneling behavior;^{296–299} in general, larger values imply at least partial through-space character, while smaller ones are associated with tunneling through conjugated π systems.²⁹⁹

An early study demonstrated that efficient excited-state electron injection did occur from sensitizers of the general type Ru(dmb)₂(L)²⁺, where dmb is 4,4'-(CH₃)₂-bpy and L contained unconjugated -(CH₂)_x-linkers between the Ru-chelating bpy moiety and one carboxylic acid group.³⁰⁰ In this same study, the acetylacetonate (acac) linker was first employed to bind sensitizers to TiO₂. Recently, the acac ligand was again employed for a proposed water oxidation sensitizer-catalyst bound to TiO₂.²²⁵ Acac is known to bind hard Ti^{IV/III} strongly and is very stable toward hydrolysis and oxidation in various aqueous pH conditions and in the presence of strongly oxidizing environments, respectively.²²⁵ For these Mn^{II}(tpy-acac)-based sensitizers, and others with catechol-containing binding groups, ultrafast injection, which was proposed based on theoretical calculations, was confirmed via femtosecond terahertz time-domain (THz-TD) spectroscopy.^{225,226} THz-TD spectroscopy allows one to spectroscopically monitor free conduction-band electrons as they have a large absorption cross section in the THz frequency domain.^{301–303} The novelty of this technique is that electron diffusion and drift can be monitored by a noncontact, nonelectrochemical means. The same research group was also successful in binding a dinuclear Mn^{IV,III}(tpy)-based sensitizer-catalyst through a μ -oxo bridge from the Mn^{IV} to a Ti^{IV} on TiO₂.²²⁷

A more systematic distance-dependent study was later reported using three Re^I(bpy)-(CH₂)_{2n}-(COOH)₂(CO)₃ Cl (*n* = 0, 1, 3) sensitizers, where it was shown that ultrafast

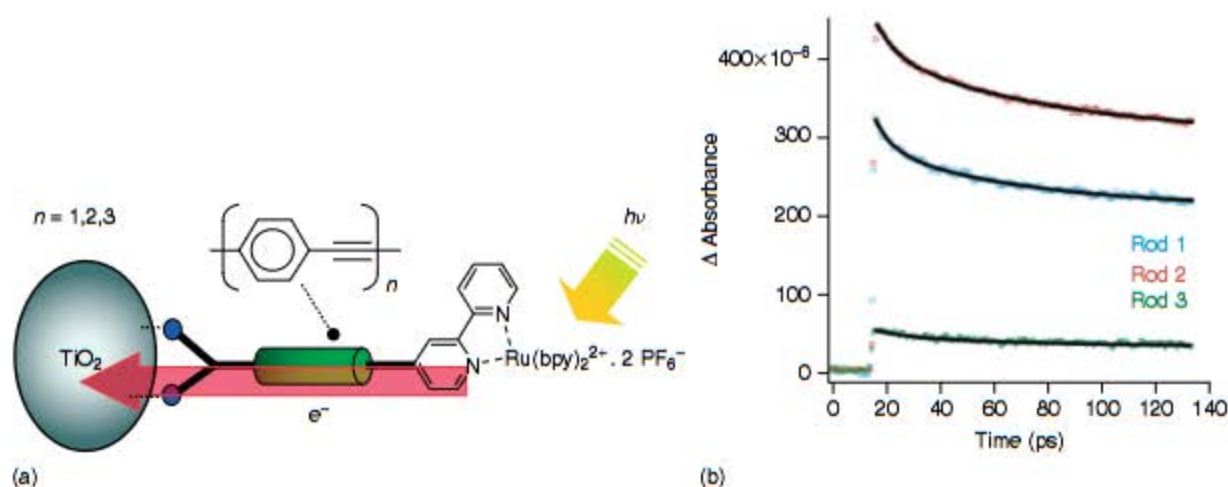


Figure 4 (a) A schematic depicting a rigid-rod, $\text{Ru}(\text{bpy})_3^{2+}$ -based sensitizer bound to a TiO_2 nanocrystallite under light excitation. (b) Single-wavelength kinetic absorption difference spectra of these TiO_2 -bound sensitizers containing rods of oligo(phenylene-ethynylene) linkers ($n = 1, 2, 3$). Although the injection yields were not distance dependent, the rates were inversely related to n . (Reproduced from Ref. 310. © American Chemical Society, 2007.)

injection into TiO_2 did not occur when electronic coupling between the surface-bound ligand and the TiO_2 surface was removed by unconjugated methylene spacers, i.e., when $n = 1$ or 3.^{207,208} For the same two sensitizers, the slower picosecond injection process could be successfully fit to a stretched exponential and the distance dependence of the injection rate could be qualitatively modeled by equation (5) using $\beta = 1.2$ for each C–C bond, indicative of nonadiabatic electron transfer. The >200-fold increase in injection rate from $n = 1$ to $n = 0$ could not be fit to such a model and was explained as adiabatic electron transfer because of a greatly increased strong electronic coupling from the lack of an unconjugated spacer moiety. Detailed comparison of the $n = 0$ with the $n = 1$ or 3 compounds was complicated by the fact that the $n = 0$ compound had significantly different photophysical and redox properties.

With three phosphonated, “black dye”-like compounds of the form $[\text{Ru}(4'\text{-PO}_3^{2-}\text{-(Ph)}_n\text{-tpy})(\text{NCS})_3]^{3-}$ ($n = 0, 1, 2$), the distance dependence of excited-state electron injection through conjugated linkers was studied.³⁰⁴ Femtosecond pump–probe transient absorption measurements revealed that the rate of each phase of an observed biphasic injection process was dependent on distance. The fast picosecond component fit nicely to an exponential distance-dependent model, equation (5), with damping factor, $\beta = 0.19 \text{ \AA}^{-1}$, while the slower component for injection was assumed to be because of injection from loosely bound or aggregated sensitizers. As this damping factor was much smaller than typical ones obtained for donor–bridge–acceptor systems in solution, it was proposed that nuclear reorganization played a negligible role in injection, a hypothesis supported by theoretical calculations.

Some novel ligand architectures that could be used to study the distance dependence for injection rates/

yields have recently been employed.³⁰⁵ Galoppini and coworkers often employ sensitizers with either a rigid-rod or tripodal linker containing at least one functional group to bind to TiO_2 .^{306–309} These have predominantly consisted of oligo(phenylene-ethynylene) linkers (E-Ph) and 1,3,5,7-tetraphenyladamantane (Ad-Tripod), respectively. A comparative excited-state electron-injection study of three rigid-rod, $\text{Ru}(\text{bpy})_3^{2+}$ -based sensitizer compounds was reported, Figure 4(a).³¹⁰ It was found that a monotonic decrease in injection rate occurred as the number of linkers was increased with a damping factor, $\beta = 0.04 \text{ \AA}^{-1}$, for both a slow and a fast injection component. A similar study on SnO_2 resulted in a value of $\sim 0.8 \text{ \AA}^{-1}$ and theoretical values were $>0.4 \text{ \AA}^{-1}$.³¹¹ Although this small distance dependence agrees rather well with the conclusions from the phosphonated compounds, these results were further complicated by the lack of the expected similar trend in injection yields, where the middle-length spacer was found to inject best, Figure 4(b). By linking the ethynylene-bpy group to the meta position of a phenyl ring, it was recently shown that the extinction coefficient was roughly half that of the para isomer.³¹² Nevertheless, the photoinduced injection yields remained independent of the position of covalent attachment, i.e., meta or para. With the use of a phosphonated-tpy ligand with and without an intervening thienyl group chelating $\text{Ru}^{\text{II}}(4'\text{-R-tpy})$, where $\text{R} = \text{H}$ or 4-bromo-2,5-dimethylphenyl, as expected the extinction coefficients practically doubled and the band red-shifted with increased conjugation.³¹³ However, contrary to what may be expected, introduction of the thienyl group between a tpy ligand and the surface-anchoring phosphonic acid group led to a faster injection rate and more favorable photoelectrochemical properties when compared to the compounds lacking the thienyl group.

In dichloromethane electrolytes with TBAI/I₂, V_{oc} values were found to be directly related to the number of phenylene-ethynylene spacer groups.^{306,307,314} As ion pairing was previously shown to occur in dichloromethane with [Ru(bpy)₂(deeb)]²⁺ and I⁻ or I₃⁻,^{315–317} it was proposed that recombination may occur with acceptors further from the TiO₂ surface for the longer tripodal sensitizers. The V_{oc} data support this distance-dependent recombination over three decades of irradiance.

The dcb ligand is structurally the same as two ina, i.e., isonicotinic acid, ligands connected in the 2 and 2' positions. The extra covalent bond in the dcb ligand increases the overall conjugation and thus lowers its LUMO energy. A comparative study of two heteroleptic Ru^{II} compounds, one with a dcb ligand and the other with two ina ligands, was undertaken; the distance dependence of injection was comparatively studied by investigating the effect of remote versus adjacent excited-state electron injection.³¹⁸ Both compounds exhibited a similar pH-dependent injection at pH > 2 even though the thexi state of the latter compound contained an electron localized on a ligand that was not bound to the TiO₂ surface. The efficient injection from sensitizers with an ina ligand has been observed for Re(bpy)(CO)₃(ina)⁺ as well.²⁰⁹

The distance dependence of excited-state injection was investigated by yet another means: core-shell architectures,^{319–323} with an insulating Al₂O₃ shell with 0.6–6 nm thickness conformally deposited on 20 nm TiO₂ nanocrystals, Figure 5(a).³⁰⁴ As electron tunneling is a factor of distance and barrier height, this architecture allowed solely the distance to be altered. These studies were somewhat hampered by ultrafast injection thought to occur at pinhole imperfections in the Al₂O₃ shell. Neglecting this ultrafast injection, it was shown that the picosecond biphasic nature of injection resulted in $\beta = 0.11 \text{ \AA}^{-1}$ and 0.04 \AA^{-1} for the fast and slow components,

respectively, Figure 5(b). As the barrier to the conduction band of bulk, crystalline Al₂O₃ is very large, dampening factors over an order-of-magnitude larger were expected. It was proposed that the electronic structure of thin alumina layers differed from that of bulk Al₂O₃.³²⁴

3.3 Reduced Sensitizer Injection

An alternative mechanism exists for photoinduced electron injection wherein the excited state is reduced prior to interfacial charge separation, Figure 3(c). This results in injection from a nonelectronically excited sensitizer. For this reason, DSSCs operating under this mechanism are appropriately termed *regenerative galvanic cells* as injection is a dark, thermodynamically favorable process.³²⁵ This alternative sensitization method has been called *supersensitization*³²⁶; the donor is termed the *supersensitizer* because of its requirement in achieving effective overall sensitization.³²⁷ A unique aspect of this mechanism is that the oxidized form of the sensitizer is never generated. Therefore, it may be particularly well suited for sensitizers that are unstable in their oxidized forms, like N3,^{117,194,328–330} or Pt^{II} sensitizers. An advantage with MLCT excited states is that the reduced form of the sensitizer is a stronger reductant than the MLCT excited state, typically by 200 to 400 mV.

Kirsch-De Mesmaeker and coworkers first reported compelling evidence for reduced ruthenium sensitizers transferring electrons to SnO₂ electrodes.³²⁷ The coincidence of Stern-Volmer constants measured by analysis of the photocurrent enhancement and photoluminescence quenching with hydroquinone donors left little doubt as to the sensitization mechanism. Additional spectroscopic evidence for photoinduced electron injection by reduced sensitizers was reported for Ru(bpy)₂(dcb)/TiO₂

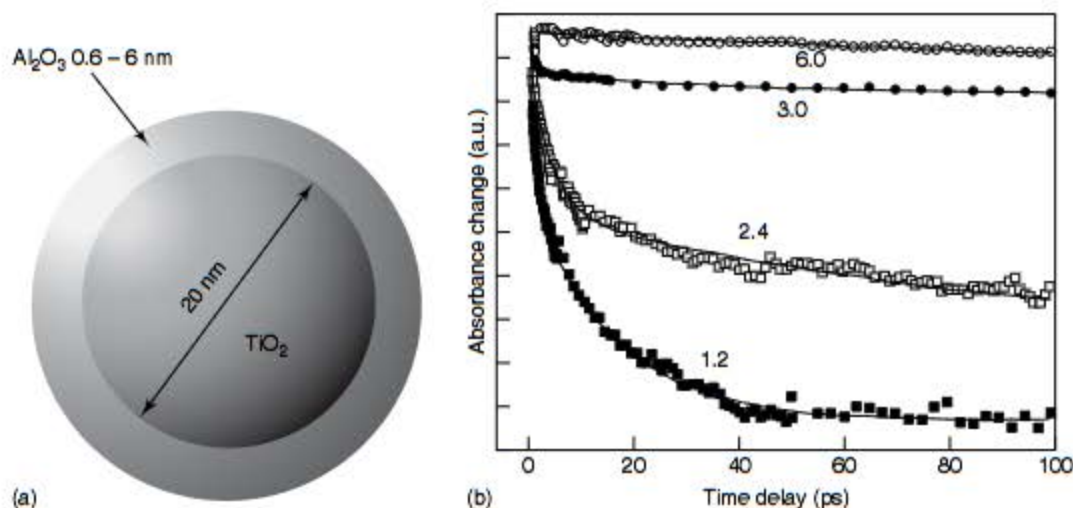


Figure 5 (a) A diagram of a TiO₂/Al₂O₃ core-shell nanoparticle. (b) Single-wavelength kinetic absorption difference spectra for Ru(4'-PO₃²⁻-tpy)(NCS)₃/TiO₂ thin films illustrating that the rate of injection was inversely related to the size of the Al₂O₃ overlayer. The Al₂O₃ overlayers' thickness in nanometers is shown. (Reproduced with permission from Ref. 304. © SPIE, 2006.)

in 0.1 M TBAClO₄ acetonitrile electrolyte with organic phenothiazine (PTZ) electron donors.³³¹ Nanosecond transient absorption data demonstrated the rapid formation of TiO₂(e⁻)/PTZ⁺, while in the absence of PTZ there was little-to-no evidence for injection. Injection was rate limited by diffusional quenching of the MLCT excited state, so the Ru^{II}(dcb⁻)(bpy)₂/TiO₂ intermediate was not directly observed.

An interesting case of reduced-sensitizer electron injection was reported with the bimetallic sensitizer (bpy)₂Ru^{II}-BL-Rh^{III}(dcb)₂/TiO₂, BL = 1,2-bis[4-(4'-methyl-bpy)] ethane.³³² About two-thirds of the MLCT excited states of the ruthenium chromophore were quenched by electron transfer to the Rh(dcb)₂ group to form a (bpy)₂Ru^{III}-BL-Rh^{II}(dcb)₂/TiO₂ charge-separated state while the remaining directly injected an electron into TiO₂.^b This observed branching ratio was proposed to result from different surface orientations. Approximately 40% of the intramolecular, charge-separated state, (bpy)₂Ru^{III}-BL-Rh^{II}(dcb)₂/TiO₂, injected electrons into TiO₂ to form (bpy)₂Ru^{III}-BL-Rh^{III}(dcb)₂/TiO₂(e⁻), while the remaining underwent back-electron transfer to form ground-state products. The Ru^{III}* injection occurred within the time resolution of the instrument, i.e., <10 ns, while injection from Rh^{II} occurred in <100 ns following light excitation.

In order to realize efficient DSSCs that operate by this mechanism, sensitizers that are potent photo-oxidants must be utilized. This stems from that fact that the I₃⁻/I⁻ redox mediator is the only redox mediator that yields high light-to-electrical power-conversion efficiencies and E°(I[•]/I⁻) is rather positive. Ru^{II} sensitizers that are strong excited-state oxidants can be prepared with ligands such as 2,2'-bipyrazine (bpz).³³³ For example, the E°(Ru^{2+*/+}) of [Ru(bpz)₂(deeb)]²⁺ was found to be greater than +1.0 V vs SCE³³⁴⁻³³⁶ (+1.24 V vs NHE³³⁷). While the excited state of this and related sensitizers were found to be efficiently quenched by iodide or phenothiazine donors, the reduced form of the compound that resulted, Ru^{II}(bpz)(bpz⁻)(deeb)/TiO₂, did not inject electrons into TiO₂.²³⁶ In fact, very similar transient absorption features were observed in solution, on TiO₂, and on insulating ZrO₂. Some improvement was observed when the semiconductor was changed to SnO₂, but the injection yields remained poor.³³⁴

Another interesting case of reductive quenching of an excited state that did not result in electron injection was reported for sensitized films in the presence of a high concentration of 1-propyl-3-methylimidazolium iodide.³³⁸ A new transient spectroscopic feature was discovered that was attributed to the reduced sensitizer, which presumably formed by reductive quenching of the excited state by iodide. The decay of this species was attributed to a back-reaction with I₃⁻ with a half-life of ~1 ms, yet it is not clear why this state did not inject electrons into TiO₂.

4 SENSITIZER REGENERATION

4.1 Intramolecular Regeneration

Considerable effort has been set forth to regenerate the oxidized sensitizer by intramolecular electron transfer. This could be considered a "hole" transfer reaction that translates the oxidizing equivalent away from the Ru^{III} metal center and, ideally, the TiO₂ surface. Very similar mechanisms are well known in the field of supramolecular photochemistry.^{180,186,339,340} To our knowledge, Wrighton and coworkers were the first to extend this photochemistry to a semiconductor electrode.³⁴¹ The ability to control hole-transfer reactions at the molecular level is important for many classes of solar cells. One can envision future-generation DSSCs where multiple hole-transfer steps translate the oxidizing equivalent from the sensitized interface directly to a counter electrode, thereby eliminating the need for the solution-based redox mediators, i.e., I₃⁻/I⁻, that are required today.

In practice, there are at least two ways in which a D⁺-Ru^{II}/TiO₂(e⁻) interfacial charge-separated state can be photogenerated. They correspond to the excited-state and reduced-state injection mechanisms described in Sections 3.2 and 3.3, respectively. Since the MLCT excited state is a weaker oxidant than is the oxidized state, it is possible to design dyads with weak donors that only react by the first mechanism, while with potent electron donors the mechanistic pathway is dependent on the relative rate constants for excited-state electron injection and intramolecular charge separation. Since excited-state injection is often found to be ultrafast, the first mechanism probably predominates even though it has not always been unambiguously identified.

It should be pointed out that in some regards N3/TiO₂ is thought to undergo a similar intramolecular, charge-transfer process. As mentioned previously, calculations show considerable hole density on the sulfur atom of the isothiocyanate ligands for N3⁺.¹⁰¹⁻¹⁰³ It is also known from electrochemical measurements that there are two closely spaced oxidations for N3, the first is predominantly metal based while the second is mainly isothiocyanate based. Therefore, in the charge-separated state, N3⁺/TiO₂(e⁻), there is likely some partial "hole transfer" from the Ru^{III} metal center to the isothiocyanate ligands. In most of the examples discussed below, the electronic coupling between the electron donor and the Ru metal center is much weaker, giving rise to complete hole hopping rather than partial charge transfer.

4.1.1 Organic Donors

Bignozzi and coworkers reported the first time-resolved spectroscopic studies of intramolecular sensitizer regeneration.^{342,343} The dyad was [Ru(4-CH₃,4'-CH₂-PTZ-bpy)(dcb)₂]²⁺, where PTZ was the organic donor phenothiazine, anchored to TiO₂ thin films and immersed in acetonitrile. In fluid methanol solution, visible-light excitation

of this dyad resulted in the creation of the MLCT excited state that was rapidly quenched by electron transfer from the PTZ group. Reductive excited-state quenching was moderately exergonic (<0.25 eV) and occurred with a rate constant of $\sim 2.5 \times 10^8$ s $^{-1}$ in methanol. When the dyad was attached to TiO₂, MLCT excitation resulted in a new charge-separated state with an electron in TiO₂ and an oxidized PTZ group, abbreviated PTZ⁺-Ru^{II}/TiO₂(e⁻). It was not possible to determine the mechanism of charge separation, yet the authors speculated that after excited-state electron injection, electron transfer from PTZ to the Ru^{III} metal center ($-\Delta G \sim 0.36$ eV) produced the charge-separated state, PTZ⁺-Ru^{II}/TiO₂(e⁻). Translation of the "hole" from the Ru^{III} metal center to the pendant PTZ moiety inhibited charge recombination by about three orders of magnitude, and a significant increase in V_{oc} resulted. Since that time, a number of dyads have been attached to TiO₂ and are discussed further below; a commonly utilized electron donor is a triarylamine moiety, NAr₃.³⁴⁴⁻³⁴⁶

After pulsed-light excitation of similar compounds, some remarkably long-lived charge-separated states were observed possessing half-lives of over half a second, as shown schematically in Figure 6(a).¹⁷⁷ Durrant, Haque, and colleagues increased this lifetime by employing Ru(4,4'-(R)₂-bpy)(dcb)₂/TiO₂ systems, where R contained one triphenylamine group, two triphenylamine groups, or a poly(vinyl-NAr₃) group of about 100 units in length, Figure 6(b).¹⁷⁶ The introduction of about 100 amines increased the half-life of the charge-separated state to over 4 s, as compared to 350 μ s and 5 ms for the other two, respectively. The kinetics for excited-state electron injection and subsequent hole transfer from the Ru^{III} metal center to the bound NAr₃ occurred within the instrument response

time, i.e. ~ 10 ns. Durrant and colleagues also studied Ru(4,4'-(R)₂-bpy)(dcb)₂/TiO₂ thin films, where R contained oligo(triphenylamine) groups at varying distances from the Ru^{II} metal center, to determine the distance dependence for back-electron transfer.^{176,177,347-349} Collectively, these data provided strong evidence that back-electron transfer rates displayed an exponential dependence on spatial separation with a dampening factor, $\beta = 0.95 \pm 0.2$ Å $^{-1}$.^{350,351}

N3 derivatives, *cis*-Ru(4,4'-(R)₂-bpy)(dcb)(NCS)₂, R = triphenylamine or CH₃, bound to TiO₂ thin films were examined in order to study the effects of Ru^{III} hole transfer to a triphenylamine moiety.¹⁶⁴ Unexpectedly, both sensitizers exhibited similar transient features with no spectral evidence for hole transfer to the amine donor. The photoelectrochemical properties of the two sensitized thin-film electrodes differed significantly, and a much larger V_{oc} value was measured for the triphenylamine-containing sensitizer. The authors speculated that the enhanced V_{oc} resulted from a larger dipole that was nascently formed on the sensitizer bearing the triphenylamine moiety. It was proposed that photoinduced electron injection into the TiO₂ acceptor states and *partial* hole delocalization from the Ru^{III} metal center to the triphenylamine moiety occurred in one concerted step.

The compound [Ru(BTL)(deeb)₂]²⁺, where BTL is [9'-[4,5-bis-(cyanoethylthio)]-1,3-dithiol-2-ylidene]-4',5'-diazfluorene, was found to have an extinction coefficient almost three times as large as Ru(bpy)₃²⁺ in the visible region.¹⁶⁵ Interestingly, the transient absorption features in solution and on TiO₂ differed greatly. In solution, a transient state was observed with spectroscopic properties characteristic of an MLCT excited state, with $\tau = 25$ ns at -40 °C, whereas when bound to TiO₂ a large positive absorption feature near

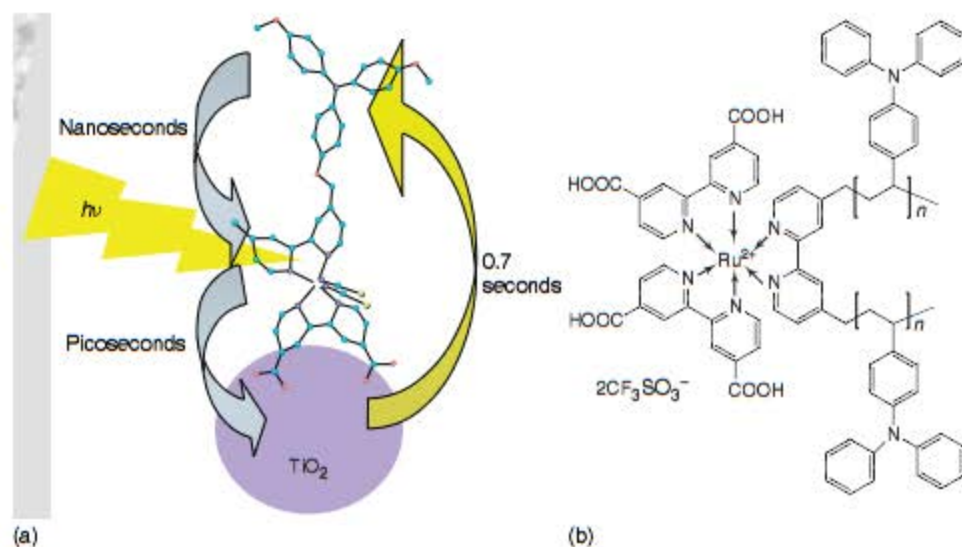


Figure 6 (a) A schematic depicting the *cis*-Ru(dmb-ether-NAr₃)(dcb)(NCS)₂ sensitizer bound to a TiO₂ nanocrystallite and the overall mechanism for photoinduced charge separation and recombination with corresponding timescales. (Taken from cover artwork.¹⁷⁷) (b) The chemical structure of the sensitizer employed to increase the half-life of the S⁺/TiO₂(e⁻) charge-separated state to over 4 s ($n = 100$). (Reproduced from Ref. 176. © Wiley-VCH, 2005.)

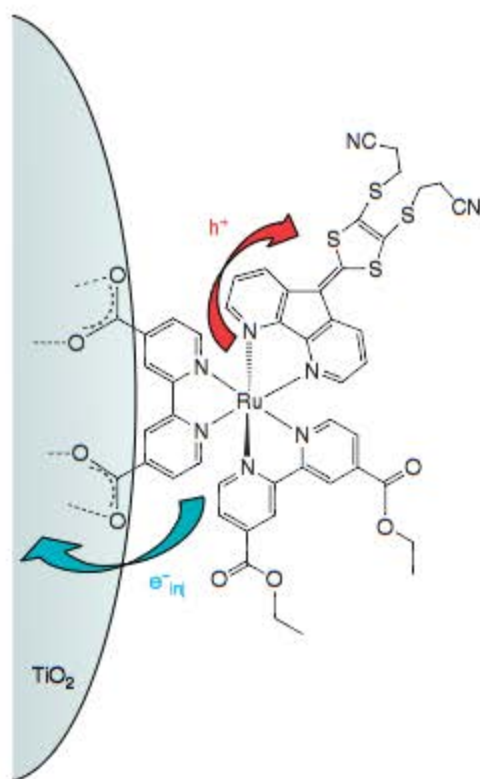


Figure 7 A schematic depicting a novel, high-extinction-coefficient sensitizer bound to a TiO_2 nanocrystallite and photoinduced electron- and hole-transfer mechanisms. This sensitizer is unique in that the extended conjugation on the free ligand is in the 3 and 3' positions. (Reproduced from Ref. 165. © American Chemical Society, 2008.)

520 nm was observed and assigned to the oxidized dithioline ligand. Within 10 ns after light excitation, an electron was injected into TiO_2 and the hole had translated from the Ru^{III} metal center to the dithioline-containing ligand, Figure 7. In fluid solution, the driving force for reductive quenching of the MLCT excited state was unfavorable.

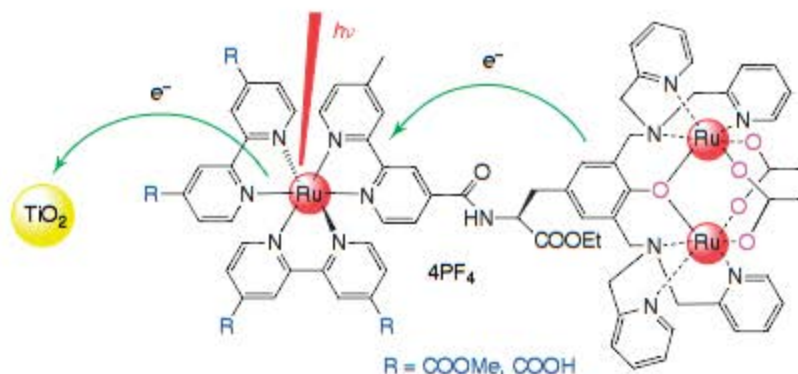


Figure 8 A schematic depicting a sensitizer employed to study intramolecular charge separation on TiO_2 thin films. Interestingly, slow intramolecular charge separation between the mononuclear Ru^{III} and dinuclear $\text{Ru}^{\text{II}}-\text{Ru}^{\text{III}}$ could be observed on the hundreds of nanoseconds timescale. (Reproduced from Ref. 353. © Wiley-VCH, 2005.)

4.1.2 Transition-Metal Donors

An advantage of using transition-metal donors is that the redox potential can be tuned over wide ranges by utilizing different ligands. The bimetallic sensitizer, $[\text{Ru}^{\text{II}}(\text{dcb})_2\text{Cl}-\text{bpa}-\text{Os}^{\text{II}}(\text{bpy})_2\text{Cl}]^{2+}$, abbreviated Ru-bpa-Os, where bpa is 1,2-bis(4-pyridyl)ethane, was anchored to TiO_2 .³⁵² Pulsed 532-nm or 416-nm light excitation of a Os-bpa-Ru/ TiO_2 thin film immersed in 1.0 M LiClO_4 acetonitrile electrolyte resulted in rapid excited-state electron injection ($\text{Ru}^{\text{II}*} \rightarrow \text{TiO}_2$) and intramolecular electron transfer ($\text{Os}^{\text{II}} \rightarrow \text{Ru}^{\text{III}}$) to ultimately form an interfacial charge-separated state with a $\text{TiO}_2(\text{e}^-)$ and an oxidized Os^{III} metal center, $\text{Os}^{\text{III}}-\text{bpa}-\text{Ru}/\text{TiO}_2(\text{e}^-)$. This same state was also generated after selective ³MLCT excitation of the Os^{II} moiety with 683-nm light. The rates of intramolecular and interfacial electron transfer were fast, $k > 10^8 \text{ s}^{-1}$, while interfacial charge recombination, $\text{Os}^{\text{III}}-\text{bpa}-\text{Ru}/\text{TiO}_2(\text{e}^-) \rightarrow \text{Os}^{\text{II}}-\text{bpa}-\text{Ru}/\text{TiO}_2$, required milliseconds for completion.³⁵²

Studies with a solution and surface-bound trinuclear ruthenium complex, $\text{Ru}^{\text{III}}-\text{Ru}^{\text{II}}(\text{L})-\text{amide}(\text{bpy})\text{Ru}^{\text{II}}(\text{dcb})_2/\text{TiO}_2$, revealed that MLCT excitation of the mononuclear Ru^{II} moiety resulted in a transient absorption spectrum indicative of $\text{Ru}^{\text{III}}-\text{Ru}^{\text{II}}(\text{L})-\text{amide}(\text{bpy})\text{Ru}^{\text{III}}(\text{dcb})_2/\text{TiO}_2(\text{e}^-)$, Figure 8.³⁵³ This intramolecular charge-separated compound was completely formed in 200 ps, at which time the injection yield was deemed to be <10%. However, at 300 ns, a spectrum consistent with $\text{Ru}^{\text{III}}-\text{Ru}^{\text{III}}(\text{L})-\text{amide}(\text{bpy})\text{Ru}^{\text{III}}(\text{dcb})_2/\text{TiO}_2(\text{e}^-)$ was observed and was shown to have a half-life of ~1 ms. This illustrates that slow hole transfer can occur over large distances under appropriate conditions.

Coordination compounds of the form $[(\text{LL})(\text{L}'\text{L}')\text{Ru}^{\text{II}}(\text{BL}')\text{Ru}^{\text{II}}(\text{LL})(\text{L}'\text{L}')]^{n+}$ were investigated on TiO_2 , where LL and L'L' are bpy and/or dcb and BL' is a bridging ligand: either tetrapyrido[3,2-a : 2', 3'-c : 3'', 2''-h : 2''', 3'''-j]phenazine (tpphz) or 1,4-bis(phen-[5,6-d]imidazol-2-yl)benzene (bfimbz), where phen is 1,10-phenanthroline.³⁵⁴

As the BL' ligands are rigid and linear heteroaromatic entities, remote, excited-state electron injection could be examined without unwanted outer-sphere ligand–surface interactions. It was shown that when BL' was tpphz—a ligand possessing π^* energetics below the π^* orbitals of the surface-bound dcB ligand— injection could be time resolved because of the excited state being localized on tpphz, away from a surface-bound dcB ligand and with less reducing power for injection. However, this slow injection was found to be not only distance- and driving force-dependent but orientation-dependent as well. When $[(\text{bpy})(\text{dcB})\text{Ru}^{\text{II}}(\text{tpphz})\text{Ru}^{\text{II}}(\text{bpy})(\text{dcB})]/\text{TiO}_2$ was employed as the sensitizer, excited-state injection could be time resolved on the nanosecond timescale whereas with $[(\text{bpy})_2\text{Ru}^{\text{II}}(\text{tpphz})\text{Ru}^{\text{II}}(\text{bpy})(\text{dcB})]/\text{TiO}_2$ it could not be, $k_{\text{inj}} > 10^8 \text{ s}^{-1}$. Using geometry optimization software, it was hypothesized that electronic coupling, and not distance from the TiO_2 surface, could explain the differences, Figure 9. The

location of the π^* orbital of the heterobinuclear complex in relation to the TiO_2 surface allowed for better electronic coupling between the sensitizer and the TiO_2 DOS even though the $N_{\text{phenazine}}\text{--Ti}$ distance was increased by over a factor of two. Photoelectrochemical measurements supported this and indicated that an increased distance for back-electron transfer enhanced the photocurrent.

4.2 Intermolecular Regeneration

In DSSCs, redox mediators are added to the external electrolyte to shuttle charges between the two electrodes. The reduced form of the mediator must regenerate the sensitizer by electron transfer prior to recombination with the injected electron. The oxidized form of the redox mediator must be reduced at the platinum counter electrode, a process not described herein. Ideally, the redox mediators do not absorb

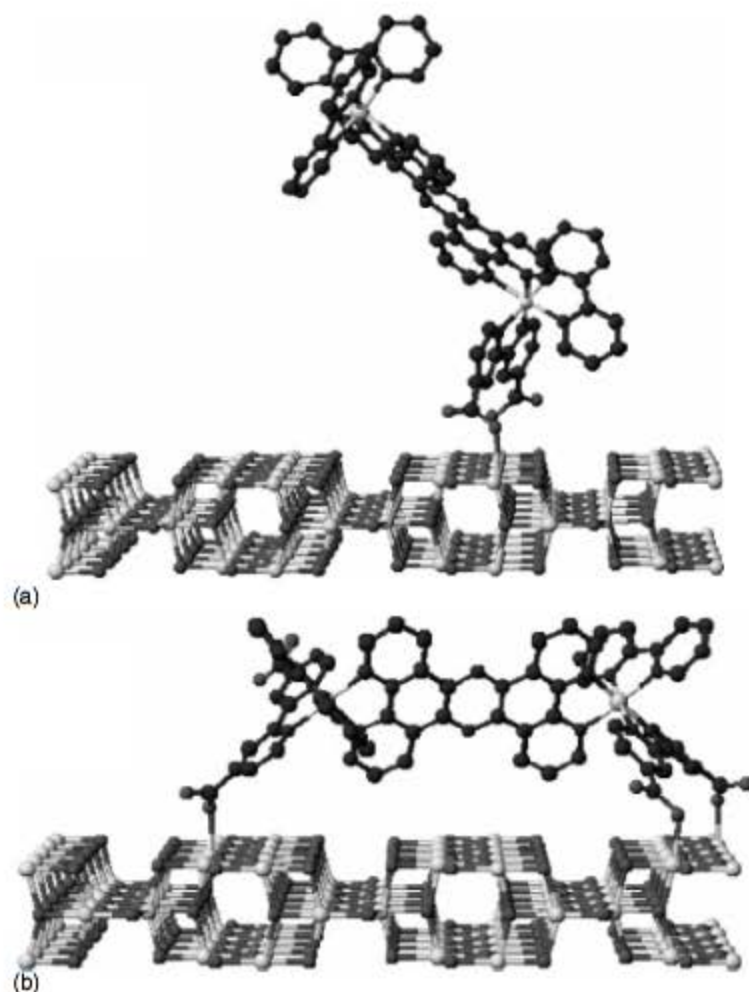


Figure 9 Density functional theory (DFT)-optimized geometry for two bimetallic Ru^{II} compounds. When a distal ligand possessed carboxylic acid functional groups capable of binding to the TiO_2 surface, the geometry of the minimized energy configuration had it binding to the surface as well (b). When the distal ligand was devoid of binding groups, it did not (a). This allowed for better electronic coupling between the sensitizer and the TiO_2 DOS, and resulted in a faster injection rate. (Reproduced from Ref. 354. © American Chemical Society, 2003.)

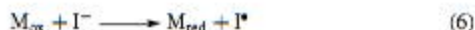
any sunlight. Although ion pairing or surface adsorption with the mediators may occur, for the organization of this article we consider these to be intermolecular electron-transfer reactions.

4.2.1 Regeneration by Iodide

Sensitizers in Solution. By far the most effective donor in DSSCs is iodide.³⁵⁵ All confirmed reports of light-to-electrical power-conversion efficiencies over 10% and state-of-the-art DSSCs require iodide.^{14–19} While many of the details of iodide oxidation at sensitized electrodes are now becoming available, it is important to point out that the aqueous redox chemistry of iodide and homogeneous reactions with transition-metal compounds have long been known.^{356–360}

A Latimer-type diagram for the aqueous redox chemistry of iodide has been previously described.²¹ Additional values and details are available in the review by Stanbury.³⁵⁶ The formal one-electron reduction potential of the iodine atom is very positive, $E^\circ(\text{I}^\bullet/\text{I}^-) = +1.33 \text{ V}$ vs NHE.³⁵⁶ Therefore, a potent oxidant is required to regenerate iodine atoms. However, another pathway exists, through which two iodides can be directly oxidized to $\text{I}_2^{\bullet-}$, $E^\circ(\text{I}_2^{\bullet-}/2\text{I}^-) = +1.03 \text{ V}$ vs NHE.³⁵⁶ On the basis of potentials alone, it is tempting to conclude that this latter pathway is the only mechanism available to oxidize sensitizers like $\text{N}3^+$, since generation of iodine atoms would be thermodynamically unfavorable by close to 250 mV.³³ However, it should be kept in mind that these reduction potentials are for standard-state conditions and that adsorption to the TiO_2 surface may have a significant effect. Walter and Elliott have provided evidence that interactions between iodide and the bpy ring may also activate iodide.³⁶¹ Furthermore, the values reported here are for aqueous electrolytes as few have been reported in acetonitrile solutions.^{362–368} There is good reason to believe that the reduction potentials will vary significantly with solvent, while only two-electron redox processes have been observed at metal electrodes.^{363,369,370}

The transition-metal redox chemistry of iodide has previously been reviewed.^{359,360} Two mechanisms have been observed, based on reactions (6) and (7):



Both are first order in transition-metal compound, M_{ox} ; while reaction (6) is first order in iodide, reaction (7) is second order in iodide. Proposed mechanisms for reaction (7), the overall third-order reaction, include I^- reacting with an $[\text{M}_{\text{ox}}, \text{I}^-]$ ion pair or M_{ox} with an $[\text{I}^-, \text{I}^-]$ ion pair. A wide variety of transition-metal compounds have been studied and linear free-energy relations for both reactions now exist. In some cases, with mild oxidants such as $\text{M}_{\text{ox}} = \text{Os}(\text{bpy})_3^{3+}$, the reverse reactions became significant.^{357–359}

Much less is known about MLCT excited-state oxidation of iodide. The reduced-sensitizer electron-injection process requires excited-state iodide oxidation followed by interfacial electron-transfer chemistry. Early studies with $[\text{Ru}^{\text{III}}(\text{bpy})_2(\text{bpy}^-)]^{2+*}$ revealed very sluggish iodide quenching, i.e., $1 \times 10^6 \text{ M}^{-1} \text{ s}^{-1}$.^{371,372} Interestingly, excited-state quenching of $[\text{Ru}^{\text{III}}(\text{bpy})_2(\text{dcb}^-)]^{2+*}$ anchored to SiO_2 appears to be much more rapid, i.e., $1 \times 10^8 \text{ M}^{-1} \text{ s}^{-1}$.³⁷³ These excited-state electron-transfer reactions have been significantly enhanced through ion pairing.^{315,317} Addition of iodide to a dichloromethane solution of $[\text{Ru}(\text{bpy})_2(\text{deeb})]^{2+}$ resulted in significant changes to the ground-state absorption. A decrease in PLI and excited-state lifetime accompanied the absorption changes consistent with both static- and dynamic-quenching mechanisms, respectively. A Benesi–Hildebrand-type analysis yielded equilibrium constants for ion pairing that were within experimental error the same as those abstracted from photoluminescence quenching data, $K_{\text{eq}} = 59\,700 \text{ M}^{-1}$. Similar behavior was observed in acetonitrile and/or with $\text{Ru}(\text{bpy})_3^{2+}$; however, roughly a two orders-of-magnitude higher iodide concentration was required. Transient absorption measurements clearly showed an electron-transfer mechanism with the appearance of $\text{I}_2^{\bullet-}$ and no evidence for iodine atom formation; thus the mechanism appeared to follow reaction (7). The cage escape yields were low, $\varphi = 0.25$, but increased to 0.50 with $\text{Ru}(\text{bpy})_3^{2+}$. Remarkably, the solid-state crystal structure of $\text{Ru}(\text{bpy})_2(\text{deeb})\text{I}_2$ showed both iodides associated with the carbonyl oxygens of the ester groups, Figure 10. One might have anticipated that coulombic repulsion would have resulted in a larger interionic distance than the $\sim 6 \text{ \AA}$ observed. If a similar structure exists in solution, the iodides would be well-positioned for a concerted reduction of $[\text{Ru}^{\text{III}}(\text{bpy})_2(\text{deeb}^-)]^{2+*}$ and formation of $\text{I}_2^{\bullet-}$. This is

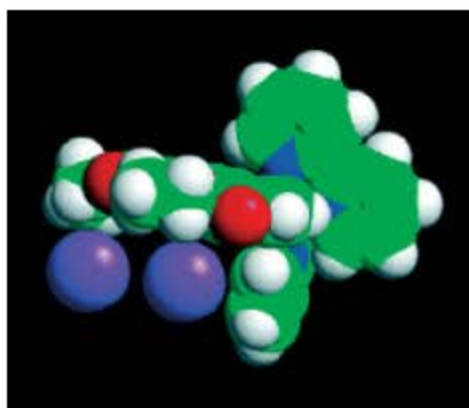


Figure 10 Space-filling representation of a single-crystal structure with two iodides associated with the deeb ligand in $[\text{Ru}(\text{bpy})_2(\text{deeb})]^{2+}$. This geometry would allow for facile reductive quenching of the excited or oxidized forms of the molecule and the proximity of a second iodide could favor $\text{I}_2^{\bullet-}$ generation as per equation (7). (Reproduced from Ref. 317. © American Chemical Society, 2006.)

an intriguing possibility as excited-state reactions that form chemical bonds are rare in all of photochemistry.

Also, recent studies in our laboratories highlighted the first evidence for iodine atoms as intermediates in the sensitized oxidation of iodide.^{374,375} In less polar acetonitrile solution containing millimolar concentrations of iodide, careful analyses of the time-resolved absorbance and photoluminescence kinetic data revealed that formation of reduced $\text{Ru}^{\text{II}}(\text{bpz}^-)(\text{bpz})(\text{deeb})^+$ occurred with a second-order rate constant of $(6.6 \pm 0.3) \times 10^{10} \text{ M}^{-1} \text{ s}^{-1}$ while that for the formation of $\text{I}_2^{\bullet-}$ was $(2.4 \pm 0.2) \times 10^{10} \text{ M}^{-1} \text{ s}^{-1}$. The lag in $\text{I}_2^{\bullet-}$ was due to the slower reaction of I^\bullet , formed via reaction (6), with an I^- to form $\text{I}_2^{\bullet-}$. Reaction of the iodine atom with iodide to make an I–I bond lowers the free energy stored in the charge-separated state by 110 mV.^{9,12} Charge recombination to yield ground-state products, $\text{Ru}^+ + \text{I}_2^{\bullet-} \rightarrow \text{Ru}^{\text{II}} + 2\text{I}^-$, is highly thermodynamically favored ($-\Delta G^\circ = 1.64 \text{ eV}$) and occurs with a rate constant of $2.1 \times 10^{10} \text{ M}^{-1} \text{ s}^{-1}$, almost ten times larger than the $\text{I}_2^{\bullet-}$ disproportionation rate constant. Unwanted charge recombination to $\text{I}_2^{\bullet-}$ has previously been proposed to lower the efficiency of DSSCs,⁵ and these data show that it can be a very fast reaction.

Sensitizer/ TiO_2 Interfaces. Fitzmaurice and Frei reported the first study of the heterogeneous reduction of Ru^{III} -polypyridyl compounds by iodide.³⁷⁶ Photoinduced electron injection into colloidal TiO_2 from $[\text{Ru}^{\text{III}}(\text{dcb})_2(\text{dcb}^-)]^{2+}$ was followed by oxidation of iodide in acidic aqueous solution. From the pseudo-first-order transient kinetics in 0.5 to 100 mM KI, a second-order rate constant for iodide oxidation of $\sim 2.5 \times 10^9 \text{ M}^{-1} \text{ s}^{-1}$ was abstracted. The transient absorption spectra were ascribed to be most consistent with formation of ion pairs.

Since that time, there have been a number of studies aimed at abstracting the rate at which the Ru^{II} form of the sensitizer is regenerated. Such experiments were usually performed by monitoring the recovery of the MLCT absorption after pulsed-laser excitation at wavelengths where the iodide oxidation products did not appreciably absorb light. While this has proven to be a reasonable method, little information regarding the mechanism(s) of iodide oxidation is obtained. Most studies of this type were performed with $\text{N3}/\text{TiO}_2$. At low iodide concentrations, the regeneration rate was found to be first order in iodide. At higher iodide concentrations, a static component was often observed. Under the 0.5 M iodide concentration of a DSSC, regeneration is often stated to be complete within 10 ns.^{20,35} The rate constant for regeneration of the oxidized sensitizer, $\text{Ru}^{\text{III}}(\text{bpy})_2(\text{dcb})/\text{SnO}_2$, by iodide was determined to be $1.2 \times 10^{10} \text{ M}^{-1} \text{ s}^{-1}$. Durrant and coworkers have recently provided evidence that the regeneration rate is dependent on the $E^\circ(\text{Ru}^{\text{III/II}})$ of the sensitizer. With $\text{Ru}(\text{dcb})_2(\text{CN})_2/\text{TiO}_2$ thin films, an intermediate was observed and assigned to a $[\text{Ru}^{\text{III}}, \text{I}^-]$ ion pair.³⁷⁷ Reaction of this with a second iodide was proposed to yield $\text{I}_2^{\bullet-}$.

The reactivity of iodide with $\text{N719}^+/\text{TiO}_2(\text{e}^-)$ increased in the presence of Li^+ and other cations with large charge-to-radius ratios.³⁷⁸ It was noted that the half-life for sensitizer regeneration abruptly shortened when the concentration of Li^+ was increased to between 10 and 50 mM. The point of zero ζ -potential (PZZP) was determined to occur at 3 mM Li^+ , a concentration slightly less than that required for the abrupt change in half-life. Also, by titration of iodide to positively charged TiO_2 particles in the presence of Mg^{2+} , the experimental data suggested that iodide adsorbed on TiO_2 within the Helmholtz layer even in the presence of sensitizers. It was concluded that the abrupt change in sensitizer regeneration occurred because of ion-pairing of iodide anions with the surface or sensitizer resulting in an increased occurrence of the faster termolecular reaction (7).

4.2.2 Regeneration by Donors Other Than Iodide

Evaluation of the reduction potentials for iodide oxidation reveals the significant problem with the I_3^-/I^- redox mediator required for champion DSSCs. Iodide is oxidized to the iodine atom at +1.33 V vs NHE and I_3^- is reduced at +0.04 V. Thus roughly a volt of free energy is lost with this redox mediator! While these are aqueous reduction potentials under standard-state conditions, there are reasons to believe that the losses are less significant in acetonitrile electrolytes. Another issue with the I_3^-/I^- redox mediator is that a facile reduction of I_3^- at the counter electrode in DSSCs is required so as to minimize the voltage loss. Platinum metal has a large exchange current density and transfer coefficient for this reaction, but it is expensive.³⁷⁹ Electrode materials like graphite do not perform as well, and the corrosive nature of the electrolyte toward less-expensive metals like silver or copper precludes their use.³⁷⁹ In addition, I_2 has an appreciable vapor pressure such that extra care must be taken to ensure a thoroughly and tightly sealed solar cell.³⁸⁰ Therefore, there is ample reason to identify alternative redox mediators for DSSCs.

Historically, one-electron-transfer, outer-sphere donors that have realized limited success in DSSCs include phenothiazine,³⁴³ ferrocene,³⁸⁰ hydroquinone,^{381,382} bromide,³⁸² SeCN^- , and SCN^- .³⁸³

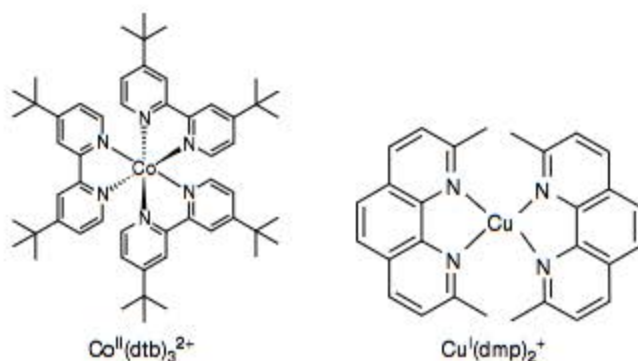
Recently, when SeCN^- - and SCN^- -based redox mediators were employed in DSSCs based on mesoporous, nanocrystalline SnO_2 electrodes sensitized with $[\text{Ru}(\text{deeb})(\text{bpy})]^{2+}$, the photocurrent was similar to that obtained using the I^-/I_3^- redox mediator.³³⁴ In addition, Wang and Grätzel observed more promising behavior with the $(\text{SeCN})_2/\text{SeCN}^-$ pseudohalide redox mediator in the 1-ethyl-3-methylimidazolium selenocyanate ionic liquid with added $\text{K}(\text{SeCN})_3$.³⁸⁴ Although this ionic liquid was found to be 35 times less viscous than the more traditional 1-propyl-3-methylimidazolium iodide ionic liquid, it was over 28 times more conductive at room temperature and could solubilize large amounts of $(\text{SeCN})_2/\text{SeCN}^-$. By transient

absorption spectroscopy, it was shown that SeCN^- and the analogous ionic-liquid-containing SCN^- could rapidly regenerate the sensitizer. It was also shown that the maximum IPCE was close to unity and the power-conversion efficiency was 7.5%. Notwithstanding, the kinetics for iodide oxidation after excited-state injection from $\text{N}_3^-/\text{TiO}_2$ in acetonitrile were found to be more rapid than that for the oxidation of SeCN^- .³⁸³

As for solution-based inorganic donors, octahedral Co^{II} diimine compounds have proven to be effective for sensitizer regeneration. One-electron-transfer, outer-sphere $\text{Co}^{\text{III/II}}$ redox mediators have led to promising light-to-electrical power-conversion efficiencies in DSSCs. The $\text{Co}^{\text{III/II}}$ self-exchange rate constants are known to be particularly sluggish, behavior that is reasonably understood by the d^6/d^7 electronic configurations that give rise to large inner-sphere reorganization energies.³⁸⁵ It is possible that these same electronic factors are responsible for the slow rates of the $\text{TiO}_2(\text{e}^-) + \text{Co}^{\text{III}}$ recombination reaction and the reasonable photocurrent efficiencies that have been reported.

The first studies of cobalt mediators were performed by Grätzel and coworkers.³⁸⁶ A DSSC based on the $[\text{Co}^{\text{III/II}}(\text{dbbip})_2]^{3+/2+}$ redox couple, where dbbip is 2,6-bis(1'-butylbenzimidazol-2'-yl)pyridine, resulted in impressive photovoltaic performance and an exchange current density of $7 \times 10^{-6} \text{ A cm}^{-2}$ in an acetonitrile/ethylene carbonate (40:60, v/v) electrolyte at a fluorine-doped tin oxide (FTO) electrode.³⁷⁹ With *cis*-Ru(4-methyl-4'-hexadecyl-bpy)(dcb)(NCS)₂/TiO₂ in an electrolyte with a 1:9 stoichiometric ratio of Co^{III} : Co^{II} , a maximum IPCE of >65% was realized, and under reduced light conditions, i.e., <0.1 suns, a power-conversion efficiency of 5.2% was also obtained.³⁸⁶ The use of a neutral sensitizer was found to be necessary in order to attenuate the adsorption of cationic redox species onto TiO₂. When $\text{Co}^{\text{II}}(\text{dbbip})_2^{2+}$ was added above a threshold of 10 mM, the second-order rate constant for regeneration was $2.9 \times 10^6 \text{ M}^{-1} \text{ s}^{-1}$, approximately an order-of-magnitude smaller than values reported for NaI. However, at 100 mM the pseudo-first-order rate constants were similar to those found with the same concentration of iodide.³⁷⁸ In support of previous work, the i_{sc} was found to be dependent on the counterion of the solution $\text{Co}^{\text{III/II}}$ redox mediator, where the perchlorate salts resulted in the highest efficiencies.³⁸⁷ Utilizing mediators where the $E^\circ(\text{Co}^{\text{III/II}})$ varied over 190 mV, a similar 180-mV variation in V_{oc} was realized. The largest V_{oc} recorded was 660 mV accompanied by a 7.9% power-conversion efficiency, again under illumination conditions of 0.1 sun.

A family of cobalt redox couples employing derivatives of bpy, phen, and tpy ligands were studied in DSSCs.³⁸⁸ The highest efficiencies were reported for the $[\text{Co}^{\text{III/II}}(\text{dtb})_3]^{3+/2+}$ perchlorate redox mediator, where dtb is 4,4'-di-*tert*-butyl-bpy (Scheme 5), and were within 80% of that of a comparable I_3^-/I^- -mediated DSSC. However, in contrast to the I_3^-/I^- redox mediator, addition of Li^+ to the cells



Scheme 5 The chemical structures of the reduced versions of the most efficient transition-metal-based redox mediators: $[\text{Co}^{\text{III/II}}(\text{dtb})_3]^{3+/2+}$ and $[\text{Cu}^{\text{II/I}}(\text{dmp})_2]^{2+/+}$

increased not only the i_{sc} but the V_{oc} as well! This was proposed to be due to a decrease in the recombination rate of $\text{TiO}_2(\text{e}^-)$ and Co^{III} , most likely from an increase in overpotential for reduction of $[\text{Co}^{\text{III}}(\text{dtb})_3]^{3+}$ at the conductive support. Cyclic voltammograms with platinum electrodes revealed sluggish interfacial, $\text{Co}^{\text{III/II}}$ electron-transfer kinetics relative to carbon and gold. Although gold was optimal in DSSCs, FTO electrodes coated with graphite nanoparticles initially outperformed those employing platinum; however, the carbon-coated FTO electrodes degraded with time. Nevertheless, the initial response was encouraging and shows promise for replacing platinum with less-expensive, carbon- and/or FTO-based materials.

It has recently been shown that upon introduction of LiClO_4 to DSSCs, the lifetime of the $\text{TiO}_2(\text{e}^-)$ ^{390,391} increased for cobalt-based redox couples, whereas it decreased for the I_3^-/I^- redox mediator. This was rationalized as being due to a cation screening effect, where the local concentration of cationic cobalt-based redox couples decreased near the TiO_2 surface when cationic Li^+ was present.^{390,391}

Although large reorganization energies and slow-electron transfer kinetics for cobalt-based redox couples are advantageous as they attenuate the unwanted, recombination reaction, $\text{TiO}_2(\text{e}^-) + \text{Co}^{\text{III}} \rightarrow \text{TiO}_2 + \text{Co}^{\text{II}}$, these characteristics are undesirable with respect to sensitizer regeneration, $\text{S}^+/\text{TiO}_2(\text{e}^-) + \text{Co}^{\text{II}} \rightarrow \text{S}/\text{TiO}_2(\text{e}^-) + \text{Co}^{\text{III}}$. Rapid sensitizer regeneration and sluggish recombination kinetics are traits that make the I_3^-/I^- redox mediator optimal. Use of a second mediator in conjunction with $[\text{Co}^{\text{III/II}}(\text{dtb})_3]^{3+/2+}$ was proposed to overcome slow regeneration while maintaining slow recombination.³⁹² Both PTZ and ferrocene were employed in DSSCs because of their small reorganization energies, rapid electron-transfer kinetics, and reduction potentials intermediate between that of $[\text{Co}^{\text{III/II}}(\text{dtb})_3]^{3+/2+}$ and the oxidized sensitizer. The oxidized sensitizer was found to recover in the presence of 0.1-M donor in the order ferrocene > PTZ > $\text{Co}(\text{dtb})_3^{2+}$ > no donor. Chronocoulometry of 1:2 molar mixtures of PTZ: Co^{II} with FTO electrodes displayed a turnover 45% faster than that for ferrocene/ Co^{II} mixtures. A

maximum IPCE of >80% was achieved. Under illumination conditions of 0.1 sun, the V_{oc} was larger than that for an equivalent DSSC employing the I_3^-/I^- redox system (0.3/0.03 M). However, the power-conversion efficiency was smaller due to mass-transport limitations of the bulky cobalt redox mediator that displayed an order-of-magnitude slower diffusion coefficient through a TiO_2 film than did I_3^- .³⁹³ Ru polypyridyl sensitizers with pendant pyrrole or pyrrolidine groups gave superior photocurrents in the presence of $[Co^{III/II}(dtb)_3]^{3+/2+}$ than in the presence of I^-/I_3^- redox mediator over the entire absorption spectrum.^{169,394} Addition of $Fe(dmb)_3^{2+}$ as a co-mediator resulted in a maximum IPCE of >80% for the best pyrrole-containing sensitizer.¹⁶⁹

The exchange current density for $[Co^{III}(dtb)_3]^{3+}$ reduction was greatly enhanced when *cis*-Os(dcb)₂Cl₂ was anchored to FTO.³⁹⁵ When employed as a counter electrode with N3/ TiO_2 in a DSSC, the i_{sc} and V_{oc} were only slightly attenuated relative to a gold counter electrode and, using a three electrode measurement, the potential of the Os(dcb)₂Cl₂/FTO counter electrode was nearly the same under open-circuit conditions.

Cu^I has a d^{10} electronic configuration and compounds like $Cu(LL)_2^+$ usually adopt a tetrahedral geometry in solution and in the solid state. The Cu^{II} form is subject to a Jahn–Teller distortion that often manifests itself in a geometry with more coplanar diimine ligands, i.e., a flattening, and a fifth ligand from solvent or a counterion axially ligated. It is possible to photoinduce these structural changes, and they have been characterized by time-resolved X-ray techniques.²³⁴ Therefore, like the $Co^{III/II}$ redox mediators, $Cu^{II/I}$ redox chemistry is accompanied by a large inner-sphere reorganization energy change and slow self-exchange rate constants, and has demonstrated some modest success as mediators in DSSCs. For example, Cu^I -diimine compounds have been studied in DSSCs.³⁹⁶ The best-performing mediators produced a maximum IPCE of ~40% and yielded a higher V_{oc} than the I_3^-/I^- redox couple under the same experimental conditions. This was attributed to a decreased dark current due to the large reorganization energy of the $Cu^{II/I}$ redox couple.

Unfortunately, the large reorganization energies for $Cu^{II/I}$ redox mediators suffer the same pitfalls as their $Co^{III/II}$ counterparts, i.e., slow sensitizer regeneration. Thus, a Cu^I compound with a distorted tetrahedral geometry was employed in order to help reduce the large reorganization energy.³⁸⁹ When $[Cu^{II/I}(dmp)_2]^{2+/+}$ (Scheme 5) was employed as the redox mediator, where *dmp* is 2,9-dimethyl-phen, a light-to-electrical power-conversion efficiency of 2.2% under 0.2-sun illumination was obtained with N719/ TiO_2 DSSCs. For a similar reason as for the Cu^I sensitizers, the methyl groups were employed to prevent planarization of the *dmp* ligands, which manifests itself in a positive shift in $E^\circ(Cu^{II/I})$. Significantly, a higher V_{oc} was realized with the $Cu^{II/I}$ mediator as compared with I_3^-/I^- under the same experimental conditions.

5 SENSITIZATION AT THE POWER POINT

The influence of the $TiO_2(e^-)$ concentration on the individual steps of the sensitization cycle, shown in Scheme 1, is generally unknown and represents an active area of investigation. Recall that the sensitization cycle consists of (i) light absorption, (ii) excited-state injection, and (iii) sensitizer regeneration/recombination. Recall that at the PP under 1-sun illumination, approximately 10 injected electrons reside in each nanocrystallite. Furthermore, aside from these Faradaic charge-transfer reactions of the sensitization cycle, there exist non-Faradaic processes that are known to accompany interfacial electron transfer. For example, it has been recognized for some time that Li^+ reversibly intercalates or binds to the surface of reduced anatase TiO_2 nanocrystallites.^{21,378,397–399} Similar, and possibly related, is the cursorily understood phenomenon where prolonged ultraviolet light soaking of an assembled DSSC yields increased power-conversion efficiencies.^{400–402} Recently, it has been shown that even visible-light soaking or forward bias in the absence of Li^+ induces what are thought to be electron transport levels that enhance DSSC performance.^{403,404} In the presence of Li^+ , intercalation into the TiO_2 lattice may impede this process, and thus it was tacitly presumed that proton intercalation was vital to the behavior.

Recent results from our laboratories suggest new directions for fundamental research and raise the question of what the term “regeneration” actually means. These new results are best understood with an example, $[Ru(dtb)_2(dcb)](PF_6)_2$. Figure 11(a) shows the absorption and photoluminescence spectra of a $Ru(dtb)_2(dcb)/TiO_2$ thin film immersed in 0.1 M $LiClO_4$ acetonitrile and in neat acetonitrile. In the presence of Li^+ , both maxima red-shifted and their intensity decreased relative to neat acetonitrile. The significant quenching of the photoluminescence intensity results from enhanced excited-state electron injection into TiO_2 as previously described herein.⁴⁰⁵

Pulsed-light excitation of $Ru(dtb)_2(dcb)/TiO_2$ in 0.1/0.5 M $LiClO_4$ /TBAI acetonitrile electrolyte resulted in the microsecond absorption difference spectrum, Figure 11(b). Under such conditions, one would expect to observe a $TiO_2(e^-)$ and I_3^- . The absorption features characteristic of I_3^- ($\lambda < 420$ nm) and $TiO_2(e^-)_s$ ($\lambda > 560$ nm) were indeed observed. However, the absorption band centered at 460 nm and the bleach at 510 nm could not be assigned to any conceivable electron-transfer products.

Spectral modeling indicated that the absorption features at 460 and 510 nm resulted from $[Ru(dtb)_2(dcb)]^{2+}$ sensitizers that were present in an environment significantly different from that which had been initially photoexcited. Spectral modeling indicated that the sensitizers that were initially photoexcited had an absorption spectrum shown in red while immediately after regeneration their spectrum was that shown in black, Figure 11(a). Overlaid on the

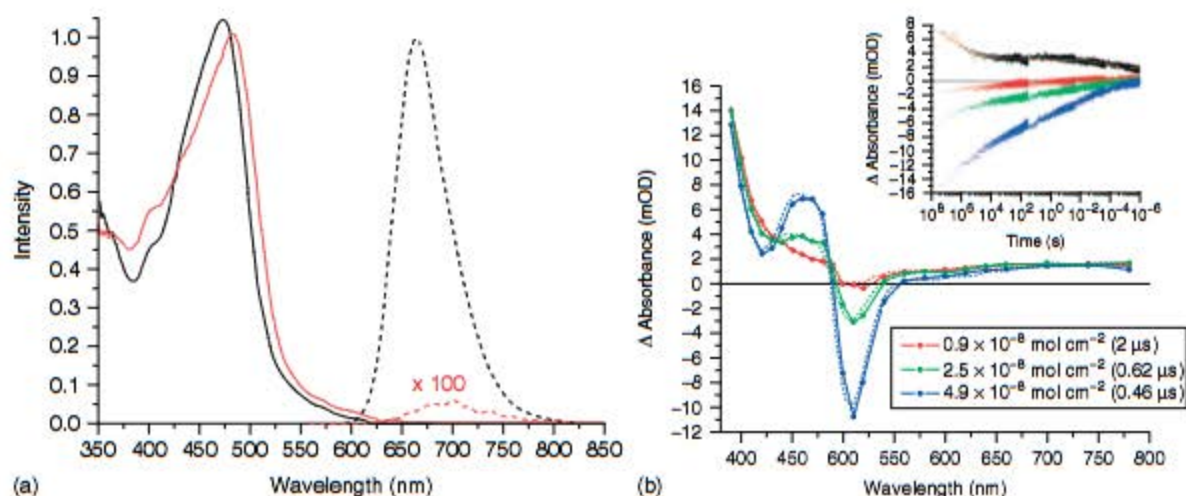


Figure 11 (a) Absorption and photoluminescence spectra of $\text{Ru}(\text{dtb})_2(\text{dcb})/\text{TiO}_2$ in 0.1 M LiClO_4 acetonitrile electrolyte (—/—) and in neat acetonitrile after removal of the LiClO_4 by 10 neat acetonitrile washings (---/---). (b) Transient absorption difference spectra for three $\text{Ru}(\text{dtb})_2(\text{dcb})/\text{TiO}_2$ thin films at the indicated surface coverages and delay times measured after pulsed 532-nm excitation in 0.1/0.5 M $\text{LiClO}_4/\text{TBAI}$ acetonitrile electrolyte. Overlaid are simulations of the data represented by dashed lines. Inset: Time-resolved, single-wavelength absorption difference spectra measured at 510 nm for each surface coverage—corresponding to cation transfer—and a single difference spectrum measured at 433 nm (—)—corresponding to I_3^- loss—due to $\text{TiO}_2(\text{e}^-) + \text{I}_3^-$ recombination. (Reproduced from Ref. 108. © American Chemical Society, 2008.)

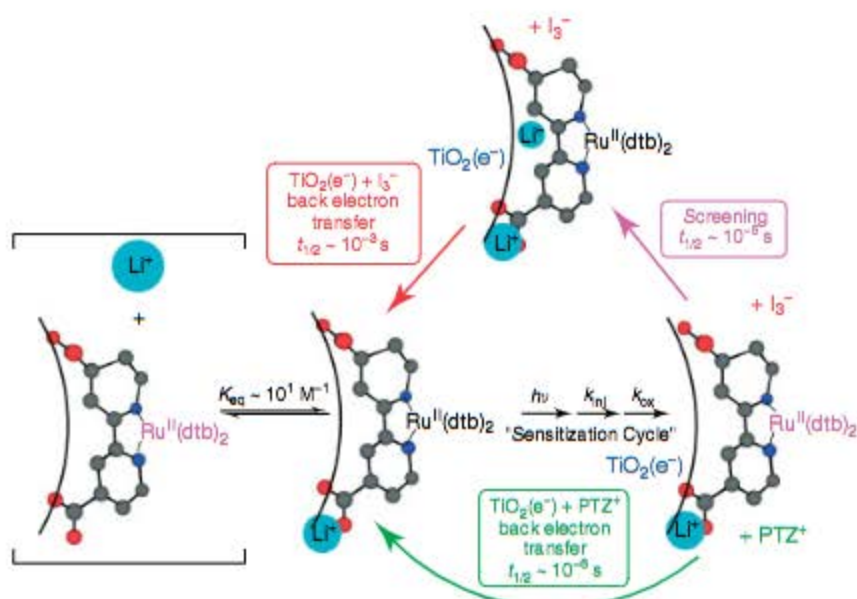
data in Figure 11(b) are simulations based on the weighted addition of (i) the absorption spectrum of I_3^- , (ii) the $\text{TiO}_2(\text{e}^-)$ absorption spectrum, and (iii) the difference in the absorption spectra of $\text{Ru}(\text{dtb})_2(\text{dcb})/\text{TiO}_2$, in the absence minus the presence of Li^+ . Similar sensitizer absorption features were observed when PTZ was used in the place of iodide. The measured spectral responses are reminiscent of those observed by electroabsorption (Stark) spectroscopy, as described above.^{252,253} While Stark effects have been observed in semiconductor nanocrystallites^{406–408} and Ru^{II} polypyridyl compounds,^{75,249–251} they were not expected in DSSCs because of the high dielectric constant of anatase TiO_2 ($\epsilon = 7–50$)⁴⁰⁹ and acetonitrile ($\epsilon = 37.5$)⁴¹⁰ and the high-ionic-strength electrolytes typically employed.^{12,301,411–425}

Recently, Hagfeldt, Boschloo, and colleagues reported similar Stark-like features in the spectroelectrochemical reduction and photoinduced absorption spectra of perylene-sensitized TiO_2 thin-film electrodes.⁴²⁶ A unique aspect of these perylene sensitizers was that they were neutral compounds that did not contain ionizable functional groups. Therefore, the sensitized thin film was not intentionally exposed to protons or Lewis-acidic cations and the origin of the effect was unlikely solely due to cations.

Results from studies by Staniszewski,¹⁰⁸ Durrant,⁴²⁷ Kamat,³⁷³ and Hagfeldt,⁴²⁶ now clearly indicate that the absorption spectra of surface-anchored molecular sensitizers are influenced by electrons injected into the metal-oxide nanoparticle. After fast excited-state electron injection into TiO_2 and regeneration by iodide, sensitizers were present in an environment distinctly different from that prior to light absorption. Significantly, the newly generated sensitizers

were in an environment that is known to be less favorable for excited-state electron injection.⁴⁰⁵ The sensitization cycle shown in Scheme 1 needs to be modified; the oxidized Ru^{III} sensitizer may be reduced to Ru^{II} on a nanosecond timescale; however, it is not brought back to the environment prior to light absorption, until slow (μs – ms) cation transfer or back-electron transfer via interfacial charge recombination as $\text{TiO}_2(\text{e}^-) + \text{I}_3^-$ has occurred. By further inspection, one realizes that the overall sensitization cycle is merely redox regenerative. In other words, the sensitizer does return to its initial formal oxidation state; however, all interfacial-related processes have not reset.

A working hypothesis emerged from the studies, which is consistent with all experimental data. This hypothesis begins with the assertion that electrons injected into TiO_2 immediately produce an electric field. This field extends roughly normal to the semiconductor–sensitizer interface and induces a Stark effect on the sensitizer absorption spectrum. A kinetic competition then exists between ionic reorganization to shield this field, termed screening,^{411,416,423} and interfacial charge recombination, magenta versus green arrows in Scheme 6. With PTZ donors, recombination was fast and screening was not clearly observed. On the other hand, with iodide donors, screening was observed prior to sluggish interfacial charge recombination, i.e. $\text{TiO}_2(\text{e}^-) + \text{I}_3^-$. To our knowledge, this was the first spectroscopic observation¹⁰⁸ and elucidation of an ionic screening process of the electric fields emanating from sensitized TiO_2 nanocrystallites. Although not shown in Scheme 6, the injected electron is found to perturb the absorption spectrum of multiple sensitizers, and not simply the sensitizer that had undergone photoinduced



Scheme 6 Solvated Li^+ in adsorption equilibrium with sensitized TiO_2 nanocrystallites. Pulsed-light excitation in the presence of electron donors results in the sensitization cycle (see Scheme 1) and yields a Ru^{II} sensitizer whose absorption spectrum is perturbed by the injected electron, behavior that is attributed to the Stark effect. With phenothiazine donors, interfacial charge recombination directly yields ground-state products. With iodide donors, charge recombination was slower, and a new dynamic process attributed to ionic reorganization, or "screening," was observed spectroscopically prior to interfacial electron transfer. (Reproduced from Ref. 36. © American Chemical Society, 2010.)

electron injection. By performing studies employing sensitized TiO_2 in the absence of external donors and on TiO_2 films co-bound with two compounds, one that served as a sensitizer and the other a reporter molecule for the Stark effect, support for the hypothesis that an injected electron influences many sensitizers was garnered.

The Stark effect may influence all of the processes outlined above related to i_{sc} and the sensitization cycle in DSSCs. Photogenerated $\text{TiO}_2(\text{e}^-)$ s that have yet to be collected in the external circuit clearly influence the absorbance spectrum of other sensitizers. The measured blue shifts and decreases of the MLCT absorption are clearly undesirable for solar light harvesting. However, for sensitizers like N3, the effect is quite small and would lead to an insignificant, $<0.001\%$ decrease in LHE at the PP under 1 sun, AM1.5 irradiation. The Stark effect yields a Ru^{II} absorption spectrum that is known to inject poorly when photoexcited.⁴⁰⁵ Excited-state injection yields are also known to decrease with excitation irradiance, yet our understanding of the origin of this behavior is lacking.^{405,428} The observations discussed here suggest that coulombic repulsion by injected electrons may be responsible. Durrant and coworkers have in fact shown that by increasing the $\text{TiO}_2(\text{e}^-)$ concentration, the half-life for recombination to the oxidized sensitizers increased by up to seven orders of magnitude.⁴²⁹ On the other hand, *complete shielding* by the supporting electrolyte would be expected to facilitate longer lived charge-separated states between the $\text{TiO}_2(\text{e}^-)$ s and oxidized sensitizers.

In agreement with previous work, the overall timescales for complete charge recombination of the injected $\text{TiO}_2(\text{e}^-)$ were microseconds to PTZ^+ ,³⁴³ tens of microseconds to milliseconds to the oxidized sensitizer,^{343,405,429} and hundreds of milliseconds to I_3^- .^{377,430,431} The electric field at the TiO_2 interface may also help clarify why recombination to cationic one-electron acceptors, like PTZ^+ or the oxidized sensitizer, is much more rapid than to anionic triiodide. The few orders-of-magnitude slower recombination kinetics seen with anionic triiodide may result from coulombic repulsion between $\text{TiO}_2(\text{e}^-)$ s and I_3^- . Synonymous to increasing the width of the space-charge layer in solid-state p-n junction solar cells, increasing the Debye length for screening should aid in the generation of even further spatially separated and longer lived anionic species, i.e., $\text{TiO}_2(\text{e}^-)$ s and I_3^- . Although speculative, the lethargic pace of this additional screening step may help explain why iodide is far superior to most other donors for redox mediation in DSSCs.

6 CONCLUSIONS

Almost two decades have passed since the celebrated Grätzel and O'Regan paper appeared in *Nature*. This article demonstrates the tremendous progress that has since been made toward developing a molecular-level understanding of charge-transfer processes at sensitized TiO_2 interfaces. The timescales and dynamics for excited-state electron

injection into TiO₂ have been quantified precisely under many experimental conditions. Regeneration of the photo-oxidized sensitizer by a variety of outer-sphere electron donors, including iodide, has also been quantified in some detail. Much less progress has been made toward our understanding of the unwanted, charge-recombination to the oxidized form of the redox mediators. This is due, at least in part, to the inefficiency of the process which makes characterization difficult. Fundamental data on the identity of the acceptor(s) as well as the reduction mechanism(s) are still lacking. Given the keen interest in these reactions, rapid progress is expected. Understanding the mechanism for charge recombination may ultimately enable the use of alternative redox mediators that are better optimized for light-to-electrical power conversion. In addition, it may prove possible to drive redox reactions to produce useful fuels that can be utilized for power when the sun is down. Inorganic chemistry has played a central role in the development of state-of-the-art, 11+0% efficient dye-sensitized solar cells. There exist exciting opportunities for inorganic chemists in the development of future-generation mesoscopic semiconductor thin films, sensitizer coordination chemistry, and redox mediators.

7 ACKNOWLEDGMENTS

This work was funded by the Division of Chemical Sciences, Geosciences, and Biosciences, Office of Basic Energy Sciences of the U.S. Department of Energy through Grant DE-DE-FC02-96ER14662. S. A. acknowledges a Johns Hopkins University Greer graduate student fellowship.

8 END NOTES

^a Analogs where one or more of the carboxylic acid groups have been deprotonated, e.g., the dianion salt of N3 with tetra-*n*-butylammonium (TBA⁺) counterions—N719,³⁴ where three covalently joined 4-carboxylic acid-pyridine substituents were employed,⁵⁰ or where hydrophobic groups were introduced in the 4 and 4' positions of one of the dcB ligands to increase stability in the presence of water.

^b We emphasize that while the scheme and this abbreviation imply that the reduction is metal based, it may in fact be ligand localized, i.e., on a dcB.

9 RELATED ARTICLES

Dye-Sensitized Solar Cells: an Overview.

10 ABBREVIATIONS AND ACRONYMS

TBA⁺ = tetra-*n*-butylammonium; bfimbz = 1,4-bis(phen-[5,6-*d*]imidazol-2-yl)benzene; bpz = bipyrazine; DFT = density functional theory; DSSCs = dye-sensitized solar cells; EXAFS = extended X-ray absorption fine spectroscopy; FTO = fluorine-doped tin oxide; HOMO = highest occupied molecular orbital; IPCE = incident photon-to-current efficiency; IVCT = Intervalence charge-transfer; LF = ligand-field; LIESST = light-induced excited spin-state trapping; LLCT = ligand-to-ligand charge-transfer; LMCT = ligand-to-metal charge transfer LPCT = ligand-to-particle charge-transfer MLCT = metal-to-ligand charge-transfer; MPCT = metal-to-particle charge transfer; NREL = National Renewable Energy Laboratory; phen = phenanthroline; PP = power point; PTZ = phenothiazine; PZZP = point of zero ζ -potential; THz-TD = terahertz time-domain; tpphz = tetrapyrido [3,2-*a* : 2', 3'-*c* : 3'', 2''-*h* : 2''', 3'''-*j*] phenazine; TRIR = time-resolved infrared; XANES = X-ray absorption near-edge structure *LHE* = *light* - *harvesting* efficiency.

11 FURTHER READING

H. Wolpher, S. Sinha, J. Pan, A. Johansson, M. J. Lundqvist, P. Persson, R. Lomoth, J. Bergquist, L. Sun, V. Sundström, B. Akermark, and T. Polivka, *Inorg. Chem.*, 2007, **46**, 638.

12 REFERENCES

1. M. I. Hoffert, K. Caldeira, A. K. Jain, E. F. Haites, L. D. D. Harvey, S. D. Potter, M. E. Schlesinger, S. H. Schneider, R. G. Watts, T. M. L. Wigley, and D. J. Wuebbles, *Nature*, 1998, **395**, 881.
2. K. Caldeira, A. K. Jain, and M. I. Hoffert, *Science*, 2003, **299**, 2052.
3. United States Department of Energy, Report of the Basic Energy Sciences Workshop on Solar Energy Utilization, in 'Basic Research Needs for Solar Energy Utilization', Department of Energy, Washington, DC, 2005.
4. United States Department of Energy Energy Information Administration. <http://www.eia.doe.gov/>. (accessed May 2009).
5. D. Lüthi, M. Le Floch, B. Bereiter, T. Blunier, J.-M. Barnola, U. Siegenthaler, D. Raynaud, J. Jouzel, H. Fischer, K. Kawamura, and T. F. Stocker, *Nature*, 2008, **453**, 379.
6. L. Louergue, A. Schilt, R. Spahni, V. Masson-Delmotte, T. Blunier, B. Lemieux, J.-M. Barnola, D. Raynaud, T. F. Stocker, and J. Chappellaz, *Nature*, 2008, **453**, 383.
7. N. S. Lewis and D. G. Nocera, *Proc. Natl. Acad. Sci. U. S. A.*, 2006, **103**, 15729.
8. J. R. Petit, J. Jouzel, D. Raynaud, N. I. Barkov, J. M. Barnola, I. Basile, M. Bender, J. Chappellaz, M. Davis, G. Delaygue,

- M. Delmotte, V. M. Kotlyakov, M. Legrand, V. Y. Lipenkov, C. Lorus, L. Pepin, C. Ritz, E. Saltzman, and M. Stievenard, *Nature*, 1999, **399**, 429.
9. U. Siegenthaler, T. F. Stocker, E. Monnin, D. Lüthi, J. Schwander, B. Stauffer, D. Raynaud, J.-M. Barnola, H. Fischer, V. Masson-Delmotte, and J. Jouzel, *Science*, 2005, **310**, 1313.
 10. N. S. Lewis, 'Powering the Planet - Global Energy Perspective', <http://nsl.caltech.edu/energy.html>. (accessed May 2009).
 11. United Nations, World Energy Assessment Report: Energy and the Challenge of Sustainability, in 'United Nations Development Program', United Nations, New York, 2003.
 12. B. O'Regan, J. Moser, M. Anderson, and M. Grätzel, *J. Phys. Chem.*, 1990, **94**, 8720.
 13. B. O'Regan and M. Grätzel, *Nature*, 1991, **353**, 737.
 14. S. Ito, M. K. Nazeeruddin, P. Liska, P. Comte, R. Charvet, P. Péchy, M. Jirousek, A. Kay, S. M. Zakeeruddin, and M. Grätzel, *Prog. Photovolt. Res. Appl.*, 2006, **14**, 589.
 15. A. G. Martin, E. Keith, H. Yoshihiro, and W. Wilhelm, *Prog. Photovolt. Res. Appl.*, 2009, **17**, 85.
 16. F. Gao, Y. Wang, D. Shi, J. Zhang, M. Wang, X. Jing, R. Humphry-Baker, P. Wang, S. M. Zakeeruddin, and M. Grätzel, *J. Am. Chem. Soc.*, 2008, **130**, 10720.
 17. Y. Chiba, A. Islam, Y. Watanabe, R. Komiya, N. Koide, and L. Han, *Jpn. J. Appl. Phys., Part 2*, 2006, **45**, L638.
 18. J. M. Kroon, N. J. Bakker, H. J. P. Smit, P. Liska, K. R. Thampi, P. Wang, S. M. Zakeeruddin, M. Grätzel, A. Hinsch, S. Hore, U. Würfel, R. Sastrawan, J. R. Durrant, E. Palomares, H. Pettersson, T. Gruszecski, J. Walter, K. Skupien, and G. E. Tulloch, *Prog. Photovolt. Res. Appl.*, 2007, **15**, 1.
 19. Y. Cao, Y. Bai, Q. Yu, Y. Cheng, S. Liu, D. Shi, F. Gao, and P. Wang, *J. Phys. Chem. C*, 2009, **113**, 6290.
 20. A. Hagfeldt and M. Grätzel, *Acc. Chem. Res.*, 2000, **33**, 269.
 21. S. Ardo and G. J. Meyer, *Chem. Soc. Rev.*, 2009, **38**, 115.
 22. G. J. Meyer, *Inorg. Chem.*, 2005, **44**, 6852.
 23. M. Grätzel, *Inorg. Chem.*, 2005, **44**, 6841.
 24. T. J. Meyer, *Pure Appl. Chem.*, 1986, **58**, 1193.
 25. P. Chen and T. J. Meyer, *Chem. Rev.*, 1998, **98**, 1439.
 26. T. J. Meyer, *Prog. Inorg. Chem.*, 1983, **30**, 389.
 27. T. J. Meyer, *Acc. Chem. Res.*, 1989, **22**, 163.
 28. A. Juris, V. Balzani, F. Barigelletti, S. Campagna, P. Belser, and A. von Zelewsky, *Coord. Chem. Rev.*, 1988, **84**, 85.
 29. S. I. Gorelsky, E. S. Dodsworth, A. B. P. Lever, and A. A. Vlcek, *Coord. Chem. Rev.*, 1998, **174**, 469.
 30. A. B. P. Lever, 'Excited State and Reactive Intermediates', American Chemical Society, Washington, DC, 1986.
 31. K. Kalyanasundaram and M. Grätzel, 'Photosensitization and Photocatalysis Using Inorganic and Organometallic Compounds', Kluwer Academic Publishers, Dordrecht, Netherlands, 1993.
 32. K. Kalyanasundaram, *Coord. Chem. Rev.*, 1982, **46**, 159.
 33. M. K. Nazeeruddin, A. Kay, I. Rodicio, R. Humphry-Baker, E. Mueller, P. Liska, N. Vlachopoulos, and M. Grätzel, *J. Am. Chem. Soc.*, 1993, **115**, 6382.
 34. M. K. Nazeeruddin, S. M. Zakeeruddin, R. Humphry-Baker, M. Jirousek, P. Liska, N. Vlachopoulos, V. Shklover, C. H. Fischer, and M. Grätzel, *Inorg. Chem.*, 1999, **38**, 6298.
 35. A. Hagfeldt and M. Grätzel, *Chem. Rev.*, 1995, **95**, 49.
 36. S. Ardo, Y. Sun, A. Staniszewski, F. N. Castellano and G. J. Meyer, Stark Effects after Excited-State Interfacial Electron Transfer at Sensitized TiO₂ Nanocrystallites, *J. Am. Chem. Soc.*, 2010, **132**, 6696.
 37. M. Grätzel, *Catech*, 1999, **3**, 4.
 38. K. Laqua, W. H. Melhuish, and M. Zander, *Pure Appl. Chem.*, 1988, **60**, 1449.
 39. G. M. Hasselman, D. F. Watson, J. R. Stromberg, D. F. Bocian, D. Holten, J. S. Lindsey, and G. J. Meyer, *J. Phys. Chem. B*, 2006, **110**, 25430.
 40. G. P. Smestad and M. Grätzel, *J. Chem. Educ.*, 1998, **75**, 752.
 41. National Renewable Energy Laboratory Reference Solar Spectral Irradiance: Air Mass 1.5. <http://rredc.nrel.gov/solar/spectra/am1.5/>. (accessed May 2009).
 42. W. Shockley and H. J. Queisser, *J. Appl. Phys.*, 1961, **32**, 510.
 43. R. T. Ross and A. J. Nozik, *J. Appl. Phys.*, 1982, **53**, 3813.
 44. A. De Vos, *J. Phys. D: Appl. Phys.*, 1980, **13**, 839.
 45. R. T. Ross and J. M. Collins, *J. Appl. Phys.*, 1980, **51**, 4504.
 46. J. R. Bolton, *Science*, 1978, **202**, 705.
 47. R. T. Ross and T.-L. Hsiao, *J. Appl. Phys.*, 1977, **48**, 4783.
 48. M. Grätzel, *Acc. Chem. Res.*, 2009, ASAP **42**(11), 1788.
 49. B. C. O'Regan and J. R. Durrant, *Acc. Chem. Res.*, 2009, ASAP **42**(11), 1799.
 50. M. K. Nazeeruddin, P. Péchy, and M. Grätzel, *Chem. Commun.*, 1997, 1705.
 51. M. K. Nazeeruddin, P. Péchy, T. Renouard, S. M. Zakeeruddin, R. Humphry-Baker, P. Comte, P. Liska, L. Cevey, E. Costa, V. Shklover, L. Spiccia, G. B. Deacon, C. A. Bignozzi, and M. Grätzel, *J. Am. Chem. Soc.*, 2001, **123**, 1613.
 52. M. Grätzel, *J. Photochem. Photobiol. C Photochem. Rev.*, 2003, **4**, 145.
 53. J. P. Paris and W. W. Brandt, *J. Am. Chem. Soc.*, 1959, **81**, 5001.
 54. F. E. Lytle and D. M. Hercules, *J. Am. Chem. Soc.*, 1969, **91**, 253.
 55. F. Felix, J. Ferguson, H. U. Guedel, and A. Ludi, *J. Am. Chem. Soc.*, 1980, **102**, 4096.
 56. G. A. Crosby, K. W. Hipps, and W. H. Elfring, *J. Am. Chem. Soc.*, 1974, **96**, 629.
 57. E. M. Kober and T. J. Meyer, *Inorg. Chem.*, 1982, **21**, 3967.
 58. A. W. Adamson and J. N. Demas, *J. Am. Chem. Soc.*, 1971, **93**, 1800.
 59. G. A. Crosby and J. N. Demas, *J. Am. Chem. Soc.*, 1971, **93**, 2841.

60. J. N. Demas and D. G. Taylor, *Inorg. Chem.*, 1979, **18**, 3177.
61. H. Yersin and E. Gallhuber, *J. Am. Chem. Soc.*, 1984, **106**, 6582.
62. H. Yersin, E. Gallhuber, A. Vogler, and H. Kunkely, *J. Am. Chem. Soc.*, 1983, **105**, 4155.
63. G. D. Hager and G. A. Crosby, *J. Am. Chem. Soc.*, 1975, **97**, 7031.
64. G. D. Hager, R. J. Watts, and G. A. Crosby, *J. Am. Chem. Soc.*, 1975, **97**, 7037.
65. R. W. Harrigan and G. A. Crosby, *J. Chem. Phys.*, 1973, **59**, 3468.
66. R. W. Harrigan, G. D. Hager, and G. A. Crosby, *Chem. Phys. Lett.*, 1973, **21**, 487.
67. K. W. Hipps and G. A. Crosby, *J. Am. Chem. Soc.*, 1975, **97**, 7042.
68. P. D. Fleischauer, A. W. Adamson, and G. Sartori, *Prog. Inorg. Chem.*, 1972, **17**, 1.
69. A. W. Adamson, *J. Chem. Educ.*, 1983, **60**, 797.
70. C. Daul, E. J. Baerends, and P. Vermooijs, *J. Am. Chem. Soc.*, 1994, **33**, 3538.
71. S. Wallin, J. Davidsson, J. Modin, and L. Hammarstrom, *J. Phys. Chem. A*, 2005, **109**, 4697.
72. A. T. Yeh, C. V. Shank, and J. K. McCusker, *Science*, 2000, **289**, 935.
73. E. M. Kober, B. P. Sullivan, and T. J. Meyer, *Inorg. Chem.*, 1984, **23**, 2098.
74. R. F. Dallinger and W. H. Woodruff, *J. Am. Chem. Soc.*, 1979, **101**, 4391.
75. D. H. Oh and S. G. Boxer, *J. Am. Chem. Soc.*, 1989, **111**, 1130.
76. M. A. Webb, F. J. Knorr, and J. L. McHale, *J. Raman Spectrosc.*, 2001, **32**, 481.
77. A. Cannizzo, F. van Mourik, W. Gawelda, G. Zgrablic, C. Bressler, and M. Chergui, *Angew. Chem., Int. Ed. Engl.*, 2006, **45**, 3174.
78. H. Yersin, W. Humbs, and J. Strasser, *Coord. Chem. Rev.*, 1997, **159**, 325.
79. S. Wallin, J. Davidsson, J. Modin, and L. Hammarström, *J. Phys. Chem. A*, 2005, **109**, 9378.
80. C. W. Chang, C. K. Chou, I. J. Chang, Y. P. Lee, and E. W. G. Diau, *J. Phys. Chem. C*, 2007, **111**, 13288.
81. R. A. Malone and D. F. Kelley, *J. Chem. Phys.*, 1991, **95**, 8970.
82. L. F. Cooley, P. Bergquist, and D. F. Kelley, *J. Am. Chem. Soc.*, 1990, **112**, 2612.
83. J. Van Houten and R. J. Watts, *J. Am. Chem. Soc.*, 1976, **98**, 4853.
84. W. Siebrand, *J. Chem. Phys.*, 1966, **44**, 4055.
85. R. Englman and J. Jortner, *Mol. Phys.*, 1970, **18**, 145.
86. K. F. Freed and J. Jortner, *J. Chem. Phys.*, 1970, **52**, 6272.
87. M. Bixon and J. Jortner, *J. Chem. Phys.*, 1968, **48**, 715.
88. G. W. Robinson and R. P. Frosch, *J. Chem. Phys.*, 1963, **38**, 1187.
89. W. Gawelda, V.-T. Pham, M. Benfatto, Y. Zaushitsyn, M. Kaiser, D. Grolimund, S. L. Johnson, R. Abela, A. Hauser, C. Bressler, and M. Chergui, *Phys. Rev. Lett.*, 2007, **98**, 057401.
90. C. Cristina, P.-S. Mirabelle, E. Amal, B. Christian, van. M. Frank, C. Andrea, and C. Majed, *Angew. Chem., Int. Ed. Engl.*, 2009, **48**, 7184.
91. W. Gawelda, A. Cannizzo, V.-T. Pham, F. van Mourik, C. Bressler, and M. Chergui, *J. Am. Chem. Soc.*, 2007, **129**, 8199.
92. C. Bressler, C. Milne, V. T. Pham, A. ElNahhas, R. M. van der Veen, W. Gawelda, S. Johnson, P. Beaud, D. Grolimund, M. Kaiser, C. N. Borca, G. Ingold, R. Abela, and M. Chergui, *Science*, 2009, **323**, 489.
93. W. Gawelda, A. Cannizzo, V.-T. Phama, A. El Nahhasa, C. J. Milnea, R. van der Veena, C. Bresslera, and M. Chergui, *Chimia*, 2007, **61**, 179.
94. W. Gawelda, V. T. Pham, R. M. van der Veen, D. Grolimund, R. Abela, M. Chergui, and C. Bressler, *J. Chem. Phys.*, 2009, **130**, 124520.
95. A. L. Smeigh, M. Creelman, R. A. Mathies, and J. K. McCusker, *J. Am. Chem. Soc.*, 2008, **130**, 14105.
96. M. Khalil, M. A. Marcus, A. L. Smeigh, J. K. McCusker, H. H. W. Chong, and R. W. Schoenlein, *J. Phys. Chem. A*, 2006, **110**, 38.
97. N. Huse, M. Khalil, T. K. Kim, A. L. Smeigh, L. Jamula, J. K. McCusker, and R. W. Schoenlein, *J. Phys. Conf. Series*, 2009, **148**, 012043.
98. H.-L. Xia, S. Ardo, A. A. Narducci Sarjeant, S. Huang, and G. J. Meyer, *Langmuir*, 2009, ASAP **25**(23), 13641.
99. A. Hauser, J. Adler, and P. Güttlich, *Chem. Phys. Lett.*, 1988, **152**, 468.
100. J. H. Alstrum-Acevedo, M. K. Brennaman, and T. J. Meyer, *Inorg. Chem.*, 2005, **44**, 6802.
101. P. Persson, R. Bergström, L. Ojamäe, and S. Lunell, Quantum-chemical Studies of Metal Oxides for Photoelectrochemical Applications, in 'Advances in Quantum Chemistry', ed. J. Sabin Academic Press, 2002, Vol. 41, p. 203.
102. H. Rensmo, S. Lunell, and H. Siegbahn, *J. Photochem. Photobiol. A Chem.*, 1998, **114**, 117.
103. H. Rensmo, S. Södergren, L. Patthey, K. Westermark, L. Vayssieres, O. Kohle, P. A. Brühwiler, A. Hagfeldt, and H. Siegbahn, *Chem. Phys. Lett.*, 1997, **274**, 51.
104. S. A. Haque, E. Palomares, B. M. Cho, A. N. M. Green, N. Hirata, D. R. Klug, and J. R. Durrant, *J. Am. Chem. Soc.*, 2005, **127**, 3456.
105. J. R. Durrant, S. A. Haque, and E. Palomares, *Coord. Chem. Rev.*, 2004, **248**, 1247.
106. L. C. T. Shoute and G. R. Loppnow, *J. Am. Chem. Soc.*, 2003, **125**, 15636.
107. D. F. Watson and G. J. Meyer, *Coord. Chem. Rev.*, 2004, **248**, 1391.

108. A. Staniszewski, S. Ardo, Y. Sun, F. N. Castellano, and G. J. Meyer, *J. Am. Chem. Soc.*, 2008, **130**, 11586.
109. H. J. Snaith, S. M. Zakeeruddin, L. Schmidt-Mende, C. Klein, and M. Grätzel, *Angew. Chem., Int. Ed. Engl.*, 2005, **44**, 6413.
110. D. Kuang, C. Klein, H. J. Snaith, J.-E. Moser, R. Humphry-Baker, P. Comte, S. M. Zakeeruddin, and M. Grätzel, *Nano Lett.*, 2006, **6**, 769.
111. D. Kuang, C. Klein, H. J. Snaith, R. Humphry-Baker, S. M. Zakeeruddin, and M. Grätzel, *Inorg. Chim. Acta*, 2008, **361**, 699.
112. P. Wang, C. Klein, R. Humphry-Baker, S. M. Zakeeruddin, and M. Grätzel, *Appl. Phys. Lett.*, 2005, **86**, 123508.
113. S. M. Zakeeruddin, M. K. Nazeeruddin, R. Humphry-Baker, P. Péchy, P. Quagliotto, C. Barolo, G. Viscardi, and M. Grätzel, *Langmuir*, 2002, **18**, 952.
114. P. Wang, S. M. Zakeeruddin, J. E. Moser, M. K. Nazeeruddin, T. Sekiguchi, and M. Grätzel, *Nat. Mater.*, 2003, **2**, 402.
115. P. Wang, C. Klein, R. Humphry-Baker, S. M. Zakeeruddin, and M. Grätzel, *J. Am. Chem. Soc.*, 2005, **127**, 808.
116. D. Kuang, S. Ito, B. Wenger, C. Klein, J. E. Moser, R. Humphry-Baker, S. M. Zakeeruddin, and M. Grätzel, *J. Am. Chem. Soc.*, 2006, **128**, 4146.
117. M. K. Nazeeruddin, S. M. Zakeeruddin, J. J. Lagref, P. Liska, P. Comte, C. Barolo, G. Viscardi, K. Schenk, and M. Grätzel, *Coord. Chem. Rev.*, 2004, **248**, 1317.
118. J. E. Kroeze, N. Hirata, S. Koops, M. K. Nazeeruddin, L. Schmidt-Mende, M. Grätzel, and J. R. Durrant, *J. Am. Chem. Soc.*, 2006, **128**, 16376.
119. L. Schmidt-Mende, J. E. Kroeze, J. R. Durrant, M. K. Nazeeruddin, and M. Grätzel, *Nano Lett.*, 2005, **5**, 1315.
120. C. Klein, M. K. Nazeeruddin, D. Di Censo, P. Liska, and M. Grätzel, *Inorg. Chem.*, 2004, **43**, 4216.
121. P. Wang, C. Klein, J.-E. Moser, R. Humphry-Baker, N.-L. Cevey-Ha, R. Charvet, P. Comte, S. M. Zakeeruddin, and M. Grätzel, *J. Phys. Chem. B*, 2004, **108**, 17553.
122. Z. Jin, H. Masuda, N. Yamanaka, M. Minami, T. Nakamura, and Y. Nishikitani, *ChemSusChem*, 2008, **1**, 901.
123. Z. Jin, H. Masuda, N. Yamanaka, M. Minami, T. Nakamura, and Y. Nishikitani, *Chem. Lett.*, 2009, **38**, 44.
124. K. L. McCall, J. R. Jennings, H. Wang, A. Morandeira, L. M. Peter, J. R. Durrant, L. J. Yellowlees, J. D. Woollins, and N. Robertson, *J. Photochem. Photobiol. A Chem.*, 2009, **202**, 196.
125. K. Kalyanasundaram, N. Vlachopoulos, V. Krishnan, A. Monnier, and M. Grätzel, *J. Phys. Chem.*, 1987, **91**, 2342.
126. N. R. de Tacconi, C. R. Chenthamarakshan, G. Yogeewaran, A. Watcharenwong, R. S. de Zoysa, N. A. Basit, and K. Rajeshwar, *J. Phys. Chem. B*, 2006, **110**, 25347.
127. M. Paulose, H. E. Prakasham, O. K. Varghese, L. Peng, K. C. Popat, G. K. Mor, T. A. Desai, and C. A. Grimes, *J. Phys. Chem. C*, 2007, **111**, 14992.
128. A. Hagfeldt, N. Vlachopoulos, S. Gilbert, and M. Grätzel, in *Electrochromic Switching with Nanocrystalline TiO₂ Semiconductor Films*, in 'Optical Materials Technology for Energy Efficiency and Solar Energy Conversion XIII', ed. V. Wittwer, C.G. Granqvist, C.M. Lampert, Freiburg, Federal Republic of Germany, SPIE, Freiburg, Federal Republic of Germany, 1994, **2255**, p. 297.
129. N. R. Kestner, J. Logan, and J. Jortner, *J. Phys. Chem.*, 1974, **78**, 2148.
130. P. F. Bernath, 'Spectra of Atoms and Molecules', 2nd edition, Oxford University Press, New York, 2005.
131. P. A. M. Dirac, *Proc. R. Soc. London, A*, 1927, **114**, 243.
132. T. D. Visser, *Am. J. Phys.*, 2009, **77**, 487.
133. J. G. Calvert, J. N. Pitts Jr, 'Photochemistry'. John Wiley & Sons, Inc., New York, 1966.
134. N. H. Damrauer, T. R. Boussie, M. Devenney, and J. K. McCusker, *J. Am. Chem. Soc.*, 1997, **119**, 8253.
135. J. A. Treadway, B. Loeb, R. Lopez, P. A. Anderson, F. R. Keene, and T. J. Meyer, *Inorg. Chem.*, 1996, **35**, 2242.
136. C. C. Phifer and D. R. McMillin, *Inorg. Chem.*, 1986, **25**, 1329.
137. V. Aranyos, J. Hjelm, A. Hagfeldt, and H. Grennberg, *J. Chem. Soc., Dalton Trans.*, 2001, **30**, 1319.
138. K. A. Walters, L. L. Premvardhan, Y. Liu, L. A. Peteanu, and K. S. Schanze, *Chem. Phys. Lett.*, 2001, **339**, 255.
139. Y. Wang, S. Liu, M. R. Pinto, D. M. Dattelbaum, J. R. Schoonover, and K. S. Schanze, *J. Phys. Chem. A*, 2001, **105**, 11118.
140. C. Klein, M. K. Nazeeruddin, P. Liska, D. Di Censo, N. Hirata, E. Palomares, J. R. Durrant, and M. Grätzel, *Inorg. Chem.*, 2004, **44**, 178.
141. P. Wang, C. Klein, R. Humphry-Baker, S. M. Zakeeruddin, and M. Grätzel, *J. Am. Chem. Soc.*, 2004, **127**, 808.
142. P. Wang, S. M. Zakeeruddin, J. E. Moser, R. Humphry-Baker, P. Comte, V. Aranyos, A. Hagfeldt, M. K. Nazeeruddin, and M. Grätzel, *Adv. Mater.*, 2004, **16**, 1806.
143. G. F. Strouse, J. R. Schoonover, R. Duesing, S. Boyde, W. E. Jones, and T. J. Meyer, Jr, *Inorg. Chem.*, 1995, **34**, 473.
144. M. Beley, J.-P. Collin, J.-P. Sauvage, H. Sugihara, F. Heisel, and A. Miehle, *J. Chem. Soc., Dalton Trans.*, 1991, **20**, 3157.
145. R. L. Blakley, M. L. Myrick, R. Pittman, and M. K. De Armond, *J. Phys. Chem.*, 1990, **94**, 4804.
146. L. Hammarström, F. Barigelletti, L. Flamigni, M. T. Indelli, N. Armaroli, G. Calogero, M. Guardigli, A. Sour, J.-P. Collin, and J.-P. Sauvage, *J. Phys. Chem. A*, 1997, **101**, 9061.
147. C. R. Hecker, A. K. I. Gushurst, and D. R. McMillin, *Inorg. Chem.*, 1991, **30**, 538.
148. J. P. Collin, S. Guillerez, J. P. Sauvage, F. Barigelletti, L. De Cola, L. Flamigni, and V. Balzani, *Inorg. Chem.*, 1991, **30**, 4230.
149. J.-P. Collin, S. Guillerez, and J.-P. Sauvage, *J. Chem. Soc., Chem. Commun.*, 1989, **25**, 776.
150. M. Beley, S. Chodorowski, J.-P. Collin, J.-P. Sauvage, L. Flamigni, and F. Barigelletti, *Inorg. Chem.*, 1994, **33**, 2543.

151. F. Barigelletti, L. Flamigni, V. Balzani, J.-P. Collin, J.-P. Sauvage, A. Sour, E. C. Constable, and A. M. W. C. Thompson, *J. Am. Chem. Soc.*, 1994, **116**, 7692.
152. R. S. Mulliken, *J. Am. Chem. Soc.*, 1952, **74**, 811.
153. J. N. Murrell, *J. Am. Chem. Soc.*, 1959, **81**, 5037.
154. S. Fukuzumi, C. L. Wong, and J. K. Kochi, *J. Am. Chem. Soc.*, 1980, **102**, 2928.
155. M. K. Nazeeruddin, Q. Wang, L. Cevey, V. Aranyos, P. Liska, E. Figgemeier, C. Klein, N. Hirata, S. Koops, S. A. Haque, J. R. Durrant, A. Hagfeldt, A. B. P. Lever, and M. Grätzel, *Inorg. Chem.*, 2005, **45**, 787.
156. S. R. Jang, C. Lee, H. Choi, J. J. Ko, J. Lee, R. Vittal, and K. J. Kim, *Chem. Mater.*, 2006, **18**, 5604.
157. D. Kuang, C. Klein, S. Ito, J. E. Moser, R. Humphry-Baker, N. Evans, F. Durrant, C. Grätzel, S. M. Zakeeruddin, and M. Grätzel, *Adv. Mater.*, 2007, **19**, 1133.
158. C. Lee, J.-H. Yum, H. Choi, S. Ook Kang, J. Ko, R. Humphry-Baker, M. Grätzel, and M. K. Nazeeruddin, *Inorg. Chem.*, 2007, **47**, 2267.
159. M. K. Nazeeruddin, T. Bessho, L. Cevey, S. Ito, C. Klein, F. De Angelis, S. Fantacci, P. Comte, P. Liska, H. Imai, and M. Grätzel, *J. Photochem. Photobiol. A Chem.*, 2007, **185**, 331.
160. A. Abbotto, C. Barolo, L. Bellotto, F. D. Angelis, M. Grätzel, N. Manfredi, C. Marinzi, S. Fantacci, J.-H. Yum, and M. K. Nazeeruddin, *Chem. Commun.*, 2008, 5318.
161. A. Abbotto, C. Barolo, J.-H. Yum, L. Bellotto, F. De Angelis, M. Grätzel, C. Marinzi, and M. K. Nazeeruddin, Ruthenium Sensitizers Based on Heteroaromatic Conjugated Bipyridines for Dye-sensitized Solar Cells, in 'Organic Optoelectronics and Photonics III, Strasbourg, France, 2008', ed. P. L. Heremans, M. Muccini, E. A. Meulenkamp, SPIE, Strasbourg, France, 2008, **6999**, p. 69990O.
162. H. Choi, C. Baik, S. Kim, M.-S. Kang, X. Xu, H. S. Kang, S. O. Kang, J. Ko, M. K. Nazeeruddin, and M. Grätzel, *New J. Chem.*, 2008, **32**, 2233.
163. F. Gao, Y. Wang, J. Zhang, D. Shi, M. Wang, R. Humphry-Baker, P. Wang, S. M. Zakeeruddin, and M. Grätzel, *Chem. Commun.*, 2008, 2635.
164. H. J. Snaith, C. S. Karthikeyan, A. Petrozza, J. Teuscher, J. E. Moser, M. K. Nazeeruddin, M. Thelakkat, and M. Grätzel, *J. Phys. Chem. C*, 2008, **112**, 7562.
165. A. Staniszewski, W. B. Heuer, and G. J. Meyer, *Inorg. Chem.*, 2008, **47**, 7062.
166. S.-R. Jang, J.-H. Yum, C. Klein, K.-J. Kim, P. Wagner, D. Officer, M. Grätzel, and M. K. Nazeeruddin, *J. Phys. Chem. C*, 2009, **113**, 1998.
167. J.-H. Yum, I. Jung, C. Baik, J. Ko, M. K. Nazeeruddin, and M. Grätzel, *Energy Environ. Sci.*, 2009, **2**, 100.
168. F. Matar, T. H. Ghaddar, K. Walley, T. DosSantos, J. R. Durrant, and B. O'Regan, *J. Mater. Chem.*, 2008, **18**, 4246.
169. D. Martineau, M. Beley, P. C. Gros, S. Cazzanti, S. Caramori, and C. A. Bignozzi, *Inorg. Chem.*, 2007, **46**, 2272.
170. D. Shi, N. Pootrakulchote, R. Li, J. Guo, Y. Wang, S. M. Zakeeruddin, M. Grätzel, and P. Wang, *J. Phys. Chem. C*, 2008, **112**, 17046.
171. Q. Yu, S. Liu, M. Zhang, N. Cai, Y. Wang, and P. Wang, *J. Phys. Chem. C*, 2009, **113**, 14559.
172. C. Y. Chen, H. C. Lu, C. G. Wu, J. G. Chen, and K. C. Ho, *Adv. Func. Mater.*, 2007, **17**, 29.
173. C.-Y. Chen, S.-J. Wu, C.-G. Wu, J.-G. Chen, and K.-C. Ho, *Angew. Chem., Int. Ed. Engl.*, 2006, **45**, 5822.
174. C. Y. Chen, S. J. Wu, J. Y. Li, C. G. Wu, J. G. Chen, and K. C. Ho, *Adv. Mater. (Weinheim, Fed. Repub. Ger.)*, 2007, **19**, 3888.
175. F. Sauvage, M. K. R. Fischer, A. Mishra, S. M. Zakeeruddin, M. K. Nazeeruddin, P. Bäuerle, and M. Grätzel, *ChemSusChem*, 2009, **2**, 761.
176. S. A. Haque, S. Handa, K. Peter, E. Palomares, M. Thelakkat, and J. R. Durrant, *Angew. Chem., Int. Ed. Engl.*, 2005, **44**, 5740.
177. N. Hirata, J.-J. Lagref, E. J. Palomares, J. R. Durrant, M. K. Nazeeruddin, M. Grätzel, and D. Di Censo, *Chem. Eur. J.*, 2004, **10**, 595.
178. F. Gao, Y. Cheng, Q. Yu, S. Liu, D. Shi, Y. Li, and P. Wang, *Inorg. Chem.*, 2009, **48**, 2664.
179. C. Lee, J.-H. Yum, H. Choi, S. Ook Kang, J. Ko, R. Humphry-Baker, M. Grätzel, and M. K. Nazeeruddin, *Inorg. Chem.*, 2008, **47**, 2267.
180. V. Balzani, L. Moggi, and F. Scandola, Towards a Supramolecular Photochemistry: Assembly of Molecular Components to Obtain Photochemical Molecular Devices, in 'Supramolecular Photochemistry', ed. V. Balzani, D. Reidel Publishing Co., Dordrecht, Holland, 1987, p. 1.
181. C. A. Bignozzi, R. Argazzi, M. T. Indelli, and F. Scandola, *Sol. Energy Mater.*, 1994, **32**, 229.
182. C. A. Bignozzi, R. Argazzi, F. Scandola, J. R. Schoonover, and G. J. Meyer, *Sol. Energy Mater.*, 1995, **38**, 187.
183. R. Amadelli, R. Argazzi, C. A. Bignozzi, and F. Scandola, *J. Am. Chem. Soc.*, 1990, **112**, 7099.
184. M. K. Nazeeruddin, P. Liska, J. Moser, N. Vlachopoulos, and M. Grätzel, *Helv. Chim. Acta*, 1990, **73**, 1788.
185. D. Holten, D. F. Bocian, and J. S. Lindsey, *Acc. Chem. Res.*, 2002, **35**, 57.
186. R. J. Forster, T. E. Keyes, and J. G. Vos, 'Interfacial Supramolecular Assemblies', John Wiley & Sons Ltd., Chichester, 2003, p. 317.
187. F. Gajardo, A. M. Leiva, B. Loeb, A. Delgadillo, J. R. Stromberg, and G. J. Meyer, *Inorg. Chim. Acta*, 2008, **361**, 613.
188. S. Altobello, R. Argazzi, S. Caramori, C. Contado, S. D. Fre, P. Rubino, C. Chone, G. Larramona, and C. A. Bignozzi, *J. Am. Chem. Soc.*, 2005, **127**, 15342.
189. T. Bessho, E. Yoneda, J.-H. Yum, M. Guglielmi, I. Tavernelli, H. Imai, U. Rothlisberger, M. K. Nazeeruddin, and M. Grätzel, *J. Am. Chem. Soc.*, 2009, **131**, 5930.

190. M. Yang, D. W. Thompson, and G. J. Meyer, *Inorg. Chem.*, 2002, **41**, 1254.
191. R. Argazzi, C. A. Bignozzi, M. Yang, G. M. Hasselmann, and G. J. Meyer, *Nano Lett.*, 2002, **2**, 625.
192. R. Argazzi, C. A. Bignozzi, T. A. Heimer, F. N. Castellano, and G. J. Meyer, *Inorg. Chem.*, 1994, **33**, 5741.
193. T. A. Heimer, E. J. Heilweil, C. A. Bignozzi, and G. J. Meyer, *J. Phys. Chem. A*, 2000, **104**, 4256.
194. H. Zabri, I. Gillaizeau, C. A. Bignozzi, S. Caramori, M.-F. Charlot, J. Cano-Boquera, and F. Odobel, *Inorg. Chem.*, 2003, **42**, 6655.
195. Y.-J. Hou, P.-H. Xie, B.-W. Zhang, Y. Cao, X.-R. Xiao, and W.-B. Wang, *Inorg. Chem.*, 1999, **38**, 6320.
196. P.-H. Xie, Y.-J. Hou, T.-X. Wei, B.-W. Zhang, Y. Cao, and C.-H. Huang, *Inorg. Chim. Acta*, 2000, **308**, 73.
197. S. R. L. Fernando, M. Y. Ogawa, *Chem. Commun.*, 1996, 637.
198. P.-H. Xie, Y.-J. Hou, B.-W. Zhang, and Y. Cao, *J. Photochem. Photobiol. A Chem.*, 1999, **122**, 169.
199. A. Kukrek, D. Wang, Y. Hou, R. Zong, and R. Thummel, *Inorg. Chem.*, 2006, **45**, 10131.
200. C. Barolo, M. K. Nazeeruddin, S. Fantacci, D. Di Censo, P. Comte, P. Liska, G. Viscardi, P. Quagliotto, F. De Angelis, S. Ito, and M. Grätzel, *Inorg. Chem.*, 2006, **45**, 4642.
201. E. M. Kober, B. P. Sullivan, W. J. Dressick, J. V. Caspar, and T. J. Meyer, *J. Am. Chem. Soc.*, 1980, **102**, 7383.
202. C. Creutz, M. Chou, T. L. Netzel, M. Okumura, and N. Sutin, *J. Am. Chem. Soc.*, 1980, **102**, 1309.
203. J. V. Caspar, E. M. Kober, B. P. Sullivan, and T. J. Meyer, *J. Am. Chem. Soc.*, 1982, **104**, 630.
204. G. H. Allen, B. P. Sullivan, and T. J. Meyer, *J. Chem. Soc., Chem. Commun.*, 1981, 793.
205. P. F. H. Schwab, S. Diegoli, M. Biancardo, and C. A. Bignozzi, *Inorg. Chem.*, 2003, **42**, 6613.
206. B. E. Hardin, E. T. Hoke, P. B. Armstrong, J.-H. Yum, P. Comte, T. Torres, J. M. J. Frechet, M. K. Nazeeruddin, M. Grätzel, and M. D. McGehee, *Nature Photon.*, 2009, **3**, 406.
207. J. B. Asbury, E. Hao, Y. Wang, H. N. Ghosh, and T. Lian, *J. Phys. Chem. B*, 2001, **105**, 4545.
208. J. B. Asbury, E. Hao, Y. Wang, and T. Lian, *J. Phys. Chem. B*, 2000, **104**, 11957.
209. G. M. Hasselmann and G. J. Meyer, *Z. Phys. Chem. (Munich)*, 1999, **212**, 39.
210. G. M. Hasselmann and G. J. Meyer, *J. Phys. Chem. B*, 1999, **103**, 7671.
211. R. Argazzi, C. A. Bignozzi, T. A. Heimer, and G. J. Meyer, *Inorg. Chem.*, 1997, **36**, 2.
212. N. A. Anderson and T. Lian, *Coord. Chem. Rev.*, 2004, **248**, 1231.
213. C. She, J. Guo, S. Irle, K. Morokuma, D. L. Mohler, H. Zabri, F. Odobel, K. T. Youm, F. Liu, J. T. Hupp, and T. Lian, *J. Phys. Chem. A*, 2007, **111**, 6832.
214. C. She, J. Guo, and T. Lian, *J. Phys. Chem. B*, 2007, **111**, 6903.
215. T. Bessho, E. C. Constable, M. Grätzel, A. H. Redondo, C. E. Housecroft, W. Kylberg, M. K. Nazeeruddin, M. Neuburger, and S. Schaffner, *Chem. Commun.*, 2008, 3717.
216. S. Sakaki, T. Kuroki, and T. Hamada, *J. Chem. Soc., Dalton Trans.*, 2002, **31**, 840.
217. N. Alonso-Vante, J.-F. Nierengarten, and J.-P. Sauvage, *J. Chem. Soc., Dalton Trans.*, 1994, **14**, 1649.
218. S. Chakraborty, T. J. Wadas, H. Hester, R. Schmehl, and R. Eisenberg, *Inorg. Chem.*, 2005, **44**, 6865.
219. P. Du, J. Schneider, F. Li, W. Zhao, U. Patel, F. N. Castellano, and R. Eisenberg, *J. Am. Chem. Soc.*, 2008, **130**, 5056.
220. J. Zhang, P. Du, J. Schneider, P. Jarosz, and R. Eisenberg, *J. Am. Chem. Soc.*, 2007, **129**, 7726.
221. W. Zhao, Y. Sun, and F. N. Castellano, *J. Am. Chem. Soc.*, 2008, **130**, 12566.
222. A. Islam, H. Sugihara, K. Hara, L. P. Singh, R. Katoh, M. Yanagida, Y. Takahashi, S. Murata, and H. Arakawa, *New J. Chem.*, 2000, **24**, 343.
223. E. A. M. Geary, L. J. Yellowlees, L. A. Jack, I. D. H. Oswald, S. Parsons, N. Hirata, J. R. Durrant, and N. Robertson, *Inorg. Chem.*, 2005, **44**, 242.
224. M. Hissler, J. E. McGarrah, W. B. Connick, D. K. Geiger, S. D. Cummings, and R. Eisenberg, *Coord. Chem. Rev.*, 2000, **208**, 115.
225. W. R. McNamara, R. C. Snocberger, G. Li, J. M. Schleicher, C. W. Cady, M. Poyatos, C. A. Schmuttenmaer, R. H. Crabtree, G. W. Brudvig, and V. S. Batista, *J. Am. Chem. Soc.*, 2008, **130**, 14329.
226. S. G. Abuabara, C. W. Cady, J. B. Baxter, C. A. Schmuttenmaer, R. H. Crabtree, G. W. Brudvig, and V. S. Batista, *J. Phys. Chem. C*, 2007, **111**, 11982.
227. G. Li, E. M. Sproviero, R. C. S. Iii, N. Iguchi, J. D. Blakemore, R. H. Crabtree, G. W. Brudvig, and V. S. Batista, *Energy Environ. Sci.*, 2009, **2**, 230.
228. E. A. M. Geary, K. L. McCall, A. Turner, P. R. Murray, E. J. L. McInnes, L. A. Jack, L. J. Yellowlees, and N. Robertson, *Dalton Trans.*, 2008, **37**, 3701.
229. L. P. Moorcraft, A. Morandeira, J. R. Durrant, J. R. Jennings, L. M. Peter, S. Parsons, A. Turner, L. J. Yellowlees, and N. Robertson, *Dalton Trans.*, 2008, **37**, 6940.
230. Z. Ning, Q. Zhang, W. Wu, and H. Tian, *J. Organomet. Chem.*, 2009, **694**, 2705.
231. E. I. Mayo, K. Kilsa, T. Tirrell, P. I. Djurovich, A. Tamayo, M. E. Thompson, N. S. Lewis, and H. B. Gray, *Photochem. Photobiol. Sci.*, 2006, **5**, 871.
232. E. Baranoff, J.-H. Yum, M. Grätzel, and M. K. Nazeeruddin, *J. Organomet. Chem.*, 2009, **694**, 2661.
233. N. Armaroli, *Chem. Soc. Rev.*, 2001, **30**, 113.
234. L. X. Chen, G. Jennings, T. Liu, D. J. Gosztola, J. P. Hessler, D. V. Scaltrito, and G. J. Meyer, *J. Am. Chem. Soc.*, 2002, **124**, 10861.

235. M. Yang, D. W. Thompson, and G. J. Meyer, *Inorg. Chem.*, 2000, **39**, 3738.
236. B. V. Bergeron and G. J. Meyer, *J. Phys. Chem. B*, 2003, **107**, 245.
237. C. Creutz, B. S. Brunschwig, and N. Sutin, *J. Phys. Chem. B*, 2006, **110**, 25181.
238. F. Liu, M. Yang, and G. J. Meyer, Molecule-to-Particle Charge Transfer in Sol-Gel Materials, in 'Handbook of Sol-Gel Science and Technology: Processing Characterization and Application; Volume II: Characterization of Sol-Gel Materials and Products', ed. R. M. Almeida, Kluwer Academic Publishers, Dordrecht, The Netherlands, 2005, Vol. 2, p. 400.
239. E. Vrachnou, M. Grätzel, and A. J. McEvoy, *J. Electroanal. Chem.*, 1989, **258**, 193.
240. E. Vrachnou, N. Vlachopoulos, and M. Grätzel, *Chem. Commun.*, 1987, 868.
241. R. L. Blackburn, C. S. Johnson, and J. T. Hupp, *J. Am. Chem. Soc.*, 1991, **113**, 1060.
242. H. Lu, J. N. Prieskorn, and J. T. Hupp, *J. Am. Chem. Soc.*, 1993, **115**, 4927.
243. S. F. Fischer and R. P. Van Duyne, *Chem. Phys.*, 1977, **26**, 9.
244. J. J. Hopfield, *Proc. Natl. Acad. Sci. U. S. A.*, 1974, **71**, 3640.
245. J. Jortner, *J. Chem. Phys.*, 1976, **64**, 4860.
246. J. Ulstrup and J. Jortner, *J. Chem. Phys.*, 1975, **63**, 4358.
247. R. P. Van Duyne and S. F. Fischer, *Chem. Phys.*, 1974, **5**, 183.
248. M. Khoudiakov, A. R. Parise, and B. S. Brunschwig, *J. Am. Chem. Soc.*, 2003, **125**, 4637.
249. L. Karki and J. T. Hupp, *Inorg. Chem.*, 1997, **36**, 3318.
250. F. W. Vance and J. T. Hupp, *J. Am. Chem. Soc.*, 1999, **121**, 4047.
251. S. J. Hug and S. G. Boxer, *Inorg. Chim. Acta*, 1996, **242**, 323.
252. S. G. Boxer, *J. Phys. Chem. B*, 2009, **113**, 2972.
253. G. U. Bublitz and S. G. Boxer, *Annu. Rev. Phys. Chem.*, 1997, **48**, 213.
254. J. A. Harris, K. Trotter, and B. S. Brunschwig, *J. Phys. Chem. B*, 2007, **111**, 6695.
255. J. Moser, S. PUNCHIHEWA, P. P. Infelta, and M. Grätzel, *Langmuir*, 1991, **7**, 3012.
256. K. A. Walters, D. A. Gaal, and J. T. Hupp, *J. Phys. Chem. B*, 2002, **106**, 5139.
257. A. Nawrocka, A. Zdyb, and S. Krawczyk, *Chem. Phys. Lett.*, 2009, **475**, 272.
258. A. Nawrocka and S. Krawczyk, *J. Phys. Chem. C*, 2008, **112**, 10233.
259. C. R. Rice, M. D. Ward, M. K. Nazeeruddin, and M. Grätzel, *New J. Chem.*, 2000, **24**, 651.
260. S. Verma, P. Kar, A. Das, D. K. Palit, and H. N. Ghosh, *J. Phys. Chem. C*, 2008, **112**, 2918.
261. G. Ramakrishna, D. A. Jose, D. K. Kumar, A. Das, D. K. Palit, and H. N. Ghosh, *J. Phys. Chem. B*, 2005, **109**, 15445.
262. P. Kar, S. Verma, A. Das, and H. N. Ghosh, *J. Phys. Chem. C*, 2009, **113**, 7970.
263. K. Schwarzburg, R. Ernstorfer, S. Felber, and F. Willig, *Coord. Chem. Rev.*, 2004, **248**, 1259.
264. D. F. Watson and G. J. Meyer, *Annu. Rev. Phys. Chem.*, 2005, **56**, 119.
265. M. G. Evans and M. Polanyi, *Trans. Faraday Soc.*, 1935, **31**, 875.
266. H. Eyring, *J. Chem. Phys.*, 1935, **3**, 107.
267. J. B. Asbury, N. A. Anderson, E. Hao, X. Ai, and T. Lian, *J. Phys. Chem. B*, 2003, **107**, 7376.
268. J. B. Asbury, Y.-Q. Wang, E. Hao, H. N. Ghosh, and T. Lian, *Res. Chem. Intermed.*, 2001, **27**, 393.
269. G. Benkő, J. Kallioinen, J. E. I. Korppi-Tommola, A. P. Yartsev, and V. Sundström, *J. Am. Chem. Soc.*, 2002, **124**, 489.
270. R. Ernstorfer, L. Gundlach, S. Felber, W. Storck, R. Eichberger, and F. Willig, *J. Phys. Chem. B*, 2006, **110**, 25383.
271. T. Hannappel, B. Burfeindt, W. Storck, and F. Willig, *J. Phys. Chem. B*, 1997, **101**, 6799.
272. J. Kallioinen, G. Benkő, P. Myllyperkiö, L. Khriachtchev, B. Skarman, R. Wallenberg, M. Tuomikoski, J. Korppi-Tommola, V. Sundström, and A. P. Yartsev, *J. Phys. Chem. B*, 2004, **108**, 6365.
273. J. Kallioinen, G. Benkő, V. Sundström, J. E. I. Korppi-Tommola, and A. P. Yartsev, *J. Phys. Chem. B*, 2002, **106**, 4396.
274. D. Kuciauskas, J. E. Monat, R. Villahermosa, H. B. Gray, N. S. Lewis, and J. K. McCusker, *J. Phys. Chem. B*, 2002, **106**, 9347.
275. A. Morandeira, G. Boschloo, A. Hagfeldt, and L. Hammarström, *J. Phys. Chem. B*, 2005, **109**, 19403.
276. P. Myllyperkiö, G. Benkő, J. Korppi-Tommola, A. P. Yartsev, and V. Sundström, *Phys. Chem. Chem. Phys.*, 2008, **10**, 996.
277. Y. Tachibana, S. A. Haque, I. P. Mercer, J. R. Durrant, and D. R. Klug, *J. Phys. Chem. B*, 2000, **104**, 1198.
278. Y. Tachibana, J. E. Moser, M. Grätzel, D. R. Klug, and J. R. Durrant, *J. Phys. Chem.*, 1996, **100**, 20056.
279. N. S. Hush, *J. Chem. Phys.*, 1958, **28**, 962.
280. N. S. Hush, *Trans. Faraday Soc.*, 1961, **57**, 557.
281. R. A. Marcus, *Annu. Rev. Phys. Chem.*, 1964, **15**, 155.
282. H. Gerischer, *Surf. Sci.*, 1969, **18**, 97.
283. H. Gerischer, *Photochem. Photobiol.*, 1972, **16**, 243.
284. R. A. Marcus and N. Sutin, *Biochim. Biophys. Rev. Bioenerg.*, 1985, **811**, 265.
285. S. Ramakrishna, F. Willig, V. May, and A. Knorr, *J. Phys. Chem. B*, 2003, **107**, 607.
286. W. Stier and O. V. Prezhdo, *J. Phys. Chem. B*, 2002, **106**, 8047.

287. F. Willig, C. Zimmermann, S. Ramakrishna, and W. Storck, *Electrochim. Acta*, 2000, **45**, 4565.
288. C. Zimmermann, F. Willig, S. Ramakrishna, B. Burfeindt, B. Pettinger, R. Eichberger, and W. Storck, *J. Phys. Chem. B*, 2001, **105**, 9245.
289. M. Thoss, I. Kondov, and H. Wang, *Chem. Phys.*, 2004, **304**, 169.
290. G. Benkő, J. Kallioinen, P. Myllyperkiö, F. Trif, J. E. I. Korppi-Tommola, A. P. Yartsev, and V. Sundström, *J. Phys. Chem. B*, 2004, **108**, 2862.
291. Y. Tachibana, M. K. Nazeeruddin, M. Grätzel, D. R. Klug, and J. R. Durrant, *Chem. Phys.*, 2002, **285**, 127.
292. S. E. Kooops, B. C. O'Regan, P. R. F. Barnes, and J. R. Durrant, *J. Am. Chem. Soc.*, 2009, **131**, 4808.
293. B. Wenger, M. Grätzel, and J.-E. Moser, *Chimia*, 2005, **59**, 123.
294. B. Wenger, M. Grätzel, and J. E. Moser, *J. Am. Chem. Soc.*, 2005, **127**, 12150.
295. T. D. M. Bell, C. Pagba, M. Myahkostupov, J. Hofkens, and P. Piotrowiak, *J. Phys. Chem. B*, 2006, **110**, 25314.
296. G. L. Closs and J. R. Miller, *Science*, 1988, **240**, 440.
297. J. F. Smalley, H. O. Finklea, C. E. D. Chidsey, M. R. Linford, S. E. Creager, J. P. Ferraris, K. Chalfant, T. Zawodzinski, S. W. Feldberg, and M. D. Newton, *J. Am. Chem. Soc.*, 2003, **125**, 2004.
298. J. F. Smalley, S. W. Feldberg, C. E. D. Chidsey, M. R. Linford, M. D. Newton, and Y.-P. Liu, *J. Phys. Chem.*, 1995, **99**, 13141.
299. H. B. Gray and J. R. Winkler, *Proc. Natl. Acad. Sci. U. S. A.*, 2005, **102**, 3534.
300. T. A. Heimer, S. T. D'Arcangelis, F. Farzad, J. M. Stipkala, and G. J. Meyer, *Inorg. Chem.*, 1996, **35**, 5319.
301. E. Hendry, M. Koeberg, B. O'Regan, and M. Bonn, *Nano Lett.*, 2006, **6**, 755.
302. G. M. Turner, M. C. Beard, and C. A. Schmuttenmaer, *J. Phys. Chem. B*, 2002, **106**, 11716.
303. M. C. Beard, G. M. Turner, and C. A. Schmuttenmaer, *J. Phys. Chem. B*, 2002, **106**, 7146.
304. B. Wenger, C. Bauer, M. K. Nazeeruddin, P. Comte, S. M. Zakeeruddin, M. Grätzel, and J.-E. Moser, in *Electron Donor-acceptor Distance Dependence of the Dynamics of Light-induced Interfacial Charge Transfer in the Dye-sensitization of Nanocrystalline Oxide Semiconductors*, 'Physical Chemistry of Interfaces and Nanomaterials V, San Diego, CA, USA, 2006', SPIE, San Diego, CA, 2006, p. 63250V.
305. K. Kilsa, E. I. Mayo, D. Kuciauskas, R. Villahermosa, N. S. Lewis, J. R. Winkler, and H. B. Gray, *J. Phys. Chem. A*, 2003, **107**, 3379.
306. E. Galoppini, *Coord. Chem. Rev.*, 2004, **248**, 1283.
307. E. Galoppini, W. Guo, P. Qu, and G. J. Meyer, *J. Am. Chem. Soc.*, 2001, **123**, 4342.
308. P. Piotrowiak, E. Galoppini, Q. Wei, G. J. Meyer, and P. Wiewior, *J. Am. Chem. Soc.*, 2003, **125**, 5278.
309. E. Galoppini, W. Guo, W. Zhang, P. G. Hoertz, P. Qu, and G. J. Meyer, *J. Am. Chem. Soc.*, 2002, **124**, 7801.
310. M. Myahkostupov, P. Piotrowiak, D. Wang, and E. Galoppini, *J. Phys. Chem. C*, 2007, **111**, 2827.
311. N. A. Anderson, X. Ai, D. Chen, D. L. Mohler, and T. Lian, *J. Phys. Chem. B*, 2003, **107**, 14231.
312. M. Abrahamsson, O. Taratula, P. Persson, E. Galoppini, and G. J. Meyer, *J. Photochem. Photobiol. A Chem.*, 2009, **206**, 155.
313. C. Houarner-Rassin, F. Chaignon, C. She, D. Stockwell, E. Blart, P. Buvat, T. Lian, and F. Odobel, *J. Photochem. Photobiol. A Chem.*, 2007, **192**, 56.
314. C. C. Clark, G. J. Meyer, Q. Wei, and E. Galoppini, *J. Phys. Chem. B*, 2006, **110**, 11044.
315. C. C. Clark, A. Marton, and G. J. Meyer, *Inorg. Chem.*, 2005, **44**, 3383.
316. C. C. Clark, A. Marton, R. Srinivasan, A. A. Narducci Sarjeant, and G. J. Meyer, *Inorg. Chem.*, 2006, **45**, 4728.
317. A. Marton, C. C. Clark, R. Srinivasan, R. E. Freundlich, A. A. Narducci Sarjeant, and G. J. Meyer, *Inorg. Chem.*, 2006, **45**, 362.
318. F. Liu and G. J. Meyer, *Inorg. Chem.*, 2005, **44**, 9305.
319. E. Palomares, J. N. Clifford, S. A. Haque, T. Lutz, and J. R. Durrant, *J. Am. Chem. Soc.*, 2003, **125**, 475.
320. A. R. Kortan, R. Hull, R. L. Opila, M. G. Bawendi, M. L. Steigerwald, P. J. Carroll, and L. E. Brus, *J. Am. Chem. Soc.*, 1990, **112**, 1327.
321. I. Bedja and P. V. Kamat, *J. Phys. Chem.*, 1995, **99**, 9182.
322. Y. Diamant, S. Chappel, S. G. Chen, O. Melamed, and A. Zaban, *Coord. Chem. Rev.*, 2004, **248**, 1271.
323. A. Zaban, S. G. Chen, S. Chappel, and B. A. Gregg, *Chem. Commun.*, 2000, 2231.
324. W. H. Rippard, A. C. Perrella, F. J. Albert, and R. A. Buhrman, *Phys. Rev. Lett.*, 2002, **88**, 046805.
325. P. Qu, G. J. Meyer, Chap. 2: Dye-Sensitized Electrodes, in 'Electron Transfer in Chemistry, Part 2', ed. V. Balzani, 2005, Vol. IV, p. 355.
326. H. Gerischer and F. Willig, *Top. Curr. Chem.*, 1976, **61**, 31.
327. I. Ortman, C. Moucheron, and A. Kirsch-De Mesmaeker, *Coord. Chem. Rev.*, 1998, **168**, 233.
328. O. Kohle, M. Grätzel, A. F. Meyer, and T. B. Meyer, *Adv. Mater. (Weinheim, Fed. Repub. Ger.)*, 1997, **9**, 904.
329. F. Cecchet, A. M. Giocacchini, M. Marcaccio, F. Paolucci, S. Roffia, M. Alebbi, and C. A. Bignozzi, *J. Phys. Chem. B*, 2002, **106**, 3926.
330. G. Wolfbauer, A. M. Bond, and D. R. MacFarlane, *Inorg. Chem.*, 1999, **38**, 3836.
331. D. W. Thompson, C. A. Kelly, F. Farzad, and G. J. Meyer, *Langmuir*, 1999, **15**, 650.

332. C. J. Kleverlaan, M. T. Indelli, C. A. Bignozzi, L. Pavanin, F. Scandola, G. M. Hasselman, and G. J. Meyer, *J. Am. Chem. Soc.*, 2000, **122**, 2840.
333. S. Ernst and W. Kaim, *Inorg. Chim. Acta*, 1986, **114**, 123.
334. B. V. Bergeron, A. Marton, G. Oskam, and G. J. Meyer, *J. Phys. Chem. B*, 2005, **109**, 937.
335. C. R. Bock, J. A. Connor, A. R. Gutierrez, T. J. Meyer, D. G. Whitten, B. P. Sullivan, and J. K. Nagle, *J. Am. Chem. Soc.*, 1979, **101**, 4815.
336. C. R. Bock, T. J. Meyer, and D. G. Whitten, *J. Am. Chem. Soc.*, 1975, **97**, 2909.
337. A. J. Bard and L. R. Faulkner, 'Electrochemical Methods: Fundamentals and Applications', 2nd edition, John Wiley & Sons, Inc., New York, 2001.
338. P. Wang, B. Wenger, R. Humphry-Baker, J. E. Moser, J. Teuscher, W. Kantlehner, J. Mezger, E. V. Stoyanov, S. M. Zakeeruddin, and M. Grätzel, *J. Am. Chem. Soc.*, 2005, **127**, 6850.
339. D. Gust, T. A. Moore, and A. L. Moore, *J. Photochem. Photobiol. B Biol.*, 2000, **58**, 63.
340. T. A. Moore, A. L. Moore, and D. Gust, *Philos. Trans. R. Soc. London, B*, 2002, **357**, 1481.
341. C. S. Christ, J. Yu, X. Zhao, G. T. R. Palmore, and M. S. Wrighton, *Inorg. Chem.*, 1992, **31**, 4439.
342. R. Argazzi, C. A. Bignozzi, T. A. Heimer, F. N. Castellano, and G. J. Meyer, *J. Am. Chem. Soc.*, 1995, **117**, 11815.
343. R. Argazzi, C. A. Bignozzi, T. A. Heimer, F. N. Castellano, and G. J. Meyer, *J. Phys. Chem. B*, 1997, **101**, 2591.
344. P. Bonhote, J. E. Moser, R. Humphry-Baker, N. Vlachopoulos, S. M. Zakeeruddin, L. Walder, and M. Grätzel, *J. Am. Chem. Soc.*, 1999, **121**, 1324.
345. K. Westermark, S. Tingry, P. Persson, H. Rensmo, S. Lunell, A. Hagfeldt, and H. Siegbahn, *J. Phys. Chem. B*, 2001, **105**, 7182.
346. Z. Ning, and H. Tian, *Chem. Commun.*, 2009, 5483.
347. J. N. Clifford, E. Palomares, M. K. Nazeeruddin, M. Grätzel, J. Nelson, X. Li, N. J. Long, and J. R. Durrant, *J. Am. Chem. Soc.*, 2004, **126**, 5225.
348. S. A. Haque, J. S. Park, M. Srinivasarao, and J. R. Durrant, *Adv. Mater.*, 2004, **16**, 1177.
349. E. Palomares, M. V. Martinez-Diaz, S. A. Haque, T. Torres, and J. R. Durrant, *Chem. Commun.*, 2004, 2112.
350. S. Handa, H. Wietasch, M. Thelakkat, J. R. Durrant, and S. A. Haque, *Chem. Commun.*, 2007, 1725.
351. C. S. Karthikeyan, H. Wietasch, and M. Thelakkat, *Adv. Mater.*, 2007, **19**, 1091.
352. C. Kleverlaan, M. Alebbi, R. Argazzi, C. A. Bignozzi, G. M. Hasselmann, and G. J. Meyer, *Inorg. Chem.*, 2000, **39**, 1342.
353. Y. Xu, G. Eilers, M. Borgström, J. Pan, M. Abrahamsson, A. Magnuson, R. Lomoth, J. Bergquist, T. Polivka, L. Sun, V. Sundström, S. Styring, L. Hammarström, and B. Akermark, *Chem. Eur. J.*, 2005, **11**, 7305.
354. B. Gholamkhash, K. Koike, N. Negishi, H. Hori, T. Sano, and K. Takeuchi, *Inorg. Chem.*, 2003, **42**, 2919.
355. M. A. Green, K. Emery, Y. Hishikawa, and W. Warta, *Prog. Photovolt. Res. Appl.*, 2008, **16**, 61.
356. D. M. Stanbury, Reduction Potentials Involving Inorganic Free Radicals in Aqueous Solution, in 'Advances in Inorganic Chemistry', ed. A. G. Sykes, Academic Press, 1989, Vol. 33, p. 69.
357. G. Nord, B. Pedersen, and O. Farver, *Inorg. Chem.*, 1978, **17**, 2233.
358. G. Nord, B. Pedersen, L. Floryan, and P. Pagsberg, *Inorg. Chem.*, 1982, **21**, 2327.
359. G. Nord, *Comm. Inorg. Chem.*, 1992, **13**, 221.
360. W. K. Wilmarth, D. M. Stanbury, J. E. Byrd, H. N. Po, and C.-P. Chua, *Coord. Chem. Rev.*, 1983, **51**, 155.
361. B. J. Walter and C. M. Elliott, *Inorg. Chem.*, 2001, **40**, 5924.
362. X. Wang and D. M. Stanbury, *Inorg. Chem.*, 2006, **45**, 3415.
363. I. V. Nelson and R. T. Iwamoto, *J. Electroanal. Chem.*, 1964, **7**, 218.
364. J. Desbarres, *Bull. Soc. Chim. Fr.*, 1961, **28**, 502.
365. A. J. Parker, *J. Chem. Soc. London A*, 1966, 220.
366. R. Alexander, E. C. F. Ko, Y. C. Mac, and A. J. Parker, *J. Am. Chem. Soc.*, 1967, **89**, 3703.
367. F. G. K. Baucke, R. Bertram, and K. Cruse, *J. Electroanal. Chem.*, 1971, **32**, 247.
368. R. Guidelli and G. Piccardi, *Electrochim. Acta*, 1967, **12**, 1085.
369. A. I. Popov and D. H. Geske, *J. Am. Chem. Soc.*, 1958, **80**, 1340.
370. V. A. Macagno, M. C. Giordano, and A. J. Arvia, *Electrochim. Acta*, 1969, **14**, 335.
371. J. N. Demas and J. W. Addington, *J. Am. Chem. Soc.*, 1976, **98**, 5800.
372. J. N. Demas, J. W. Addington, S. H. Peterson, and E. W. Harris, *J. Phys. Chem.*, 1977, **81**, 1039.
373. C. Nasr, S. Hotchandani, and P. V. Kamat, *J. Phys. Chem. B*, 1998, **102**, 4944.
374. J. M. Gardner, J. M. Giaimuccio, and G. J. Meyer, *J. Am. Chem. Soc.*, 2008, **130**, 17252.
375. J. M. Gardner, M. Abrahamsson, B. Farnum, and G. J. Meyer, *J. Am. Chem. Soc.*, 2009, ASAP **131**(44), 16206.
376. D. J. Fitzmaurice and H. Frei, *Langmuir*, 1991, **7**, 1129.
377. J. N. Clifford, E. Palomares, M. K. Nazeeruddin, M. Grätzel, and J. R. Durrant, *J. Phys. Chem. C*, 2007, **111**, 6561.
378. S. Pelet, J. E. Moser, and M. Grätzel, *J. Phys. Chem. B*, 2000, **104**, 1791.
379. P. J. Cameron, L. M. Peter, S. M. Zakeeruddin, and M. Grätzel, *Coord. Chem. Rev.*, 2004, **248**, 1447.
380. B. A. Gregg, F. Pichot, S. Ferrere, and C. L. Fields, *J. Phys. Chem. B*, 2001, **105**, 1422.
381. J. Desilvestro, M. Grätzel, L. Kavan, J. Moser, and J. Augustynski, *J. Am. Chem. Soc.*, 1985, **107**, 2988.

382. N. Vlachopoulos, P. Liska, J. Augustynski, and M. Grätzel, *J. Am. Chem. Soc.*, 1988, **110**, 1216.
383. G. Oskam, B. V. Bergeron, G. J. Meyer, and P. C. Searson, *J. Phys. Chem. B*, 2001, **105**, 6867.
384. P. Wang, S. M. Zakeeruddin, J. E. Moser, R. Humphry-Baker, and M. Grätzel, *J. Am. Chem. Soc.*, 2004, **126**, 7164.
385. N. Sutin and C. Creutz, *J. Chem. Educ.*, 1983, **60**, 809.
386. H. Nusbaumer, J. E. Moser, S. M. Zakeeruddin, M. K. Nazeeruddin, and M. Grätzel, *J. Phys. Chem. B*, 2001, **105**, 10461.
387. H. Nusbaumer, S. M. Zakeeruddin, J.-E. Moser, and M. Grätzel, *Chem. Eur. J.*, 2003, **9**, 3756.
388. S. A. Sapp, C. M. Elliott, C. Contado, S. Caramori, and C. A. Bignozzi, *J. Am. Chem. Soc.*, 2002, **124**, 11215.
389. S. Hattori, Y. Wada, S. Yanagida, and S. Fukuzumi, *J. Am. Chem. Soc.*, 2005, **127**, 9648.
390. S. Nakade, T. Kanzaki, W. Kubo, T. Kitamura, Y. Wada, and S. Yanagida, *J. Phys. Chem. B*, 2005, **109**, 3480.
391. S. Nakade, Y. Makimoto, W. Kubo, T. Kitamura, Y. Wada, and S. Yanagida, *J. Phys. Chem. B*, 2005, **109**, 3488.
392. S. Cazzanti, S. Caramori, R. Argazzi, C. M. Elliott, and C. A. Bignozzi, *J. Am. Chem. Soc.*, 2006, **128**, 9996.
393. J. J. Nelson, T. J. Amick, and C. M. Elliott, *J. Phys. Chem. C*, 2008, **112**, 18255.
394. A. Grabulosa, M. Beley, P. C. Gros, S. Cazzanti, S. Caramori, and C. A. Bignozzi, *Inorg. Chem.*, 2009, **48**, 8030.
395. M. J. Scott, J. J. Nelson, S. Caramori, C. A. Bignozzi, and C. M. Elliott, *Inorg. Chem.*, 2007, **46**, 10071.
396. M. Brugnati, S. Caramori, S. Cazzanti, L. Marchini, R. Argazzi, and C. A. Bignozzi, *Int. J. Photoenergy*, 2007, **2007**, 80756.
397. B. Enright, G. Redmond, and D. Fitzmaurice, *J. Phys. Chem.*, 1994, **98**, 6195.
398. H. Lindstrom, S. Södergren, A. Solbrand, H. Rensmo, J. Hjelm, A. Hagfeldt, and S. E. Lindquist, *J. Phys. Chem. B*, 1997, **101**, 7710.
399. H. Lindstrom, S. Södergren, A. Solbrand, H. Rensmo, J. Hjelm, A. Hagfeldt, and S. E. Lindquist, *J. Phys. Chem. B*, 1997, **101**, 7717.
400. B. O'Regan and D. T. Schwartz, *Chem. Mater.*, 1998, **10**, 1501.
401. B. A. Gregg, S.-G. Chen, and S. Ferrere, *J. Phys. Chem. B*, 2003, **107**, 3019.
402. S. Ferrere and B. A. Gregg, *J. Phys. Chem. B*, 2001, **105**, 7602.
403. Q. Wang, Z. Zhang, S. M. Zakeeruddin, and M. Grätzel, *J. Phys. Chem. C*, 2008, **112**, 7084.
404. Q. Wang, Z. Zhang, S. M. Zakeeruddin, and M. Grätzel, *J. Phys. Chem. C*, 2008, **112**, 10585.
405. C. A. Kelly, F. Farzad, D. W. Thompson, J. M. Stipkala, and G. J. Meyer, *Langmuir*, 1999, **15**, 7047.
406. E. F. Hilinski, P. A. Lucas, and Y. Wang, *J. Chem. Phys.*, 1988, **89**, 3435.
407. D. J. Norris, A. Sacra, C. B. Murray, and M. G. Bawendi, *Phys. Rev. Lett.*, 1994, **72**, 2612.
408. S. H. Szczepankiewicz, J. A. Moss, and M. R. Hoffmann, *J. Phys. Chem. B*, 2002, **106**, 7654.
409. C. L. Olson, J. Nelson, and M. S. Islam, *J. Phys. Chem. B*, 2006, **110**, 9995.
410. CRC, 'Handbook of Chemistry and Physics'. 73rd edition, CRC Press, Boca Ration, 1992.
411. B. A. Gregg, *Coord. Chem. Rev.*, 2004, **248**, 1215.
412. J. Nelson, *Phys. Rev. B*, 1999, **59**, 15374.
413. G. Schlichthorl, S. Y. Huang, J. Sprague, and A. J. Frank, *J. Phys. Chem. B*, 1997, **101**, 8141.
414. K. Schwarzbarg and F. Willig, *J. Phys. Chem. B*, 1999, **103**, 5743.
415. L. Dloczik, O. Ileperuma, I. Lauermaun, L. M. Peter, E. A. Ponomarev, G. Redmond, N. J. Shaw, and I. Uhlendorf, *J. Phys. Chem. B*, 1997, **101**, 10281.
416. A. Zaban, A. Meier, and B. A. Gregg, *J. Phys. Chem. B*, 1997, **101**, 7985.
417. A. Zaban, S. Ferrere, and B. A. Gregg, *J. Phys. Chem. B*, 1998, **102**, 452.
418. B. A. Gregg, *J. Phys. Chem. B*, 2003, **107**, 13540.
419. R. Könenkamp, *Phys. Rev. B*, 2000, **61**, 11057.
420. V. Kytin, T. Dittrich, J. Bisquert, E. A. Lebedev, and F. Koch, *Phys. Rev. B*, 2003, **68**, 195308.
421. P. Hoyer and H. Weller, *J. Phys. Chem.*, 2002, **99**, 14096.
422. L. Brus, *Phys. Rev. B*, 1996, **53**, 4649.
423. D. Cahen, G. Hodes, M. Grätzel, J. F. Guillemoles, and I. Riess, *J. Phys. Chem. B*, 2000, **104**, 2053.
424. J. Bisquert, D. Cahen, G. Hodes, S. Ruhle, and A. Zaban, *J. Phys. Chem. B*, 2004, **108**, 8106.
425. C. L. Olson, *J. Phys. Chem. B*, 2006, **110**, 9619.
426. U. B. Cappel, E. A. Gibson, A. Hagfeldt, and G. Boschloo, *J. Phys. Chem. C*, 2009, **113**, 6275.
427. I. Montanari, J. Nelson, and J. R. Durrant, *J. Phys. Chem. B*, 2002, **106**, 12203.
428. A. Kay, R. Humphry-Baker, and M. Grätzel, *J. Phys. Chem.*, 1994, **98**, 952.
429. S. A. Haque, Y. Tachibana, D. R. Klug, and J. R. Durrant, *J. Phys. Chem. B*, 1998, **102**, 1745.
430. C. Bauer, G. Boschloo, E. Mukhtar, and A. Hagfeldt, *J. Phys. Chem. B*, 2002, **106**, 12693.
431. A. N. M. Green, R. E. Chandler, S. A. Haque, J. Nelson, and J. R. Durrant, *J. Phys. Chem. B*, 2005, **109**, 142.